Solubilization Strength Characterization of Parenteral Solutions Containing Polysorbate 80 in Support of Extractable & Leachable Studies

Dissertation

zur Erlangung des akademischen Grades

"Doktor der Naturwissenschaften"

Fachbereich Chemie, Pharmazie, Geographie und Geowissenschaften

Johannes Gutenberg-Universität, Mainz

vorgelegt von

Adrian Benedict Strobel

geb. in Offenbach am Main

Mainz 2021

1. Berichterstatter: [redacted]

2. Berichterstatter: [redacted]

Tag der mündlichen Prüfung: 18.11.2021

Table of Contents

List of Figures

List of Tables

Acronyms and Abbreviations

AET	Analytical evaluation threshold
API	Active pharmaceutical ingredient
CAS	Chemical Abstracts Service
CAS-RN	CAS registry number
CAZ	Carbazole
CMC	Critical micelle concentration
COSMO-RS	Conductor-like screening model for realistic solvation
COSMOmic	COSMO-RS for micelles
CSA	Chemical safety assessment
CTAB	Cetyltrimethylammonium bromide
DEHP	Di(2-ethylhexyl) phthalate
Dextrose	D-Glucose
DNT	2,4-Dinitrotoluene
EDTA	Ethylenediaminetetraacetic acid
EtOH	Ethanol
E & L	Extractables and leachables
FDA	United States Food and Drug Administration
GC	Gas chromatography
HLB	Hydrophobic-lipophilic balance
HSA	Human serum albumin
HS-GC	Headspace gas chromatography
HSP	Hansen solubility parameters
ICH	International Council for Harmonisation of Technical Requirements for Pharmaceuticals for Human Use
IPA	Isopropanol (isopropyl alcohol)
IUPAC	International Union of Pure and Applied Chemistry
LC	Liquid chromatography
LDPE	Low density polyethylene
LSER	Linear solvation energy relationship

MEKC	Micellar electrokinetic chromatography
MLC	Micellar liquid chromatography
MS	Mass spectrometry
MTM	Mass transport modeling
Naph	Naphthalene
NMR	Nuclear magnetic resonance
NaCl	Sodium chloride
NVOC	Non-volatile organic chemical
OECD	Organization for Economic Co-operation and Development
PDMS	Polydimethyl siloxane
Ph.Eur.	European Pharmacopoeia
PTFE	Polytetrafluoroethylene
PRCA	Pure red cell aplasia
PS 20	Polysorbate 20
PS 80	Polysorbate 80
PSP	Partial solvation parameters
Q3E	ICH quality guideline on the assessment and control of extractables and leachables
QSAR	Quantitative structure-activity relationship
SCT	Safety Concern Threshold
SDS	Sodium dodecyl sulfate
Surfactant	Surface active agent
UFZ	Helmholtz-Center for Environmental Research
UNIFAC	Universal quasichemical functional group activity coefficients
USP	United States Pharmacopeia
UV	Ultraviolet
VHOC	Very hydrophobic organic chemical
VOC	Volatile organic chemical
v/v	Volume per volume
w/v	Weight per volume

Symbols

A	Peak area
A_i	Hydrogen bond acidity (LSER solute descriptor)
Air	Headspace reference phase
B_i	Hydrogen bond basicity (LSER solute descriptor)
B_i^0	Adjusted hydrogen bond basicity (LSER solute descriptor)
C_i	(Molar) concentration of a solute
C_i^0	Initial concentration of a solute
D_i	Diffusion coefficient of a solute
Dex	Dextrose
E_i	Excess molar refraction (LSER solute descriptor)
$EtOH$	Ethanol
$Extr$	Polymer extract
e, s, a, b, v, c	LSER system parameters
f_A	Weight or volume based fraction of substance A in solution
i	Solute, solvated chemical
IPA	Isopropanol
$K_{i,1/2}$	Molar partition coefficient of a solute between phase 1 and 2
$K_{i,1/2}^x$	Mole fraction partition coefficient of a solute between phase 1 and 2
k_S	Setschenow/ salting constant
$LDPE$	Low density polyethylene
log	Logarithmic
m_i	Mass of a solute
M	Medium

Mic	Micellar phase
n_i	Amount of solute
NaCl	Sodium chloride
n_{agg}	Surfactant aggregation number
O	Octanol
P	Polymer
PDMS	Polydimethyl siloxane
$\mathrm{PS\ 80}$	Polysorbate 80 (micellar phase)
r	Chromatographic response factor
S_i	Solubility of a solute or dipolarity/ polarizability (LSER solute descriptor)
Surf	Surfactant
$\mathrm{Surf(Mic)}$	Micellized surfactant (surfactant in micelles)
tot	Total
V	Volume
$\overline{V}$	Molar volume
V_i	Scaled molecular volume according to McGowan (LSER solute descriptor)
W	Water
X_i	Mole fraction concentration
κ_i	Molar solubilization ratio of a solute
γ_i	Activity coefficient of a solute

1. Introduction

Leaching is a physical process occurring between clinically relevant solutions and materials, where chemical material constituents (leachables) migrate towards the solution [1]. Polymers are essential parts of contact materials in pharmaceutical applications, showing advantageous properties in production, storage, and application of medicines. They are cost efficient, flexible, and provide inertness to environmental stresses to the medicinal product [2]. Nonetheless, polymeric contact materials are a source of leachables that have the potential to negatively impact the safety and efficacy of a drug product, with injectable parenteral formulations carrying an elevated patient risk due to direct administration to the bloodstream [3]. Experimental assessment of patient exposure to material constituents is therefore demanded and carried out in extractable and leachable (E & L) studies [4]. Here, drug products with high extraction strength towards contacting polymers, often elicited by formulated solubilizers such as surfactants, promote leaching which ultimately increases patient exposure [5].

As leachable studies directly examine the drug product, they pose analytical and logistical obstacles due to a complex analytical matrix, cost, and availability of drug product in early development [6]. In lieu of conclusive studies of leachables in the clinically relevant drug product, extraction studies employing alcohol-water mixtures as simulating solvents, intended to mimic pharmaceutical formulations, can obtain suitable projections of final leachable levels under accelerated conditions [7]. The preparation of suitable simulating solvent mixtures affords quantitative knowledge of the major solubilization mechanisms under operation in the clinically relevant product formulation. In turn, this requires characterization of solubilization behavior mediated by individual excipients and information on the excipient composition in parenteral drug products [8, 9]. A strongly solubilizing excipient that is extensively employed in parenteral formulations is polysorbate 80 (PS 80), a nonionic surfactant that forms micelles in aqueous solution [10, 11].

Beside the consideration of solubilization mechanisms, thorough understanding of the physicochemical aspects of diffusion of migrants in polymers as well as partitioning between polymers and contact solutions enables the prediction of time-dependent leachable accumulation in pharmaceutical solutions. Both preparation of tailored simulating solvents and prediction of final leachable accumulation in a drug product are expected to support the work of E & L practitioners by delivering information to develop appropriate methods and testing protocols [12].

Accordingly, this thesis aims to provide the background of E & L testing on both pharmaceutical contact materials and parenterally applied drug formulations. The challenges encountered by practitioners in the field of E & L, as well as opportunities for improvement, especially through robust scientific approaches, will be presented. In particular, model equations predicting partition equilibria will be utilized to gain insights into the underlying physicochemical processes that influence the migration of leachables. The derivation and application of these models is a central subject of this work, which intends to expand the body of knowledge related to the physicochemical aspects of the E & L field.

1.1 Background

1.1.1 Materials in Contact with Pharmaceutical Solutions

Pharmaceutical solutions are in contact with various materials during manufacture, storage, and use of a drug product. Multiple interactions between solution and contact material can occur, including adsorption of solution constituents to the material's surface, penetration (swelling) of the material by the pharmaceutical solvent or leaching of chemicals (leachables) from the contact material into the solution [13, 14]. These events pose inherent risks concerning the stability, safety, and efficacy of the final drug product due to loss of necessary pharmaceutical ingredients or presence of unwanted impurities. Stringent monitoring is required to preclude adverse effects of material contact, with emphasis on liquid dosage forms for parenteral application which have i) a high likelihood of interaction and ii) a high degree of concern associated with the route of administration [3] (Table 1).

Materials of construction in pharmaceutical processes include metals, glass, and polymers [15]. While leaching of chemicals can occur from all these materials [16, 17], polymers (rubbers and plastics) are of special interest when in contact with pharmaceutical solutions. Organic and inorganic residues from polymer manufacture including solvents, mono- and oligomers, catalysts as well as polymer additives like stabilizers, plasticizers, or coloring agents and their potential degradation products may remain in the finished material [18]. The total pool of potential leachables embedded in the polymer matrix is referred to as extractables.

Extraction of unwanted chemical species from contact materials is an overarching problem in a drug product's life cycle demanding expert analysis. Compounds originating from a contact material are scrutinized within a chemical safety assessment (CSA), covering extractable, simulating, and leachable studies to determine their identity and quantity and a toxicological risk assessment derived from the presented data [3, 19, 20]. While the toxicological risk posed by the leachable itself requires investigation, chemical or physical reaction of a leachable with a drug product constituent may also negatively affect quality and safety attributes of the product [21]. Therapeutic biological proteins especially offer many sites for reaction with leachables and see increased market authorization [22]. Hence, the manufacture process of biopharmaceuticals is monitored for contamination of the process stream with leachables [23, 24]. However, biomanufacturing also involves one or several purification steps where leachables can be cleared, preventing their accumulation in the final drug product [25, 26].

Leaching of material constituents with final human exposure is well documented [27-29]. A case that received considerable public attention is discussed below (Chapter 1.1.4) [30].

Table 1. Examples of Packaging Concerns for Common Classes of Drug Products. Adapted from FDA[a)] Guidance for Industry [3].

Degree of concern associated with the route of administration	**Likelihood of packaging component-dosage form interaction**		
	High	**Medium**	**Low**
Highest	Inhalation aerosols/ solutions, injections and injectable suspensions	Sterile powders and powders for injection, inhalation powders	
High	Ophthalmic solutions/ suspensions, transdermal ointments/ patches, nasal aerosols/ sprays		
Low	Topical solutions/ suspensions, topical/ lingual aerosols, oral solutions/ suspensions	Topical/ oral powders	Oral tablets/ capsules

a) U.S. Food and Drug Administration

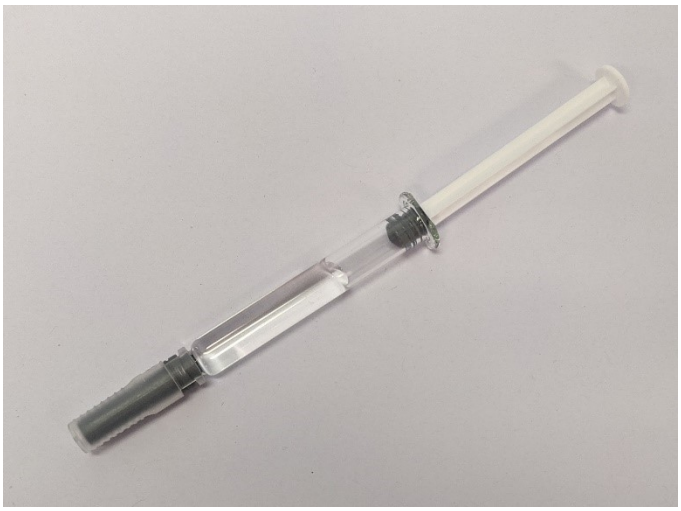

Figure 1. Prefillable syringe system that serves as primary packaging for parenterally applied medicinal products.

Figure 2. Rubber vial stoppers as potential source of leachables.

1.1.2 Extractables and Leachables

Studies on extractables and leachables (E & L) serve as a means to gather data on unwanted impurities from contact materials a patient may be exposed to when receiving a drug product. From the data collected in a CSA, final patient exposure to individual chemical compounds is calculated and critically reviewed by toxicologists, based on the daily intake and timespan of the treatment [31], as required for the market authorization of a drug product.

Extractable studies aim to explore organic and inorganic chemicals that can be extracted from a material in a timely manner and under laboratory conditions [32]. Strong solvents (or appropriate solvent mixtures), high temperatures, and comminution of the material are used to achieve exhaustive extraction of the material. Orthogonal experimental and analytical methods, e.g. utilizing different extraction solvents in addition to liquid and gas chromatography, are employed to address the chemical variety of extractables as expressed by their polarity, volatility, charge and size [33, 34]. In particular, polarity-driven extraction through choice of suitable extraction solvents has been identified as a fundamental concept to accomplish the objectives of E & L testing [35, 36].

An important aspect of extractable studies is the confirmed identification of the compounds by chemical name, structure, and, if available, CAS registry number. Mass spectrometry (MS) analysis against chemical libraries and authentic reference standards are regularly used to help ascertain the extractable's identity [37]. This, in turn, allows a compound-specific toxicological assessment where the necessary information about the chemical(s) in question can be retrieved and applied for evaluation of possible patient exposure.

An extractable study provides – assuming that extractable compounds could be identified – information on identity and amount of potential leachables [38], aiding experimental design of further studies by anticipating compound profiles and possible degradation products. The quantitative extractable profile of a material also reveals compounds of interest for later analyses based on physicochemical data, e.g. a chemical's aqueous solubility. For instance, below the analytical evaluation threshold (AET), extractables and leachables require no identification and toxicological assessment (subject to some constraints) [39, 40]. To chromatographically implement the AET, standards representing the lowest detection and quantification concentration based on the AET are measured to help differentiate between the signals that require identification and those that do not. Since analytical responses can vary between reference and unknown substances, an analytical uncertainty factor is applied to the AET to offset the different response factors [41]. The AET itself depends on the daily dose of a medicine and is derived from a safety concern threshold (SCT), below which the daily intake of any leachable would be of no concern towards patient safety, including carcinogenic leachables [42]. Figure 3 illustrates the connection between chromatographic data from an extractable and a leachable study. While Figure 3 displays this connection adequately, more signals above the AET that do not require elucidation are likely to be found in an actual experimental chromatogram, relating to e.g. extraction solvents or the drug product matrix.

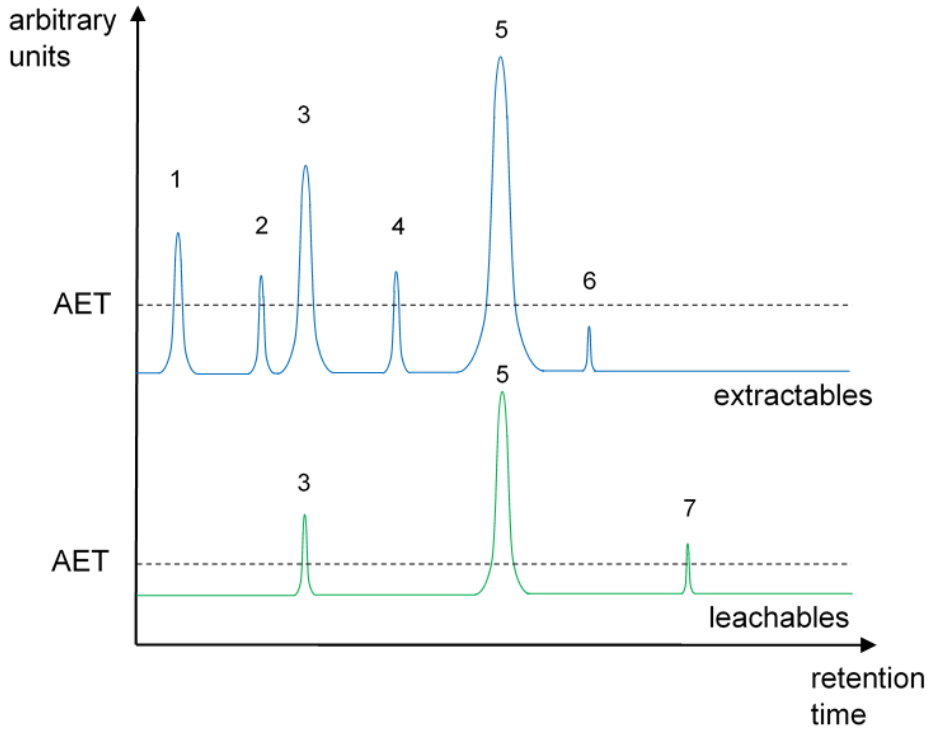

Figure 3. Overlay of idealized chromatograms from an extractable and a leachable study on contact material and drug product, respectively. From the upper chromatogram, chemical structure of five compounds (1-5) is elucidated, while one compound (6) below the AET is disregarded. Compounds 3 and 5 are likewise identified in the following leachable study on the drug product, where a degradant (7) from one of the extractables is additionally found.

Leachable studies are performed directly on a drug product or placebo thereof and not, contrary to extractable studies, on the material [43]. In leachable studies, the accumulation of leachables in the drug product is assessed until the designated shelf life of the product has been reached. While they appear ideal to deduce actual patient exposure from the quantitative chemical profile elucidated, leachable studies are time-intensive and analytically challenging to perform. Not only are leachables most often present at trace levels, pharmaceutical solutions are generally difficult matrices to analyze, which can render the task of determining all leachables that have migrated to a solution impossible [44]. It is therefore of great interest to the E & L community to establish a correlation between extractables from a material and a final quantitative leachable profile found in a drug product without having to perform rigorous and time-consuming leachable studies [45].

An expedient way to project realistic leachable levels are extraction studies using simulating solvents. For plastic packaging of parenteral drugs and process materials, these studies are typically carried out with 50% v/v alcohol (ethanol or isopropanol) in water mixtures as a simulating solvent to represent the polarity-driven extraction strength of a pharmaceutical formulation [7]. Extraction studies using simulating solvents (or briefly: simulation studies) serve as an intermediate step between extractable and leachable studies and are performed under accelerated conditions, while attempting to match the leaching propensity of the drug product as closely as possible with a simple solvent mixture [15].

At present, alcohol-water mixtures (cosolvent mixtures) used in simulation studies disregard the individual composition of pharmaceutical formulation constituents and their quantitative effect on solubilization of potential leachables. The solubilization capacity of a formulation is hence frequently overestimated when represented by such a simulating solvent [7]. As a result, data from

a simulation study may not be representative of the final leachable profile by failing to simulate quantitative solubilization mechanisms in a drug product. In Figure 4, the impact of different simulating solvent compositions on an extraction profile generated in a simulation study is displayed in overlayed chromatograms. Here, a reduction in the employed alcohol fraction leads to identification of fewer and less intense signals above the AET.

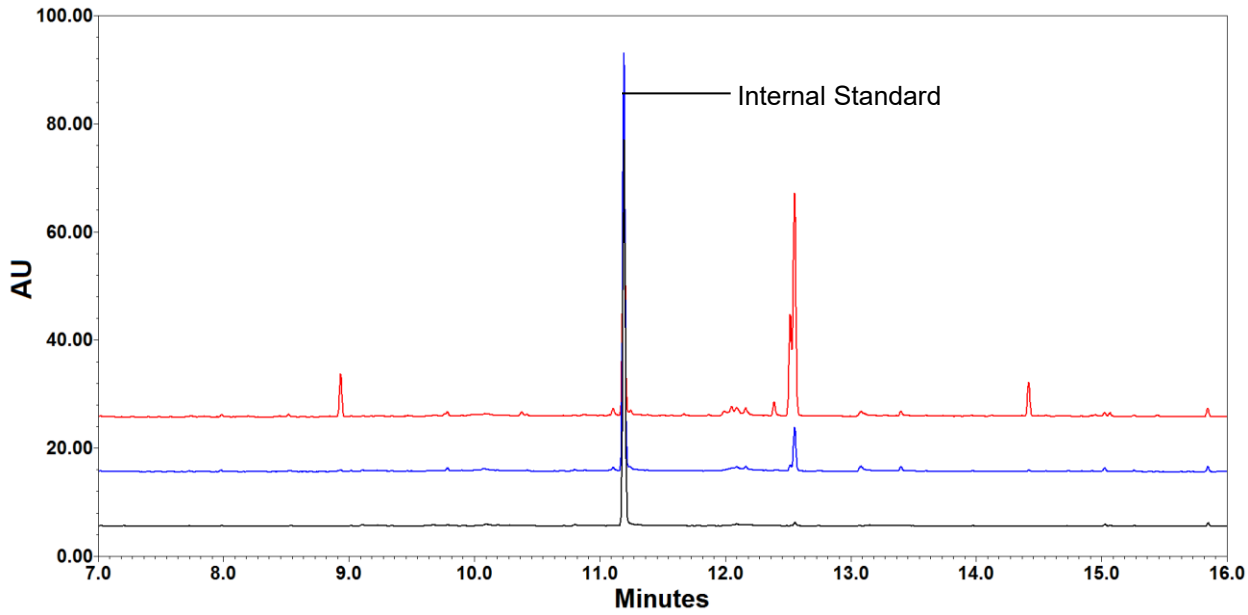

Figure 4. Overlay plot of in-vial rubber stopper extracts generated with different IPA in water mixtures over 24 h at 30°C. Back-extracted with dichloromethane for GC chromatography and detected with a flame ionization detector. Red line = 50% v/v IPA in water; blue line = 30% v/v IPA in water; black line = 20% v/v IPA in water.

There are currently several best practice recommendations for the chemical assessment of extractables and leachables from polymers [15, 22, 32, 43, 46, 47], targeting different process materials in the drug product lifecycle, e.g. container closure systems or biomanufacturing components. The International Council for Harmonisation (ICH), with its goal to streamline quality, safety, and efficacy aspects of human medicines worldwide [48], offers quality guidelines for monitoring and determination of drug product impurities under the abbreviation Q3. The quality guideline on the assessment and control of extractables and leachables (Q3E), for which development was recently initiated, aims to harmonize regulatory guidance of E & L monitoring, establishing a structured, risk-based approach [49].

In addition to a more formalized evaluation system introduced in Q3E, small molecule mass transport modeling (MTM) can be implemented to support CSAs by exploration of physical factors impacting leaching [47]. Similar molecular modeling approaches have already been successfully implemented for food contact materials [50-53]. Several applications of MTM can be considered, including:

- the calculation of alcohol content for suitable simulating solvents based on the extraction strength of a pharmaceutical solution or
- the estimation of final leachable levels in a drug product, based on a material's quantitative extraction profile and the drug product composition

In this work, the necessary physicochemical concepts (i.e., models and associated parameters) for MTM, which enable the robust prediction of solubilization in parenteral formulations and simulating solvents as well as mass transfer from polymers to these solutions, are presented or

established. Furthermore, these concepts will be applied to foresee ultimate leachable concentrations in the clinically relevant contact solution within a well-defined system.

1.1.3 Parenteral Formulations

Supporting a predictive concept for solubilization, the constituents of pharmaceutical contact solutions of relevance to E & L testing and their associated solubilization mechanisms require characterization. Critically, the extraction strength of a drug product towards contact materials depends on the composition of the excipients. Even though the active pharmaceutical ingredient (API) is responsible for the therapeutic activity of a formulation, it only constitutes a small weight fraction of the formulation, with excipients comprising the remaining major fraction [22, 54].

Parenteral formulations are sterile preparations for injection, infusion or implantation in the human body, according to the European Pharmacopoeia (Ph. Eur. 10) [55]. In these preparations, excipients are formulated assuming pharmaceutical inactivity (i.e., drug product efficacy depends solely on the API). Nonetheless, some excipients are known to interact with the human body by influencing drug uptake or metabolization as well as causing pain, fever, or swelling at the injection site, among other immune responses [56-58]. Such interactions are especially relevant when a drug product is applied via injection. Concerning the safety of the applied medicine, injectable administration carries higher patient exposure to formulation constituents, as it enters the systemic organism completely without presystemic metabolisation [59]. Both these points limit the choice of excipients and their respective amounts suitable for formulation in a parenterally applied drug product.

Similar risk categorization can be applied to formulations in contact with manufacture or packaging materials. Here, liquid formulations have the highest potential to extract material constituents, thus bearing the highest potential patient exposure to leachables from the material [3]. As acknowledged by regulatory agencies, besides inhalable formulations, liquid parenteral formulations therefore require the highest amount of scrutiny in CSAs (see Table 1).

A majority of authorized liquid parenteral formulations contain water for injection as the main solvent [11, 60], which justifies focus on aqueous based parenteral formulations within the scope of this work. Besides water for injection, these formulations contain additional excipients to ensure a safe, compatible, and effective drug product. Each excipient employed in a formulation serves one or more distinct pharmaceutical purposes, whereby it can be categorized. In aqueous based parenteral formulations, typical excipient classes include cosolvents, solubilizing or thickening agents (surfactants and polymers), chelating agents, preservatives (antioxidants and antimicrobials), buffers, tonicifying agents, and lyoprotectants (only in lyophilized products that are diluted in an aqueous medium before use) [11, 61-64]. Frequently formulated excipients and their respective excipient class are displayed in Table 2. While the identity of excipients encountered differs from drug product to drug product, no essential difference between excipients formulated in biological or (conventional) small molecule drugs can be established [65].

Table 2. Important parenteral excipient classes and representative excipients. Adapted from [11] and [61].

Excipient class	Representative excipients
Solvents and cosolvents	Water for injection, ethanol, glycerin, propylene glycol
Solubilizing, wetting, suspending, emulsifying or thickening agents[a)]	Polysorbate 20/80, poloxamer 188, sodium carboxy methyl cellulose, polyvinyl pyrrolidone
Chelating agents	Disodium/calcium EDTA[b)]
Antioxidants	Sodium bisulfite, sodium metabisulfite, sodium ascorbate
Antimicrobial preservatives	Benzyl alcohol, thiomersal, methyl/propyl paraben
Buffers	Acetate, citrate, phosphate with various counterions
Bulking agents, lyophilization protectants, tonicity adjusters	Sodium chloride, glycerin, dextrose, trehalose, sucrose, mannitol

a) surfactants/ polymers
b) ethylenediaminetetraacetic acid

1.1.4 Eprex® Case

Below, a prominent case of leachable accumulation in a parenteral drug product is presented, showcasing why chemical safety assessments are indispensable for parenteral formulations that include potent solubilizers like PS 80.
In 1998, human serum albumin (HSA) was replaced by polysorbate 80 as a protein stabilizer in pre-filled syringes of Eprex®, a recombinantly produced human erythropoietin analogue. The formulation change was mandated by concerns over the use of human blood derived products like HSA, which could contain viral or prionic contaminations [66, 67]. Over the following years, cases of pure red cell aplasia (PRCA) increased significantly in patients with chronic renal disease receiving the new formulation subcutaneously. Ultimately, leachables from the syringe plunger were found in pre-filled syringes with uncoated rubber stoppers, prompting the report of those leachables as the root cause of erythropoietin antibody formation and PRCA incidence. The increase of leachables can be correlated to the introduction of PS 80 to the formulation [30].
In a clinical study of subcutaneously administered epoetin alfa prefilled syringes, antibody formation occurred in two patients [68]. Investigations showed an elevated content of soluble tungsten species, originating from the barrel syringe manufacture, in some prefilled syringes [69]. Further tests showed tungsten induced epoetin aggregation, which may lead to increased immunogenicity, depending on the nature of aggregation, specifically disulfide bonding. The authors proposed tungsten species as root cause for PRCA in the Eprex® case. However, this does not explain the sudden increase of PRCA cases when PS 80 was introduced to the Eprex® formulation, since comparable amounts of tungsten must have been present beforehand.
Richter *et al.* [70] later conducted studies on uncoated rubber closures with polysorbate solutions and found an increase in high molecular weight proteins (aggregates) induced by leachables. The authors concluded that this aggregation caused an increase in PRCA cases, as discussed previously. The effectivity of a fluoropolymer-coated rubber stopper preventing leachable accumulation was demonstrated in a technical investigation [71], where leachables were only found

in formulations with PS 80 as a solubilizer in contact with uncoated rubber stoppers. Identical, but coated rubber stoppers did not leach rubber constituents, even if the contacting formulation contained PS 80. Since 2003, fluoropolymer-coated rubber stoppers have replaced uncoated stoppers in Eprex® formulations and the incidence of PRCA cases has dropped consequently [30]. Regardless of the underlying mechanism leading to protein aggregation, it should be self-evident that a reduction of leachables and impurities in general is beneficial for patient safety. A leachable-mediated product defect may be complex or even impossible to track down completely [72], as the above summary shows.
Fortunately, in parallel to this incident, industry guidelines detailing container closure system testing were published by regulatory authorities [3, 19]. Manufacturers now likewise must provide safety data for previously authorized drug products in which excipients have been exchanged. This process could have elucidated leaching of molecular constituents of the syringe system before the product was released to the market, necessitating e.g. a change of system or construction materials like the rubber plunger.
The immense technical and analytical expenditures related to E & L testing are warranted for cases when leaching of material constituents are probable due to the nature of the material or the contact solution, as in the given example. However, it is also beneficial to identify cases where no significant leaching, based on the underlying physicochemical processes governing leachable accumulation, is expected, and consequently amend the analytical procedure in CSAs.

1.1.5 Objectives

From the above, the objectives of this thesis are presented. The solubilization of organic chemicals in parenteral formulations must be quantified to determine the extraction strength of the solution towards contacting materials. To this end, quantitative descriptions of solubilization mechanisms exerted by excipients in parenteral formulations are needed. Thermodynamic models connecting solubilization to physicochemical parameters are required to estimate relevant parameters of solubilization in aqueous solutions containing excipients without further experimental input. Where possible, such models are collected from the literature and investigated for their predictive power. The effect that the combination of excipients has on aqueous solubilization is explored subsequently. Since no comprehensive model allowing estimation of the solubilizing propensity of PS 80 in solution has yet been reported, an intuitive, semi-empirical modeling approach is presented. Utilizing experimental data, a robust and accurate model equation is constructed. In addition, thermodynamic models are gathered from the literature that allow the alignment of simulating solvents with PS 80 solutions and parenteral formulations. Finally, the calculated extraction strength of a contact solution is verified in an experimental case study that provides a clinically relevant leaching scenario.

2. Theory

2.1 Mass Transport Modeling

Mass transport modeling (MTM) aims to provide pre-experimental data assisting the investigation of pharmaceutical contact materials. The principles governing mass transport of small molecule chemicals from contact materials to a process stream, drug product, or body fluid are diffusion, partitioning, and solubility [9]. In combination, a quantitative, time-dependent description of the migration process is possible with knowledge of these parameters and the dimensions of material and contacting product.

The mass flux J of a chemical in a material or solution, following along the gradient of chemical potential, is proportional to the diffusion coefficient D_i [73], according to Fick's first law:

$$J = -D_i \frac{\partial C_i}{\partial x} \quad (1)$$

where C_i is the concentration of the chemical and x is its relative position. While diffusion is comparatively fast in aqueous solutions ($D_{i,W} \approx 10^{-5}$ m^2 s^{-1}), D_i is multiple magnitudes lower in polymers [74]. The net diffusion ceases once chemical equilibrium between the contact phases is reached, where concentrations in contact material and drug product or extraction solvent remain constant.

Attainment of chemical equilibrium in the contact medium depends on the employed polymer material(s), the volumes of medium and polymer, the contact surface area, current temperature, the total time of contact, and respective diffusion and partition coefficients [75]. If no equilibrium is attained within the products shelf life, leachable concentration in the drug product is typically dependent on the rate-limiting diffusion characteristics of the polymer (i.e., diffusion-controlled) [50]. Since polymers are also employed as food contact materials, extensive research into the field of polymer diffusion and migration to foodstuffs has been conducted. As a result, several diffusion models for the estimation of diffusion coefficients in polymers $D_{i,P}$ have been proposed, based on atomic first principles or semi-empirical approaches [74, 76-80]. Moreover, numerical software tools with integrated estimation of $D_{i,P}$ to plot migration curves from polymers to contact solutions (e.g. food simulants) have been developed and applied successfully [81], demonstrating that chemical migration inside polymers can be reasonably forecast. For leachables related to pharmaceutical process equipment, a successful application of estimated diffusion coefficients from extractable data has recently been published [82]. Owed to this research background, modeling of diffusion constants in polymers and, by extension, modeling of migration to foodstuffs has already been implemented in international regulations for food contact plastic materials [83, 84], in contrast to the concept of MTM introduced here. The main difference between the concept of migration modeling as officially recognized in the food industry and MTM is that the former does not deploy precise predictions of partition coefficients, rather aiming to divide migrants into two groups of low and high solubility in the respective foodstuff [50]. As many material constituents in pharmaceutical applications (elastomers, thermoplastics) allow for comparatively high diffusivity of migrants [74, 85], chemical equilibrium can often be attained within the drug products shelf life. Here, thermodynamic partition equilibria dictate the level of leachables (partition-controlled scenario), with equilibrium concentrations described by a partition coefficient K_i [79, 86]. Leaching from a contact polymer was found essentially unaffected by the magnitude of the partition coefficient until approximately 60% of the leachable have migrated to the contact medium [87], which helps as a threshold to differentiate between partition- and diffusion-controlled migration scenarios described

above. A comparison of partition- and diffusion-controlled migration of leachables and an example of total extractable transfer are illustrated in Figure 5 for two identical products with different shelf lives.

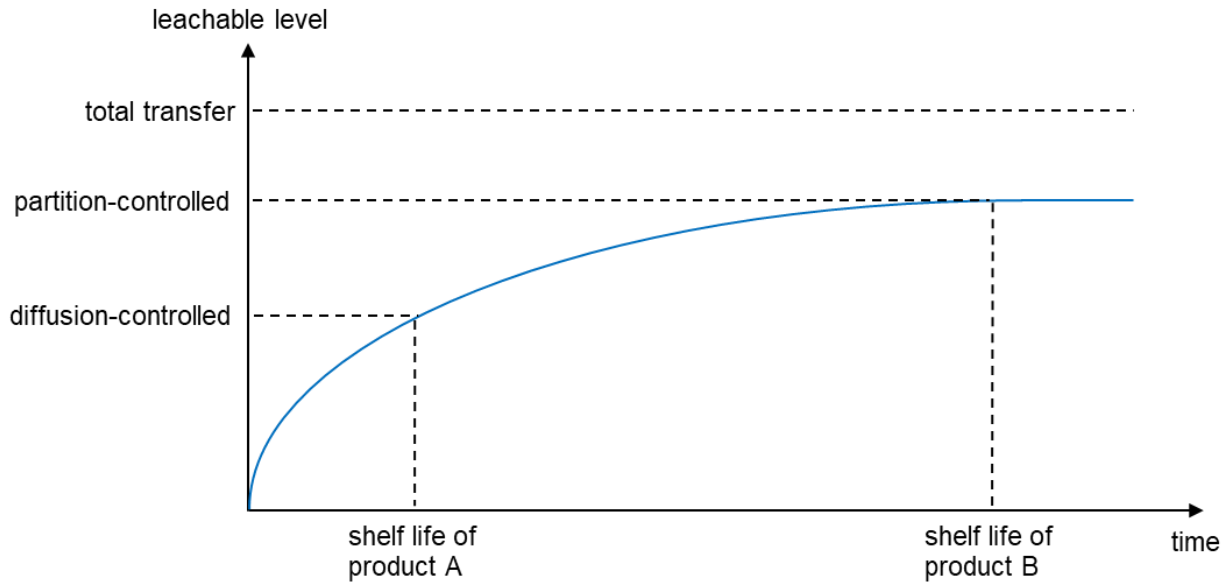

Figure 5. Migration of a leachable into two identical drug products with different shelf lives. Product shelf life determines whether migration is predominantly controlled by the diffusion (product A) or the partition coefficient (product B) of a leachable. Total transfer assumes complete migration of a leachable from the contact material to the drug product, i.e. a hypothetical, worst-case scenario where the partition equilibrium is disregarded.

The partition coefficient $K_{i,P/M}$ for a solute i between polymer (P) and contact medium (M), e.g. process stream, formulation, or bodily fluid, is established from differential concentrations (C) in both phases:

$$K_{i,P/M} = \frac{C_{i,P}}{C_{i,M}} \tag{2}$$

$$C_{i,M} = \frac{C_{i,P}^{0}}{\frac{V_M}{V_P} + K_{i,P/M}} \tag{3}$$

with V as the volume of the respective phase. If the partition coefficient $K_{i,P/M}$, phase ratio V_M/V_P and initial leachable concentration in polymer $C_{i,P}^{0}$ are established or can be predicted, the ultimate leachable concentration $C_{i,M}$ can be forecast. From the parameters in eq. (3), $K_{i,P/M}$ is a suitable physicochemical constant to model, as phase ratio and $C_{i,P}^{0}$ are unique to the system in question and must be determined individually. $K_{i,P/M}$, and any other partition coefficient discussed here, is understood to include both adsorption and absorption phenomena to each respective phase, while the subscript i signifies that the chemical is solvated in the surrounding phase. Conveniently, these solvated chemicals are also referred to as solutes. Figure 6 offers a comprehensible overview of the influence of $D_{i,P}$ and $K_{i,P/M}$ on migration of leachables from a polymer to a contact medium.

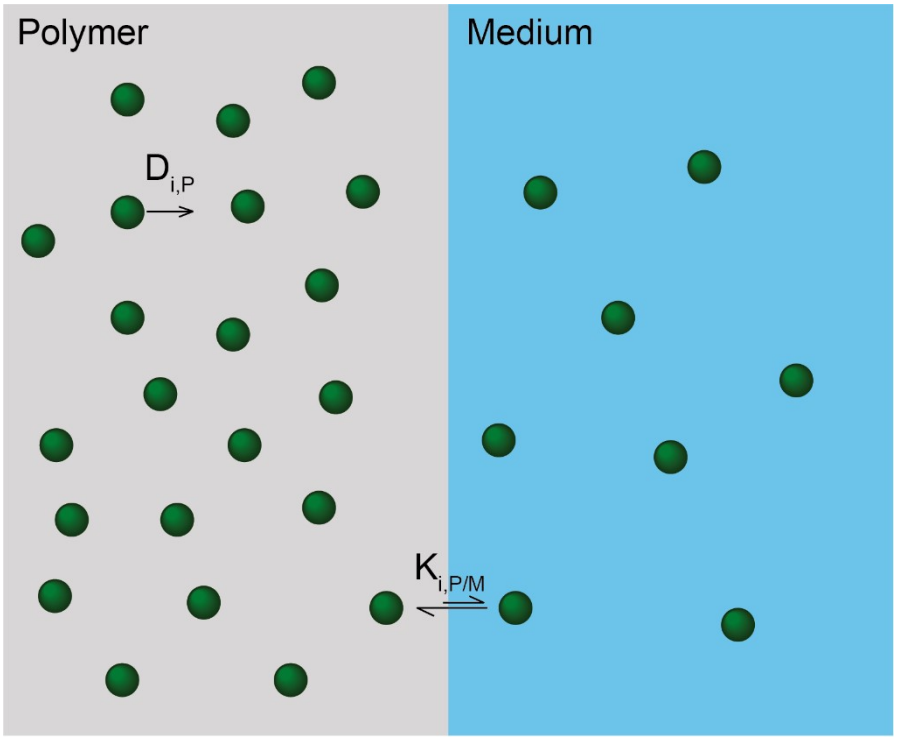

Figure 6. Migration of leachables from polymer to contact medium. Leachables (green circles) are initially only present in the polymer phase (left side). The mass flux of leachables proportional to $D_{i,P}$ towards the medium (right side) begins upon contact between the phases and ends when chemical equilibrium, as described by $K_{i,P/M}$, is reached.

Final leachable concentration in the clinically relevant medium $C_{i,M}$ is subject to its solubilization strength, described via differential limiting solubilities in aqueous medium ($S_{i,M}$) and pure water ($S_{i,W}$) and ideally expressed on a logarithmic scale. As limiting solubility and equilibrium concentrations are thermodynamically connected, a hypothetical partition coefficient can be constructed:

$$\log \frac{S_{i,M}}{S_{i,W}} \approx \log K_{i,M/W} \tag{4}$$

where $K_{i,M/W}$ is the hypothetical partition coefficient between medium and water. The expression of $K_{i,M/W}$ by the differential limiting solubilities is suitable as long as the activity coefficient of the solute at infinite dilution (γ_i^{∞}) is similar to that at saturation (γ_i^{sat}) [88], which implies that individual solutes interact only with the solvent and not with each other.
$\mathrm{Log}\, K_{i,M/W}$ affords an expedient way to establish $\log K_{i,P/M}$ via a thermodynamic cycle:

$$\log K_{i,P/M} = \log K_{i,P/W} - \log K_{i,M/W} \tag{5}$$

with $\log K_{i,P/W}$ as the logarithmic partition coefficient between a polymer and water. Since models for the prediction of $\log K_{i,P/W}$ can be retrieved from the literature [86, 89-91], eq. (5) can be implemented to avoid determination or prediction of $\log K_{i,P/M}$ for the many possible polymer-medium combinations encountered in chemical safety assessments.

While both diffusion and partition coefficients are necessary to establish time-dependent chemical migration, the equilibrium concentration, as described by the partition coefficient, defines a worst-case value for leachable accumulation in the clinically relevant drug product, as evidenced by Figure 5. Hence, within a risk-based approach, partition equilibria become decisive parameters to assess the criticality of polymer contact.

Both partition coefficients to and limiting solubilities in pharmaceutical solutions can be leveraged to infer the composition (i.e., alcohol content) of simulating solvents. As with medium solubilization strength, cosolvent mixture strength at a given alcohol volume fraction f_C can be calculated from the logarithm of differential limiting solubilities in the cosolvent-water mixture (S_{i,f_C}) and water:

$$\log \frac{S_{i,f_C}}{S_{i,W}} \approx \log K_{i,f_C/W} \tag{6}$$

where $\log K_{i,f_C/W}$ is the hypothetical logarithmic partition coefficient between the cosolvent-water mixture and pure water. Several model equations for calculation of the cosolvent mixture strength (or solubilization strength) of alcohol-water mixtures have been proposed [92-95]. A particularly practical, yet convenient approach to establish $\log K_{i,f_C/W}$ was presented by Abraham *et al.* for ethanol- and isopropanol-water mixtures in the form of linear solvation energy relationships (LSERs) [96, 97]. The premise of these model equations will be elucidated in Chapter 2.5.

Now, from a given medium solubilization strength $\log K_{i,M/W}$, adjusting the alcohol fraction f_C until $\log K_{i,M/W} \approx \log K_{i,f_C/W}$ yields a simulating solvent tailored towards a specific drug formulation, which usually also aligns their extraction strength towards a contacting material. However, some interactions between a contact solution and a polymer alter the extraction strength specifically without a change in solubilization. Depending on the polymer, solvents can permeate and therefore swell the matrix [98], while some of the pharmaceutical solution constituents have the potential to adsorb to the polymer surface [99]. Both processes may alter the extraction strength of the medium towards a contact polymer and need to be considered when extrapolating extraction strength from solubilization strength.

Figure 7 depicts an overview of simulating solvent alignment, i.e. the relation of medium solubilization and solvent strength as well as respective extraction strengths.

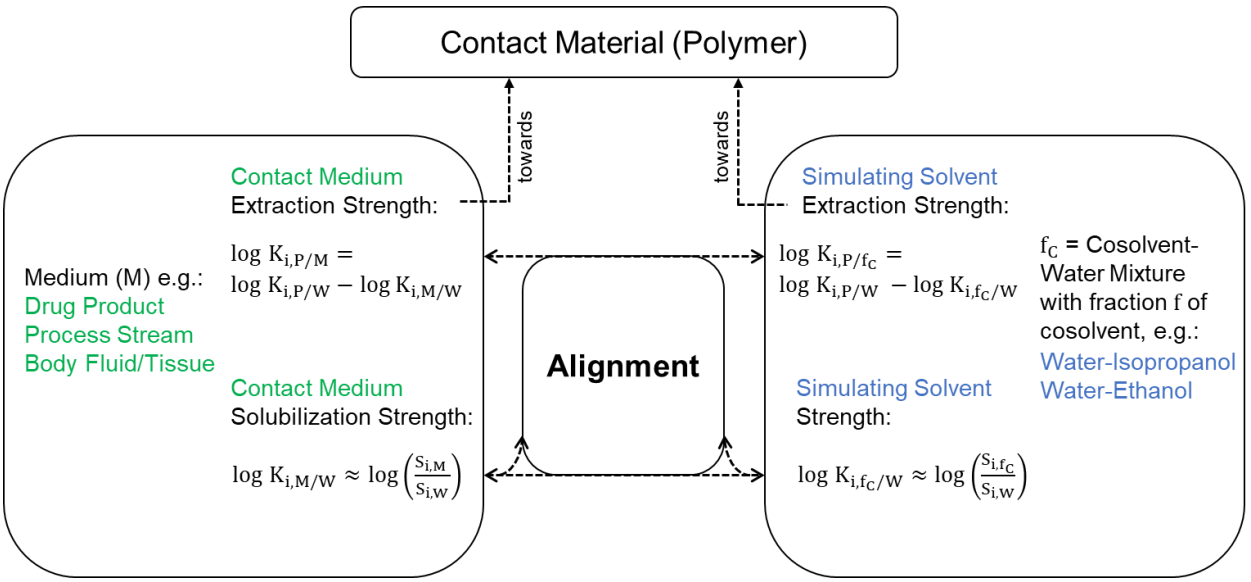

Figure 7. Quantitative description of medium, solvent, and extraction strengths and alignment of simulating solvents with the clinically relevant contact medium.

2.2 Solubilization Characteristics of Parenteral Excipients

Beyond their pharmaceutical purpose, excipients can modify the solubilization capacity of aqueous formulations. An increase in aqueous solubilization promotes leaching of chemicals from contact materials and thus needs quantitative understanding and characterization [100]. As elaborated above (1.1.3), a distinction between preparations of chemical and biological actives is unnecessary, as the aforementioned solubilization mechanisms exerted by excipients may be encountered in either of those preparations and solubilization is deemed unaffected by the API. When initially evaluating an aqueous pharmaceutical preparation for its solubilization propensity, the following questions have to be addressed for each excipient formulated:

1) Does this excipient influence solubilization of chemicals in water at the concentration it is formulated?
2) If so, can the effect be quantitatively described for individual chemicals by one or more equations based on the aqueous concentration of the excipient?
3) Are there any physicochemical models that allow prediction of the solubilization propensity of an aqueous solution of the excipient?
4) Are the input parameters for the model accessible and comprehensible (and thus suitable for mass transport modeling)?

If the excipient influences aqueous solubilization and the requirements stated in questions 2) – 4) can be fulfilled, the solubilization strength of an aqueous solution of the excipient can be quantitatively predicted. However, as many formulations are more complex and contain multiple excipients, alterations of the solubilization mechanisms are possible through interaction between the excipients [8]. In this case, it must be ascertained if and to what extent such interactions are possible. Solubilization in complex pharmaceutical formulations will be experimentally determined as part of this thesis (Chapter 4.3).
Below, the most critical solubilization mechanisms encountered in aqueous parenteral formulations, namely cosolvency, salting in/ out, cosolute-mediated solubilization, complexation,

and micellization, are discussed. It is attempted to answer the four question that were formulated above for commonly employed representatives from the different excipient classes.

Water-miscible cosolvents, such as short-chain alcohols (e.g. ethanol, polyethylene glycol, glycerol), are potent solubilizers in pharmaceutical applications. They break the strong hydrogen bonds between water molecules that are responsible for high solute cavity formation energies in solution [101]. Solubility of nonpolar and even many polar chemicals is increased as a result, depending on the fraction of cosolvent f_C in water [102]. Multiple quantitative cosolvent models have been successfully applied to calculate solubility as a function of f_C, including predictive models based on group contribution or quantum chemical theory and correlative models that utilize log-linear single parameter relations or (excess) free energy-related properties [94, 96]. Here, correlative models relying on chemical parameters are deemed more accessible and comprehensible to practitioners, for example in the field of E & L.

Antimicrobial preservatives (e.g. benzyl alcohol, 2-phenoxyethanol, parabens) are employed to preserve pharmaceutical preparations and multidose products in particular. In aqueous solution, some antimicrobials are also capable of solubilizing chemicals if present at sufficient concentrations [103]. A concentration dependent solubilization in water can be proposed for antimicrobials in the same manner as for cosolvents [104]. However, the antimicrobials listed above are not fully water-miscible like cosolvents. In the context of this work, partially water-miscible organic excipients influencing solubilization will be referred to as cosolutes instead. As these antimicrobials are typically not considered solubilizers in aqueous media, a quantitative description of their solubilizing properties in water and suitable solubilization models have yet to be presented.

Physiological salts and sugars establish required tonicity in parenteral formulations, with sodium chloride (NaCl) and D-glucose (dextrose) as frequently used excipients. Dissociated salts like NaCl modify structuring in water, thereby influencing water solubility ($S_{i,W}$) of nonelectrolytes, commonly referred to as salting in/ out, depending on whether S_i is in- or decreased [105, 106]. The influence of individual electrolytes on aqueous solubility is quantified via the Setschenow equation:

$$\log \frac{S_{i,W}}{S_{i,Salt}} = C_{Salt}\, k_{i,S} \tag{7}$$

where $S_{i,Salt}$ is the solubility of the chemical in the electrolyte solution, C_{Salt} is the concentration of the electrolyte in mol L^{-1} and $k_{i,S}$ (L mol^{-1}) is the Setschenow or salting constant (positive for salting out and negative for salting in). Experimental Setschenow constants can be retrieved from the literature for many hydrophobic chemicals in different aqueous electrolyte solutions [107, 108]. For the same chemical, the salting effect of electrolytes can be ranked in a series according to Hofmeister [109], who initially devised a series of electrolyte solutions according to the precipitation tendency of proteins. In the series, ions with high charge densities (i.e., smaller anions and cations) typically cause salting-out of chemicals, while ions with low charge densities (large anions and cations with low charge) can even increase chemical solubility (salting-in) [110]. In comparison to other salts, sodium chloride displays a minor salting-out effect. A highly accurate predictive model estimating the Setschenow constant $k_{i,S}$ for chemicals in NaCl solutions has been presented [111], enabling the calculation of solubilization strength of aqueous NaCl solutions from experimental parameters.

While solubilization of chemicals is affected by sugars in aqueous solutions, no clear classification of their solubilizing mechanism has been presented so far. The terms “cosolvency” [112, 113], “salting in/ out” [114] and “sugaring in/ out” [115] have been proposed in the literature. According to the nomenclature introduced above for antimicrobial preservatives, the term cosolute is most

appropriate in the context of this work. The solubilizing effect of highly water-soluble sugars like dextrose is best explained by their own solubilization in water. Like ionic species, sugars bind solvating water molecules which are then no longer available to other solutes [113, 116, 117]. However, a reverse trend leading to increased solubility can be observed at higher sugar concentrations for some solutes, depending on the sugar in solution [112]. Solubilization in highly concentrated sugar solutions is similar to solubilization in cosolvent-water mixtures [118], where weaker intermolecular bonding of solvent molecules facilitates cavity formation in solution. As individual sugars can in- or decrease solubility of chemicals, no simple relationship between sugar concentration and solubilization comparable to the Setschenow equation can be established [114, 115, 119]. Simple solubilization modeling of a limited number of solutes in sugar solutions has been carried out [120, 121], but no model that enables solubilization prediction for a larger chemical domain has been reported so far.

Complexing agents are employed in parenteral formulations to bind ligands through molecular interactions and dramatically increase their solubility in water [122]. The equilibrium of formation for a 1:1 complex between the complexing agent and a solute molecule is formally indicated by the formation constant K_i, analogous to partition coefficients introduced previously. Complexation is utilized in parenteral delivery of hydrophobic small molecule drugs. Water-soluble cyclic glucose oligomers (cyclodextrins) offer cavities in which organic molecules can be included to promote bioavailability, stability or aqueous solubility [123]. Desired properties of cyclodextrins are achieved by varying the number of glucose units or through chemical modification of the hydroxyl units [124].

Specific complexation of ions (chelation) sees widespread use in pharmaceutical formulations to capture metal ions that promote undesired oxidation, typically with a salt of ethylenediaminetetraacetic acid (EDTA) as the chelating agent of choice [10]. As EDTA forms highly stable complexes with divalent cations ($\log K_i \geq 10$) [125], the extent of ion complexation depends solely on EDTA concentration. No effect on solubilization of organic solutes is expected when EDTA is formulated since it preferably chelates inorganic metal cations.

Finally, surfactants solubilize chemicals within micelles formed by multiple aggregated surfactant molecules. Surfactant mediated solubilization warrants a separate, in-depth discussion of the mechanistic principles surrounding micellar aggregation and approaches to model solubilization in surfactant solutions, which follows in the subsections below.

Typical excipients and their concentrations encountered in aqueous parenteral formulations, their pharmaceutical purpose and solubilization mechanism are compiled in Table 3 [61-64, 122, 126]. In this selection of excipients, the principle constituent classes are represented to allow a categorized inspection of their solubilization mechanisms.

Table 3. Typical parenteral excipients, common concentration(s), purpose, and solubilization mechanism in a formulation.

Excipient	Common concentration(s) (%[a)])	Pharmaceutical Purpose	Solubilization mechanism
Polysorbate 80	0.01, 0.1, 0.5	Solubilization Stability	Micellization
Ethanol	10	Solubilization	Cosolvency
Benzyl alcohol	1.5	Microbial preservation	Cosolute
Sodium chloride	0.9	Tonicity	Salting in/ out
Disodium EDTA	0.11	Stability	Complexation
Dextrose	5	Tonicity, lyophilization protectant, bulking agent	Cosolute

a) w/v, except for ethanol (v/v).

2.3 Surfactants

Surfactants (surface-active agents) are amphiphilic molecules whose distinct properties allow them to be used in many fields including separation processes in industry and environmental remediation, food processing, and pharmaceutical industry [127-131]. They can be categorized based on their overall ionization as anionic (e.g. sodium dodecyl sulfate), cationic (e.g. cetyltrimethylammonium bromide), zwitterionic (e.g. phospholipids) and nonionic (e.g. polysorbates) surfactants. Nonionic surfactants are particularly favored in parenteral applications for their high tolerability [10]. They increase aqueous solubility of small molecule drugs through incorporation into micelles [65] or stabilize biopharmaceuticals by reducing aggregation of proteins [132].

Containing both strongly hydrophilic and hydrophobic moieties in a single molecule, surfactants exhibit particular behavior in solution. They generally show strong solubilization of organic compounds when the critical micelle concentration (CMC) is exceeded [133]. Beyond this concentration, micellar aggregates of multiple surfactant monomers form as a separate pseudophase in water, with a hydrophilic shell of polar surfactant head groups surrounding a hydrophobic core of nonpolar surfactant tails [134]. The solubilizing effect of surfactants is usually attributed to the formation of micelles [135], and the sudden increase of solubilization can indeed be utilized to find the CMC [136]. Nonetheless, solubilization of very hydrophobic chemicals below the CMC through pre-micellar surfactant aggregation has been determined [137].

The micellar core, shell, and interfacial region between core and shell are all capable of solubilization, and solutes are solubilized in either of those regions according to molecular interactions (e.g., nonpolar alkanes towards the micellar core region) [138, 139]. As a result, solubility enhancement of organic chemicals in aqueous surfactant solution past the CMC can be observed macroscopically compared to pure water.

The macroscopic effect of surfactant mediated solubilization can be represented by a hypothetical partition coefficient based on the differential equilibrium solubilities in a solution with a weight-based fraction f of surfactant and in water, in line with the construction of partition coefficients between cosolvent-water mixtures and water [88]:

$$K_{i,f_{Surf}/W} \approx \frac{S_{i,f_{Surf}}}{S_{i,W}} \quad (8)$$

Micellar solubilization in water can further be thermodynamically characterized by means of a partition coefficient between the micellar phase (Mic) and water, i.e. relating equilibrium concentrations in the micelle and the adjacent water phase, on either a mole fraction or molar scale:

$$K^{X}_{i,Mic/W} = \frac{X_{i,Mic}}{X_{i,W}} \quad (9)$$

$$K_{i,Mic/W} = \frac{C_{i,Mic}}{C_{i,W}} \quad (10)$$

$$K^{X}_{i,Mic/W} = K_{i,Mic/W} \frac{\overline{V}_{Mic}}{\overline{V}_{W}} \quad (11)$$

with $K^{X}_{i,Mic/W}$ and $K_{i,Mic/W}$ as mole fraction and molar partition coefficient, $X_{i,Mic}$ and $X_{i,W}$ as micellar and aqueous mole fraction, $C_{i,Mic}$ and $C_{i,W}$ as the concentration in micellar and aqueous phase, $\overline{V}_{Mic}$ and $\overline{V}_{W}$ as molar volume of micellized surfactant and water, respectively [140]. Unlike $K_{i,f_{Surf}/W}$, $K_{i,Mic/W}$ is independent of surfactant concentration and can be utilized to ascertain solute affinity towards the micellar phase. $K_{i,Mic/W}$ quantitatively relates to $K_{i,f_{Surf}/W}$ by the volumetric fraction of micellized surfactant in solution, $f_{Surf(Mic)}$:

$$K_{i,Mic/W} = \frac{K_{i,f_{Surf}/W} - f_{W}}{f_{Surf(Mic)}} \quad (12)$$

$$f_{Surf(Mic)} = C_{Surf(Mic)}\,\overline{V}_{Surf(Mic)} \;\; ; \;\; f_{W} = 1 - f_{Surf(Mic)} \quad (13a; b)$$

with f_{W} as the volumetric fraction of water and $C_{Surf(Mic)}$ as the concentration of micellized surfactant, which is equal to the total concentration of surfactant minus its CMC. Figure 8 shows a cross-section through an assembled micelle with three solutes of different polarity solvated in the micellar environment.

While partitioning commonly describes the phase transfer of a chemical between two distinct phases, partitioning between micelles and water is a special case. Micelles are non-homogenous in size, fully solvated in and saturated with water, and finely dispersed in the surrounding aqueous phase [134]. Therefore, “pseudophase” is an expedient term to describe micelles in aqueous solution.

In addition to micellar solubilization, surfactants interact with contact materials by adsorption to the materials surface. Permeation of chemicals from surfactant solutions through polymers into an acceptor solution was shown to be slowed by surfactants interacting with migrants at the polymer surface [99]. Reduced migration kinetics could therefore also be observed between a two-phase system of polymer and surfactant solution, e.g. when chemicals leach from contact polymers to pharmaceutical solutions containing surfactants during storage of a drug product, in comparison to surfactant-free contact solutions.

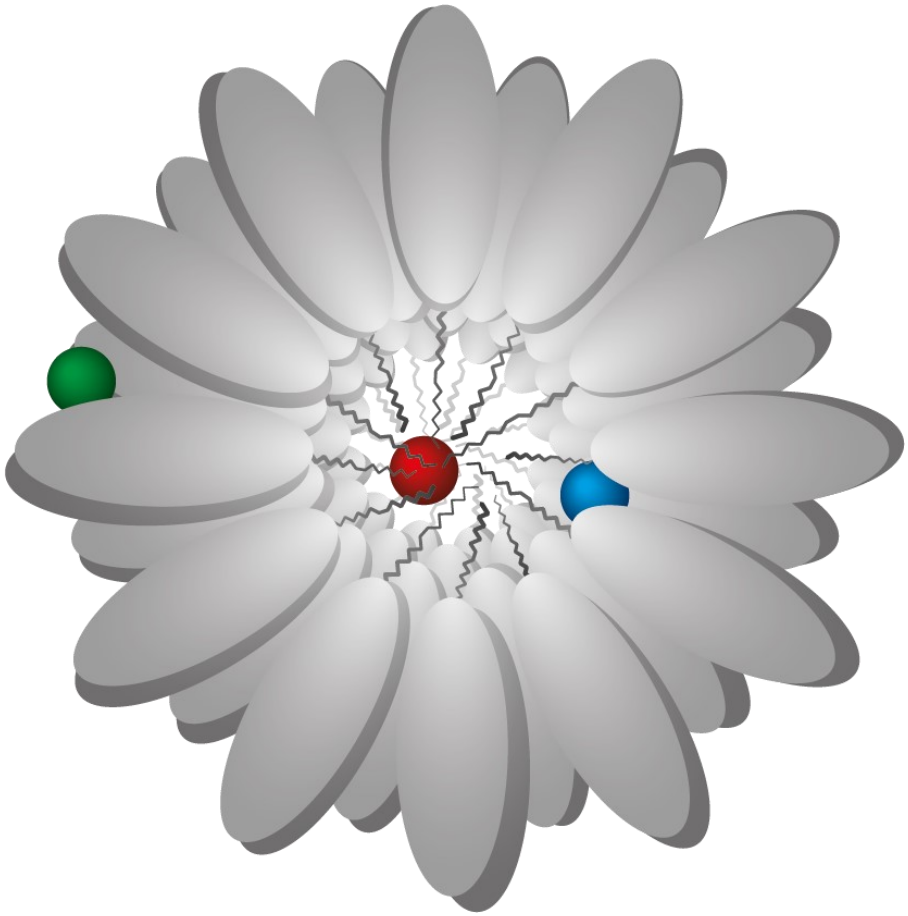

Figure 8. Three-layer cross-section through a globular micelle in water loaded with different solutes. The outer ellipses are the polar parts of individual surfactant molecules, while the nonpolar tails of surfactant molecules point inwards. Inside the micelle, the red sphere represents a solute solvated in the nonpolar micellar core region, where van-der-Waals interactions are predominant. The blue sphere represents a solute solvated in the interfacial region between micelle core and head region, and the green sphere represents a solute solvated in the polar region of the micelle close to its exterior, where hydrogen-bonding interactions are more prevalent.

2.3.1 Polysorbate 80

Polysorbate 80 (polyoxyethylene (20) sorbitan monooleate, PS 80) is an ester of polyethoxylated sorbitan and oleic acid. It is one of the most frequently formulated parenteral excipients, used in both chemical and biological preparations of active pharmaceutical ingredients [11, 61, 141].
The hydrophobic-lipophilic balance (HLB) is a scale for hydrophobicity of surfactant molecules, where surfactants are ordered from 0 (entirely hydrophobic) to 20 (entirely hydrophilic) [142]. For PS 80, this value is 15, indicating a largely hydrophilic surfactant molecule with a comparatively small hydrophobic hydrocarbon tail. In fact, PS 80s micelle core region only contributes 2.4% to the total micellar volume [143].
Commercially available, compendial-grade PS 80 products are multi component mixtures, with the aforementioned ester polyoxyethylene (20) sorbitan monooleate as a lead structure [144] (Figure 9). Hundreds of chemical structures relating to the lead structure can be found in a PS 80 product, originating from the presence of different fatty acids, varying degrees and sites of ethoxylation,

and degradation products from hydrolysis or oxidation [145-147]. Pharmacopeial monographs consequently define minimum and maximum fatty acid fractions permitted in compendial PS 80 products, which are presented in Table 4.

Both hydrolysis and autoxidation of the PS 80 molecule can impact micellar partitioning behavior of chemicals to PS 80 micelles [148], with hydrolysis generating degradation products with varying characteristics and autoxidation potentially influencing the solubilization characteristics of the unsaturated hydrocarbon core through altered molecular interactions [149]. Whether differences in PS 80 product composition impact its solubilization characteristics is therefore of interest for formulation scientists and E & L practitioners alike.

The effect of PS 80 on leaching of chemicals from plastic materials has recently been investigated [5, 7, 8, 150]. The specific solubilization characteristics of PS 80 were mimicked by cosolvent-water mixtures, such as ethanol- and isopropanol-water mixtures, exploring possible configurations of simulating solvents for pharmaceutical solutions. Nonetheless, no attempt has been made towards a general and quantitative model for PS 80 solubilization in aqueous solution, incorporating all relevant molecular solute-micelle interactions.

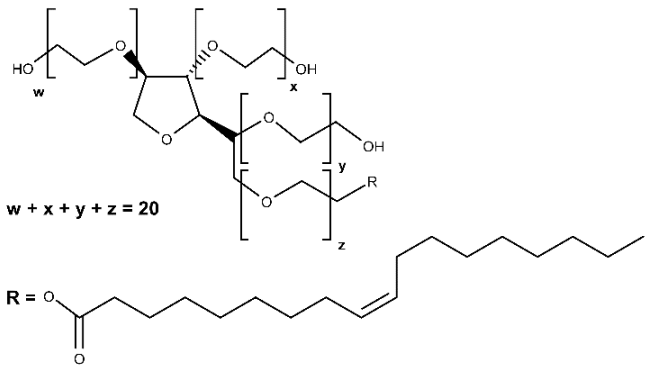

Figure 9. Polysorbate 80 lead structure.

Table 4. Boundary fatty acid fractions in polysorbate 80 products, according to Ph.Eur. and USP monographs.

Fatty acid	Content limit PS 80
Myristic acid	< 5%
Palmitic acid	< 16%
Palmitoleic acid	< 8%
Stearic acid	< 6%
Oleic acid	> 58%
Linoleic acid	< 18%
Linolenic acid	< 4%

Table 5. Parameters of polysorbate 80 and its micelles in aqueous solution. Values of choice for this work are written in bold text, where applicable.

M[a] (g mol^{-1})	CMC (mM)	$\bar{V}_{PS80(Mic)}$[b] (L mol^{-1})	n_{agg}[c]
1309.66	**0.012** [151]	**1.173** [153]	46-66[d] [153]
	0.011 [152]	1.183 [154]	120[e] [156]
		1.198 [155]	45.7[f] [157]

a) Molar mass
b) Molar volume of micellized PS 80
c) Aggregation number
d) 25°C, 1.00% w/v
e) 25°C, 0.13% w/v
f) 22°C, 0.20% w/v

2.4 Predictive Models for Micellar Partitioning

A model that relates partitioning of solutes between micelles and water is indispensable to quantitatively characterize solubilization in solutions containing surfactants like PS 80. Several approaches allow estimation of partitioning between or solubility in gaseous, liquid, and solid phases or pseudophases [158-162]. Solute partitioning can be forecast based on single physicochemical solute parameters, e.g. the octanol-water partition coefficient $\log K_{i,Octanol/Water}$ ($\log K_{i,O/W}$). $\mathrm{Log}\ K_{i,O/W}$, also often denoted as $\log P$ in the literature, is one of the most utilized experimental physicochemical parameters to scale hydrophobicity of organic chemicals [163]. Log-linear equations constructed from $\log K_{i,O/W}$ can be retrieved for many biphasic partition systems, including PS 80 micelles to water [164]. Nonetheless, estimations based solely on $\log K_{i,O/W}$ can be unreliable, as the system cannot fully characterize all molecular interactions between a given solute-solvent pair [161].

More recently, first principle atomistic methodologies have been applied to partitioning between micelles and water. Fundamental approaches like COSMO-RS (Conductor-like Screening Model for Realistic Solvation) or UNIFAC (Universal Quasichemical Functional Group Activity Coefficients) relate molecular information, such as surface area, surface charge, group contributions, or volume to thermodynamic parameters (chemical potential or activity). Both methods allow an ab initio prediction that does not rely on specific experimental data, e.g. $\log K_{i,O/W}$. COSMO-RS and UNIFAC were utilized to calculate partitioning of nonionic solutes from water to ionic sodium dodecyl sulfate (SDS) and nonionic Triton X-100 micelles [165]. For ionizable solutes, COSMO-RS was used to successfully model partitioning between nonionic surfactant micelles and water at various pH values [166]. Furthermore, a combination of COSMO-RS and molecular dynamics termed COSMOmic (COSMO-RS for micelles) can simulate specific structural properties of micelles (i.e., the anisotropic spacial orientation of polar shell and nonpolar core regions) and chemical potential of solutes therein, improving partition projections [167, 168].

Still, ab initio models require expert knowledge for efficient use, making them inappropriate for broad application under regulatory aspects in the context of E & L. A more practical and robust approach for practitioners in the field of E & L are linear solvation energy relationships (LSERs). LSERs are semi-empirical equations connecting free energy related parameters, such as K_i, to physicochemical properties of solvents and solutes [169]. They have been used in various scientific fields [170] and provide accurate estimations in their domain of applicability.

2.5 Construction and Application of Linear Solvation Energy Relationships (LSERs)

Abraham-type linear solvation energy relationships (LSERs) are among the most widely accepted and robust models used to predict partition coefficients of organic compounds between two homogenous phases [171]. Using experimentally calibrated solute descriptors specific to a molecule, the potential physicochemical interactions of solutes and surrounding solvent phases can be quantitatively described with the LSER equation:

$$\log K_i = eE_i + sS_i + aA_i + bB_i^0 + vV_i + c \quad (14)$$

Solute descriptors (capitals in eq. (14)) carry chemical meaning, with $\mathbf{E_i}$ as the excess molar refraction, $\mathbf{S_i}$ as the dipolarity/ polarizability, $\mathbf{A_i}$ and $\mathbf{B_i^0}$ as the hydrogen bond acidity and basicity, respectively, and $\mathbf{V_i}$ as the scaled molecular volume according to McGowan. The $\mathbf{B_i^0}$ descriptor replaces the $\mathbf{B_i}$ descriptor for applications where the organic phase contains water (e.g., micelles), thus affecting hydrogen bonding interactions of solutes with hydrogen accepting moieties in the organic phase and varies from the ordinary B_i descriptor for few compounds, including anilines. Scaling of solute descriptors is adjusted to span a similar numerical range for the descriptors of most chemicals. Saturated hydrocarbons serve as a reference for solute descriptors and have their E_i, S_i, A_i and B_i^0 descriptors set to zero by default. The system parameters (lower case letters in eq. (14)) $\mathbf{e}$, $\mathbf{s}$, $\mathbf{a}$, $\mathbf{b}$, $\mathbf{v}$ and $\mathbf{c}$ are complementary fitting parameters determined via multiple linear regression for individual two-phase systems [172]. LSER equation (14) is, in principle, applicable to all non-ionized, small molecule solutes. A graphical abstract of the regression of an LSER model is provided in Figure 10.

The quality of solute descriptors is vital for the accuracy of the predicted $\log K_i$. E_i, S_i, A_i, and B_i^0 themselves rely on accurately determined experimental data. Few chemical classes have been shown to be poorly predictable using available LSER solute descriptors, including siloxanes [173], which can be identified as leachable substances from polydimethyl siloxane elastomers used in pharmaceutical processes and packaging [174]. If no experimentally determined set of solute descriptors is available for a solute, calculation of descriptors with quantitative structure-activity relationship (QSAR) software tools is possible [175]. The QSAR predicted descriptors are currently far less precise than experimentally determined descriptors [176], therefore introducing larger errors in the calculation of $\log K_i$.

A recently introduced approach could overcome the necessity for experimental determination of LSER molecular descriptors. Termed partial solvation parameters (PSPs), it is based on classical Hansen solubility parameters (HSPs) [177], which define the cohesive energy density in a material through molecular dispersion, polarity, and hydrogen bonding. PSPs share several similarities with the LSER system [178]. Just like LSER descriptors, PSPs have chemical meaning, but can be independently calculated via different routes, with physicochemical information stemming from e.g. COSMO-RS or existing LSER descriptors from eq. (14) [179, 180]. Unlike the LSER approach, solubilization and partition predictions from PSPs have not been extensively utilized, but show promising results for pharmaceutically relevant systems [181], and are of great interest considering their potential to rationalize molecular descriptors in the future.

The chemical domain of LSER partitioning models is restricted by the capabilities to accurately determine $\log K_i$. A precise measurement of small solute concentrations or mole fractions can be difficult, depending on the chemical nature of solute and surrounding phase. For example, large errors are encountered when the aqueous concentration of very hydrophobic organic chemicals

(VHOCs) in water to organic phase partitioning is measured, as the equilibrium concentration of the solute in water is extremely low due to sparse aqueous solubility of VHOCs [176]. Moreover, VHOCs adsorb to laboratory equipment like glassware when solvated in water, reducing the freely dissolved and analytically obtainable chemical concentration [182]. In this scenario, partitioning is erroneously observed as a two-phase thermodynamic process, although it occurs between three phases (water, organic phase, and glassware) that all have ad- or absorbed relevant amounts of the solute. In consideration of the difficulties associated with experimental determination of certain partition coefficients and solute descriptors, it is imperative to review and, where necessary, exclude any inaccurate experimental data from LSER regressions to retain model precision.

Partitioning of solutes between two coherent phases is typically measured by equilibrating both phases and then sampling each phase individually to determine respective solute concentrations [183]. In contrast to coherent liquid or solid phases, the micellar pseudophase is not directly accessible for in situ sampling as it is colloidally dispersed in the aqueous phase. Various methods of determination have been used successfully to mitigate this circumstance by ascertaining the concentration ratio of a solute between the phases.

In a reference phase approach, solute concentration in micelles is indirectly inferred from a third phase in contact with either a surfactant solution or water [184, 185]. Since some molecules partition to micelles, solute accumulation in the reference phase is reduced when in contact to surfactant solutions in comparison to water. From the resulting difference, a partition coefficient between micelles and water can be established. Other methods are based on liquid chromatography with micellar solutions as eluents. In micellar liquid chromatography (MLC), the analyte interacts with both stationary phase and surfactant micelles present in the mobile phase. Here, strong interactions with micelles lead to faster elution of the analyte [186]. Micellar electrokinetic chromatography (MEKC) is a modified capillary electrophoresis method based on electrokinetic migration of charged micelles along an electroosmotic flow [187]. Again, partitioning of nonionic solutes to the charged micelles increases solute velocity inside the capillary. MEKC is, however, limited to the use of charged surfactants that are entrained by the electroosmotic flow. In both methods, micelle partitioning of analytes can be inferred from their retention time.

To obtain a LSER model equation for micellar partitioning with broad applicability, it is helpful to broaden the chemical diversity of compounds for model calibration, by both choice of suitable chemicals for experimental determination and inclusion of literature data. Many studies published in the literature report differential solubilities in surfactant solution and water [140]. With aqueous equilibrium solubility $S_{i,W}$ and solubility in surfactant solution $S_{i,f_{Surf}}$, the hypothetical partition coefficient $K_{i,f_{Surf}/W}$ between surfactant solution and water can be established according to eq. (8) and converted to the micelle-water partition coefficient $K_{i,Mic/W}$ with eqs. (12) and (13).

LSER equations have been reported for ionic SDS [188, 189] and cetyltrimethylammonium bromide (CTAB) [187] micelle to water partitioning, as well as fasted state simulated intestinal fluid, which contains biological surfactants that form micelles [190]. The studies demonstrated that model equations for micelle to water partitioning can be constructed with acceptable predictability.

As no such model has yet been published for the frequently formulated excipient PS 80, establishing a quantitative LSER model from experimental data on PS 80 micelle to water partitioning ($\log K_{i,PS80/W}$) is a central objective of this work. Solubilization of chemicals at a given PS 80 concentration can be foreseen with the presented equations and predictions of $\log K_{i,PS80/W}$.

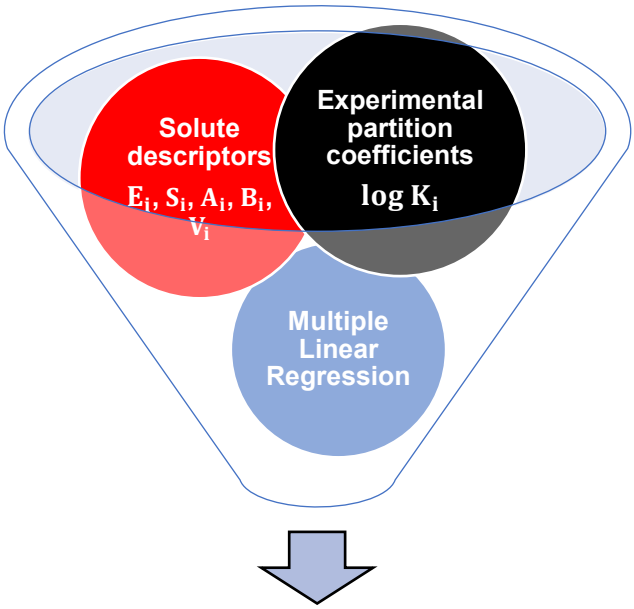

Figure 10. Graphical abstract of LSER model construction.

3. Materials and Methods

3.1 Materials

Chemicals were commercially sourced from various vendors, with a minimum purity of 97%. PS 80 was of compendial grade unless noted otherwise. The chemicals were used without further purification. Water for all experiments was passed through a Milli-Q A10 Ultrapure Water Purification System (Millipore, Eschborn, Germany).
Low density polyethylene (LDPE) sheets (200 µm thickness) were obtained from Polifilm Extrusion GmbH (Weißandt-Gölzau, Germany). Polydimethyl siloxane (PDMS) sheets (800 µm thickness) were sourced from CS Hyde (Lake Villa, IL).
A list of all solutes, their LSER descriptors, and general chemical information can be found in the appendix (Table A1).

3.2 Methods

The following experimental procedures were carried out in triplicate and average results reported. Experimental logarithmic octanol-water partition coefficients ($\log K_{i,O/W}$) were retrieved from the EPI Suite™ program, version 4.11, U.S. Environmental Protection Agency, Washington, D.C. Statistical analysis and multiple linear regression for LSER equations were carried out with GraphPad Prism, version 9.0.0, GraphPad Software, San Diego, California.

3.2.1 Polysorbate 80 Micelle to Water LSER Partition Model

For experimental determination of logarithmic partition coefficients $\log K_{i,PS80/W}$ that were included in the LSER model regression, two different experimental methods were employed, based on the volatility of solutes. For sufficiently volatile solutes (volatile organic chemicals, VOC), the headspace of a sample vial served as a reference phase for solute partitioning measurements. For the remaining non-volatile solutes (non-volatile organic chemicals, NVOC), LDPE strips were chosen to serve as a reference phase. Only compounds with experimental LSER substance descriptors available (see Table A1 and Table A2) were included to avoid introduction of errors associated with QSAR prediction of substance descriptors.

Table 6. Preparation scheme for reference phase partitioning samples.

Batch		Nominal amount spiked per solute (µg)	Volume reference phase[c] (mL)	Volume solution (mL)	PS 80 concentration (% w/v)	Sample preparation	Analysis	Test solute $\log K_{i,O/W}$[e] range
VOC[a]	1	200	17	5	10, 15	none	HS-GC/MS	0.5-2.7
VOC	2	25	17	5	5, 10, 15, 20	none	HS-GC/MS	0.9-3.3
VOC	3	10	17	5	1, 2	none	HS-GC/MS	2.6-4.5
VOC	4	10	17	5	1, 2	none	HS-GC/MS	2.5-4.0
VOC	5	2.5	17	5	1, 2	none	HS-GC/MS	4.1-4.9
VOC	6	2.5	17	5	1, 2	none	HS-GC/MS	3.4-6.1
NVOC[b]	1	100	0.5	4	4, 8	Ex. Acetone[d]	LC/UV	0.9-3.0
NVOC	2	100	0.5	4	1, 2	Ex. Acetone	LC/UV	1.7-3.1
NVOC	3	40	0.5	4	1, 2	Ex. Acetone	LC/UV	2.0-3.4
NVOC	4	40	0.5	40	1, 2	Ex. Acetone	LC/UV	3.3-4.6

a) Volatile organic chemicals (applied in headspace method).
b) Non-volatile organic chemicals (applied in polymer method).
c) For VOC: reference phase air/ headspace, for NVOC: reference phase LDPE.
d) Extraction of LDPE with acetone (72 h, 40°C, 150 rpm orbital shaker).
e) Logarithmic octanol water partition coefficient retrieved from EPI Suite™ v4.11.

3.2.1.1 Headspace Reference Phase Partitioning

Determination of $K_{i,PS80/W}$ for volatile solutes as input for the LSER model regression was carried out by means of batch equilibrium partition experiments. Aqueous polysorbate 80 solutions at multiple concentrations (two at a minimum) were prepared by weighing the appropriate amount of surfactant in a volumetric flask, addition of approximately half of the water required, dissolution of polysorbate using a magnetic stir bar, and making up to the desired volume. PS 80 solutions were stored at 8°C in amber glass vials for up to one month. 22 mL headspace vials were filled with 5 mL of either water or polysorbate 80 solutions, see Table 6. Spike solutions of chemical compound batches were prepared in LC gradient grade methanol (Merck Millipore). From those spike solutions, serial dilutions serving as calibration standards for GC measurements were prepared in dimethyl formamide (Merck Millipore). Solutes were introduced by adding 5 µL of the respective methanolic spike solutions. The low volume of methanol ensured no interaction with both headspace and micelle partitioning from water, as well as micelle formation in water. The resulting concentrations of the solutes were well below the aqueous solubility limit of each solute.

After spiking, vials were tightly closed with 20 mm polytetrafluoroethylene (PTFE)/ silicone septa aluminum crimp caps (Klaus Ziemer GmbH, Langerwehe, Germany).
Headspace vials were shaken on an orbital shaker set to 150 rpm (IKA KS 501 digital, IKA, Germany) at 25°C for at least 2 hours to achieve equilibrium between water, headspace, and micelles (if present). Equilibration time was determined by sampling the headspace of fresh vials in 30 minute intervals until subsequent measured peak areas were constant.
After equilibration, the headspace of the vials was analyzed at 25°C in a HS-GC/MS coupled system and the peak area of the respective solutes were recorded. Details on the HS-GC/MS measurement are reported in the appendix (Table A3).
Under the mass balance assumption for a vial containing only water and a solute (i), the following applies:

$$\mathrm{m_{i,tot}} = \mathrm{m_{i,W}} + \mathrm{m_{i,Air}} \tag{15}$$

with $\mathrm{m_i}$ as the mass of solute in either water (W) or the headspace above (Air) and $\mathrm{m_{i,tot}}$ equal to the initial amount of solutes introduced to the vial with the spike solution.
The partition coefficient $\mathrm{K_{i,W/Air}}$ represents equilibrium distribution between water and air in the vial:

$$\mathrm{K_{i,W/Air}} = \frac{\mathrm{C_{i,W}}}{\mathrm{C_{i,Air}}} = \frac{\mathrm{m_{i,W}}\ \mathrm{V_{Air}}}{\mathrm{m_{i,Air}}\ \mathrm{V_W}} \tag{16}$$

with $\mathrm{C_i}$ as concentration in either water or air and V as respective volume of each phase.
Inserting eq. (16) in eq. (15) and solving for $\mathrm{C_{i,Air}}$ gives:

$$\mathrm{C_{i,Air(W)}} = \frac{\mathrm{m_{i,tot(W)}}}{\mathrm{V_{Air(W)}} + \mathrm{V_W}\ \mathrm{K_{i,W/Air}}} \tag{17}$$

for a vial with pure water, which similarly applies to vials containing a PS 80 solution $(\mathrm{PS80})$ instead:

$$\mathrm{C_{i,Air(PS80)}} = \frac{\mathrm{m_{i,tot(PS80)}}}{\mathrm{V_{Air(PS80)}} + \mathrm{V_{PS80}}\ \mathrm{K_{i,f_{PS80}/Air}}} \tag{18}$$

with $\mathrm{K_{i,f_{PS80}/Air}}$ as the surfactant solution to air partition coefficient and $\mathrm{V_{PS80}}$ as the volume of surfactant solution.
Headspace concentration above either water or surfactant solution is then proportional to the chromatographic peak area A with the chromatographic response factor r constituting the proportionality constant:

$$\mathrm{A_{i,W}} = \mathrm{r}\ \mathrm{C_{i,Air(W)}}\ ;\ \mathrm{A_{i,f_{PS80}}} = \mathrm{r}\ \mathrm{C_{i,Air(PS80)}} \tag{19a; b}$$

If the chromatographic response is linear in the concentration range studied, r is equal in eqs. (19a; b). Inserting eqs. (19a; b) in eqs. (17) and (18), cancelling out r, yields:

$$\frac{\mathrm{A_{i,f_{PS80}}}}{\mathrm{A_{i,W}}} = \frac{\mathrm{m_{i,tot(PS80)}}\left(\mathrm{V_{Air(W)}} + \mathrm{V_W}\ \mathrm{K_{W/Air}}\right)}{\mathrm{m_{i,tot(W)}}\left(\mathrm{V_{Air(PS80)}} + \mathrm{V_{PS80}}\ \mathrm{K_{f_{PS80}/Air}}\right)} \tag{20}$$

After rearrangement:

$$K_{i,f_{PS80}/Air} = \frac{A_{i,W}}{A_{i,f_{PS80}}} \frac{m_{i,tot(PS80)}}{m_{i,tot(W)}} \left(\frac{V_{Air(W)}}{V_{PS80}} + \frac{V_W K_{i,W/Air}}{V_{PS80}} \right) - \frac{V_{Air}}{V_{PS80}} \quad (21)$$

Division by the water to air partition coefficient $K_{i,W/Air}$ leads to:

$$K_{i,f_{PS80}/W} = \frac{A_{i,W}}{A_{i,f_{PS80}}} \frac{m_{i,tot(PS80)}}{m_{i,tot(W)}} \left(\frac{V_{Air(W)}}{V_{PS80} K_{i,W/Air}} + \frac{V_W}{V_{PS80}} \right) - \frac{V_{Air}}{V_{PS80} K_{i,W/Air}} \quad (22)$$

With $K_{i,f_{PS80}/W}$ as surfactant solution to water partition coefficient.
In the experimental setup presented here, $V_{Air(W)} = V_{Air(PS80)}$, $V_W = V_{PS80}$, and $m_{i,tot(W)} = m_{i,tot(PS80)}$, simplifying eq. (22) to:

$$K_{i,f_{PS80}/W} = \frac{A_{i,W}}{A_{i,f_{PS80}}} \left(\frac{V_{Air(W)}}{V_{PS80} K_{i,W/Air}} + 1 \right) - \frac{V_{Air}}{V_{PS80} K_{i,W/Air}} \quad (23)$$

Inserting $K_{i,f_{PS80}/W}$ in eq. (12) gives the micelle to water partition coefficient $K_{i,PS80/W}$.
$K_{i,W/Air}$ values were retrieved from a comprehensive literature source [191] or calculated with the LSER equation presented therein and are reported with the respective $\log K_{i,PS80/W}$.
Linearity of the detector response to ensure a constant response factor r was verified by recording calibration curves over the response range observed for the samples.

3.2.1.2 Polymer Reference Phase Partitioning

In an approach similar to the headspace reference method in 3.2.1.1, air as the reference phase was now substituted by LDPE to determine $K_{i,PS80/W}$ for a set of non-volatile solutes as data for LSER model regression. Ultrapure water was replaced by 10 mM Na_2HPO_4/ NaH_2PO_4 (final pH = 6.0) buffer solution to suppress ionization of ionizable solutes in water. LDPE sheets serving as reference partition phase were prepared for experimental use by cutting them into 2 cm wide strips followed by extraction in n-hexane, methanol and twice in Milli-Q water (24 h each) on an orbital shaker set to 150 rpm at room temperature. Solvent to polymer volume ratio exceeded 50:1 in all instances. Solvent residuals were evaporated at 60°C for 30 minutes in a drying cabinet. Any residual water on the polymer sheets was wiped off with lint-free paper tissues (Kimberly-Clark, Dallas, TX). The extracted polymer strips were stored in glass jars with 24 mm PTFE lined screw caps (Agilent Technologies, Santa Clara, CA) until use. Before each experiment, polymer strips were cut into appropriate sizes and weighed to assure uniform mass distribution. The calibration standards for LC measurements were prepared in acetone and acetonitrile-buffer mixtures. For solvent-buffer mixtures, 50/50 v/v acetonitrile/ phosphate pH 6.0 and 25/75 v/v acetonitrile/ ammonium acetate pH 9.0 were employed.
LDPE polymer strips were cleaved longitudinally, reducing adhesion to the walls of the vial, and placed in appropriately sized screw-cap glass vials (see Table 6). Vials were filled with buffer or PS 80 solution, spiked with 5 µL concentrated methanolic solutions of analytes as above (3.2.1.1), tightly closed with 13 mm PTFE lined screw caps, and shaken at 120 rpm for at least four weeks at 25°C to equilibrate the polymer strips with the solution.
After equilibration, polymer strips were removed from the vials with acetone-rinsed forceps, wiped dry with lint-free tissue to remove any adhering solution droplets, placed in 16 mL amber glass vials filled with 10 mL acetone, and closed with 15 mm PTFE lined silicone screw caps. Extraction

was carried out at 40°C for 72 h on an incubating orbital shaker set to 150 rpm (IKA KS 4000 i control, IKA, Germany). The extraction solvent was subsequently concentrated to 1.5 mL under a gentle stream of nitrogen.
Recovery samples were prepared by adding blank polymer strips to extraction vials and spiking solutes to the extraction solvent, extracting and concentrating the solvent as detailed above. All solutes showed recovery rates of 80% or higher from the concentrated extraction solvent. Extracts were analyzed in a LC/UV system (Table A4) and peak areas of the respective solutes determined.
Analogous to the headspace reference method, the following relations apply accordingly:

$$A_{i,W} = r \cdot C_{i,Extr(W)} \; ; \; A_{i,f_{PS80}} = r \cdot C_{i,Extr(PS80)} \qquad (24a; b)$$

with $C_{i,Extr}$ as the concentration of solute in the polymer extract.
$C_{i,Extr}$ relates to the concentration in the polymer $C_{i,P}$:

$$C_{i,P(W)} = \frac{C_{i,Extr(W)}\, V_{Extr(W)}}{V_{P(W)}} \; ; \; C_{i,Pol(PS80)} = \frac{C_{i,Extr(PS80)}\, V_{Extr(PS80)}}{V_{P(PS80)}} \qquad (25a; b)$$

with V_{Pol} and V_{Extr} representing polymer and extract volumes, respectively. As $V_{P(W)} = V_{P(PS80)}$ and $V_{Extr(W)} = V_{Extr(PS80)}$, $C_{i,Extr}$ is directly proportional to $C_{i,P}$. Partitioning to the headspace above the solution can be neglected since the chemicals tested in this setup are non-volatile. Replacing the headspace reference phase Air with the polymer reference phase P, eqs. (15)-(23) presented for headspace partitioning apply likewise. Instead of $K_{i,W/Air}$ values, experimental $K_{i,W/P}$ values were used to correct measured peak areas.
Required $K_{i,W/P}$ values were collected by additionally probing the solution of vials containing no PS 80 (i.e., buffered water) by direct injection in the LC/UV system. As aqueous concentration of solutes in batch “NVOC 4” was below the analytical detection threshold of the system, the aqueous phase was extracted with 2 mL n-hexane as detailed above. 1 mL n-hexane was removed after the extraction and blown to dryness under a stream of nitrogen. The crystalline residue was taken up in 1 mL acetone. Recovery samples for this procedure indicate a recovery of at least 85% for all solutes in the batch. External calibration series were prepared for each compound batch and used to calculate $K_{i,W/P}$ from equilibrium concentrations in polymer and water.

3.2.1.3 Solubility Method

Measurement of the excess solubility in surfactant solutions (solubility method) has been widely applied to determine micellar partitioning. For several of the non-volatile chemicals, values for $K_{i,PS80/W}$ were determined with both the solubility method and the reference phase method for comparison of the two (see Chapter 4.1.2.4).
Briefly, the partitioning of solutes between micelles and water can be inferred by determining the equilibrium solubility of a compound in water ($S_{i,W}$) and, in parallel, in PS 80 solution ($S_{i,f_{PS80}}$). Saturated solutions of individual compounds were prepared by weighing excess chemical into 4 mL glass vials and addition of 4 mL water or PS 80 solution. Vials were closed with screw caps with 13 mm PTFE lined septa and placed on an orbital shaker set to 150 rpm at 25°C for at least one week. After equilibration, all vials were centrifuged at 10,000 x g (Sorvall Primo, Thermo Fisher Scientific, Waltham, MA) for 30 minutes to separate the pure compound from the

supernatant. Samples were taken from the clear supernatant and, when necessary, diluted with methanol before injection into the LC/UV system (see Table A4). Equilibrium between the liquid phase and the solid chemical was ascertained by determining $S_{i,W}$ once more upon doubling the initial equilibration time.
With eqs. (8) and (12), $K_{i,PS80/W}$ can then be inferred from $S_{i,f_{PS80}}$, $S_{i,W}$, and the fraction of micellized PS 80, $f_{PS80(Mic)}$.

3.2.1.4 Micelle Partitioning Data from the Literature

To complement the experimental values from this work, PS 80 micelle to water partitioning data were also retrieved from literature sources and used in the LSER model regression. Reported data were all based on the solubility method presented in 3.2.1.3. As a prerequisite for data inclusion, the following experimental features were required in the publications: equilibrium of excess pure compound with the solution, agitation of the sample vessel to ensure best possible contact of solvent and chemical, and a separation technique ensuring a particle-free solution [192]. Acceptable experimental temperatures ranged between 20-25°C.
Where necessary, mole fraction partition coefficients $K^{X}_{i,Mic/W}$ were converted to concentration based partition coefficients $K_{i,Mic/W}$ using eq. (11). When only $S_{i,W}$ and the molar solubilization ratio of surfactant, κ_i (mol/mol), were reported, $S_{i,f_{Surf}}$ was calculated as follows:

$$\kappa_i = \frac{n_{i(Mic)}}{n_{PS80(Mic)}} \tag{26}$$

$$S_{i,f_{PS80}} = S_{i,W} + \kappa_i \, C_{PS80(Mic)} \tag{27}$$

With: $n_{i(Mic)}$ amount of solute i in micelles, $n_{PS80(Mic)}$: amount of PS 80 in micelles and $C_{PS80(Mic)}$: molar concentration of surfactant in micelles. An arbitrary value for PS 80 concentration from the experimental method section was chosen to derive $C_{PS80(Mic)}$.

3.2.2 Simulating Solvent Alignment

One of the goals pursued with the prediction of micelle to water partitioning is the alignment of solubilization strength of alcohol-water mixtures with the solubilization strength of PS 80 solutions for the preparation tailored simulating solvents. From the initial information of partitioning between PS 80 micelles and water in the form of $\log K_{i,PS80/W}$, concentration dependent quantitative solubilization in a PS 80 solution can be calculated using eq. (12). In a similar manner, quantitative solubilization of alcohol-water mixtures employed as simulating solvents can be derived at incremental alcohol concentrations, directly through hypothetical mixture to water partition coefficients. The relevant LSER model equations for ethanol- and isopropanol-water systems, published by LSER pioneer M. Abraham [96, 97], can be retrieved from the appendix. The necessary LSER model for the calculation of $\log K_{i,PS80/W}$ will be established and discussed beforehand.

For the alignment of simulating solvent composition with the solubilization strength of PS 80 solutions, five toxicologically relevant chemicals with tabulated and diverse LSER descriptors were chosen from a list of leachable compounds [193] that have a “moderate” to “intermediate” associated risk score, as detailed in the publication. Calculations are performed at four different PS 80 concentrations: 0.01%, 0.1%, 0.5%, and 1.0% w/v in water. Table 7 lists the chosen chemicals and their respective experimental LSER solute descriptors.

Table 7. List of test leachables for simulating solvent alignment and their respective LSER descriptors.

Compound	CAS-RN	LSER descriptors					Source
		E_i	S_i	A_i	B_i^0	V_i	
Pyridine	110-86-1	0.64	0.84	0.00	0.47	0.675	[194]
Benzothiazole	95-16-9	1.30	1.21	0.00	0.47	0.969	[195]
Ethylbenzene	100-41-4	0.61	0.51	0.00	0.15	0.998	[196]
Butylbenzyl phthalate	85-68-7	1.30	1.73	0.00	1.01	2.459	[197]
Dodecyl acrylate	2156-97-0	0.14	0.62	0.00	0.42	2.254	Abraham Absolv[a)]

a) Personal database of M.H. Abraham included in UFZ tool.

3.2.3 Interactions of Parenteral Excipients Affecting Solubilization

The aqueous solubilization characteristics of selected parenteral excipients isloated and in combination were assessed by the solubility method presented above (3.2.1.3). As a quantitative parameter describing solubilization, the medium solubilization strength $\log K_{i,M/W}$, defined by differential solubilities in the respective medium ($S_{i,M}$) and water ($S_{i,W}$), was determined. $\mathrm{Log}\, K_{i,M/W}$ was ascertained in different media for 2,4-dinitrotoluene, naphthalene, and carbazole. Detailed physicochemical information on the three test chemicals can be retrieved from the appendix (Table A1).

Formulations containing the chosen parenteral excipients were prepared as follows, depending on the individual composition:

For excipient mixtures containing PS 80, the appropriate amount of surfactant was weighed in a 1 L volumetric flask and dissolved in water, as described previously. If the excipient mixture also contained a 10% volumetric fraction of ethanol, PS 80 was dissolved directly in the ethanol-water mixture. For the preparation of the individual mixtures, the necessary amount of benzyl alcohol, NaCl, EDTA, and/ or dextrose was weighed in a 100 mL volumetric flask and subsequently filled

to approximately half the total volume with either water, aqueous PS 80 solution, or PS 80 in ethanol-water mixture. To dissolve the excipients, flasks were placed on a magnetic stirrer and a stir bar was added to the flask. Once all excipients were dissolved, the volumetric flasks were filled to the indicated mark with the appropriate solvent as delineated above. After preparation, excipient mixtures were stored at 8°C in 100 mL amber glass vials until use to suppress degradation of PS 80. In total, 38 different excipient mixtures (formulations) were prepared containing either 0%, 0.01%, 0.1%, or 0.5% w/v PS 80 (Table 8).

Table 8. Excipients and respective concentrations used to determine interactions affecting solubilization behavior in parenteral formulations.

Excipient	Concentration(s) (%)
Polysorbate 80	0.01, 0.1, 0.5
Ethanol	10
Benzyl alcohol	1.5
Sodium chloride	0.9
Disodium EDTA	0.11
Dextrose	5

3.2.4 Migration Case Study

Leachable migration was tested in a simulated polymer contact scenario to assess the accuracy of thermodynamic model predictions in a realistic scenario resembling drug product to packaging contact. Dedicated 100 mL vessels for the migration tests were constructed by adding an additional opening at the lower side of the flask (Figure 11). Polymer disks used for migration experiments were punched out of whole sheets with metal rings (40 mm diameter) and extracted as detailed previously (3.2.1.2).

Polymer disks loaded with a cocktail of five non-volatile solutes (Table 9), three of which represent potential leachables according to Ph. Eur. 10, were weighed, placed on an aluminum disk, and inserted in the bottle cap, which was subsequently screwed on the 100 mL flask with the polymer disk facing the flask interior. The outer edges of the polymer were in contact with the bottle opening, while the remaining part of the polymer faced the bottle interior and thus contacted the solution.

Polymer disks were loaded with desired solutes as follows:

The pre-extracted polymer disk was placed in a 100 mL screw cap bottle, and 20 mL of a 50% v/v methanolic stock solution containing the desired solutes were added (loading step). Bottles were rotated on an orbital shaker (150 rpm) at room temperature. At two intervals of 48 h each, aliquots of 40 mL water were added, resulting in a total volume of 100 mL in the flask. One week after the initial step, the disks were removed from the bottles, wiped dry with lint-free tissue, and immediately used. The final mass of all solutes did not exceed 0.5% w/w in the polymer (Table 11).

Contact media included pH 6.0 phosphate buffered water, 20% and 50% (v/v) ethanol-water mixtures representing simulating solvents, 0.01%, 0.1%, 0.5% w/v PS 80 solutions, and three placebo formulations containing 0.5% PS 80 and other parenteral excipients (Table 10). The contact solutions were prepared as elaborated previously (3.2.3). The custom-made flasks were

filled with 50 mL of the desired medium. Solute migration from polymer to medium was initiated by turning the flasks upside down, resulting in direct contact between polymer and medium.
100 µL samples were taken after 1 h, 2 h, 8 h, 24 h, 78 h, 1 week, 2 weeks, 4 weeks, 6 weeks, and 8 weeks. After 8 weeks, polymer disks were removed from the bottle cap, wiped dry with lint-free tissue, weighed, and extracted in 50 mL acetone at 40°C for 1 week on an incubating orbital shaker. Again, 100 µL samples were taken from the extraction solvent.
All samples were diluted with 900 µL 50/50 v/v methanol/ 0.1% formic acid before injection into the LC-MS system (see Table A5). Detection limit for all compounds was around 1 ng/mL.

Table 9. Chemicals and polymer loading in case study.

Compound	CAS	$\log K_{i,O/W}$	$\log K_{i,PDMS/W}$ [c)]	$\log K_{i,LDPE/W}$ [d)]
1,2-Benzanthraquinone	2498-66-0	3.8	3.13	3.43
Di-(2-ethylhexyl) phthalate[a)]	117-81-7	7.6	6.52	6.10
9-Phenylcarbazole	1150-62-5	5.0	4.97	5.44
Oleamide[a)]	301-02-0	8.0	6.68	6.36
3,5-Di-tert-butyl-4-hydroxybenzaldehyde[b)]	1620-98-0	4.2	2.36	1.81

a) Plastic additive according to Ph. Eur. 10.
b) Degradant of plastic additive according to Ph. Eur. 10.
c) PDMS to water partition coefficient, calculated with LSER model eq. (A1) [198].
d) LDPE to water partition coefficient, calculated with LSER model eq. (A2) (unpublished results, T. Egert (Boehringer Ingelheim)).

Table 10. Placebo formulations used in the migration case study.

Placebo 1		Placebo 2		Placebo 3	
Excipient	**Concentration**	**Excipient**	**Concentration**	**Excipient**	**Concentration**
PS 80	0.5%	PS 80	0.5%	PS 80	0.5%
Benzyl alcohol	1.5%	Benzyl alcohol	1.5%	Ethanol	10%
NaCl	0.9%	NaCl	0.9%	Benzyl alcohol	1.5%
		EDTA	0.11%	NaCl	0.9%
		Dextrose	5.0%	EDTA	0.11%
				Dextrose	5.0%

Table 11. Average load of model leachables in PDMS and LDPE disks.

Compound	average load (µg/disk)	
	PDMS	LDPE
1,2-Benzanthraquinone	143.22	140.21
Di-(2-ethylhexyl) phthalate	174.57	177.34
9-Phenylcarbazole	205.14	203.37
Oleamide	166.71	70.78
3,5-Di-tert-butyl-4-hydroxybenzaldehyde	16.58	7.55

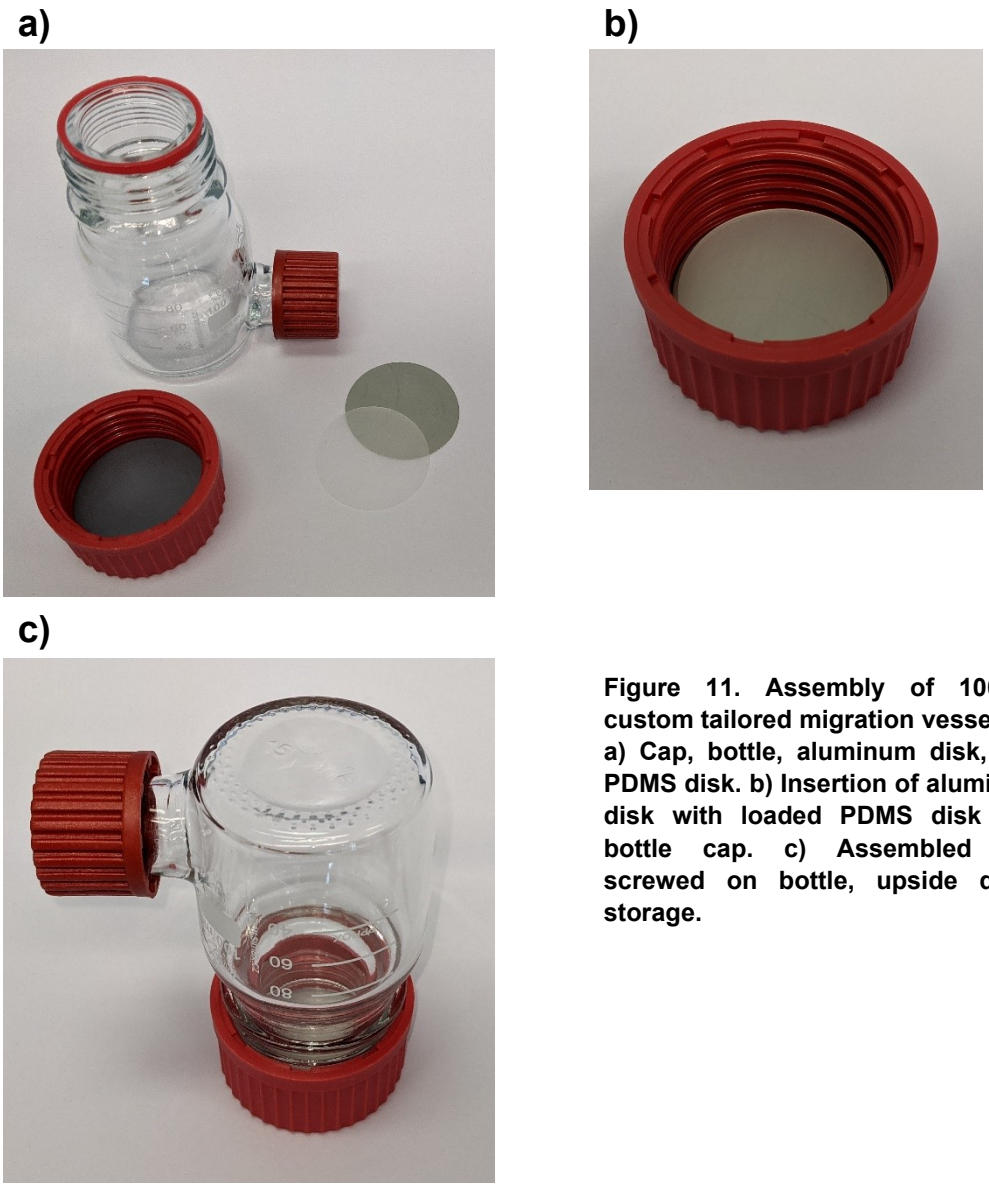

Figure 11. Assembly of 100 mL custom tailored migration vessel. a) Cap, bottle, aluminum disk, and PDMS disk. b) Insertion of aluminum disk with loaded PDMS disk into bottle cap. c) Assembled cap screwed on bottle, upside down storage.

4. Results and Discussion

4.1 Polysorbate 80 Micelle to Water LSER Partition Model

4.1.1 Results

In total, 75 $\log K_{i,PS80/W}$ values were measured (46 by means of the headspace and 29 by means of the polymer reference phase method) at 25°C and tabulated below (Table 12). Triplicate measurements showed very good repeatability of measured partition coefficients between PS 80 and water, with standard deviations (SDs) of 0.04 log units on average for all experimental values. Additionally, 37 $\log K_{i,PS80/W}$ values were retrieved from literature sources (Table 13).

The literature search identified 14 publications fulfilling the aforementioned criteria, thus providing PS 80 micelle to water partition coefficients for a total of 37 organic compounds. A major portion of literature values consists of drug solubilities, since PS 80 is a potent solubilizer with research in this field carried out over many decades [199, 200]. Other compounds of interest in the literature encompass hydrophobic chemicals of environmental concern with surfactants such as polysorbates used for environmental remediation of toxic organic chemicals [201, 202].

$\mathrm{Log}\ K_{i,PS80/W}$ values span over 6 log units from 0.16 (tetrahydrofuran) to 6.64 (dodecane), while molar masses range from 69.11 g mol^{-1} (butyronitril) to 1202.61 g mol^{-1} (cyclosporin). Many solutes from literature data sets exhibit strong hydrogen bond donor and acceptor functions, therefore complementing the solutes showing predominantly weak hydrogen bonding from this study, i.e. resulting in an overall chemically diverse range of test solutes. To demonstrate this, chemicals in the data set were grouped based on chemical functionality. The groups contain 17 alkanes/-enes/-ynes, 10 halogenated and 8 aromatic hydrocarbons, 3 heterocyclic aromatics, 11 alcohols, 6 aldehydes and ketones, 3 (thio)ethers, 8 carboxylic acids, 9 amines, 5 nitro compounds, one nitrile, 7 barbiturates, and finally, 15 chemicals with multiple functionalities.

Data accumulated above allows the construction of model equations that can predict PS 80 micelle to water partition coefficients of new chemicals when necessary descriptors are provided. For LSER equations, solute descriptors were obtained mainly from the database offered by the Helmholtz-Center for Environmental Research (UFZ) [203], and a small portion gathered from individual literature sources (Table A1 and Table A2). Multiple linear regression of experimentally determined $\log K_{i,PS80/W}$ (complete data set) against LSER solute descriptors results in the following relationship:

$$\log K_{i,PS80/W} = -0.226 + 0.945\ E_i - 1.021\ S_i - 0.151\ A_i - 3.378\ B_i^0 + 3.645\ V_i \quad (28)$$

$$n = 112,\ R^2 = 0.969,\ SD = 0.219$$

LSER predicted $\log K_{i,PS80/W}$ of the complete data set are tabulated in Table 12 and 13 with respective residuals. Below the tables, Figures 16 and 17 show the distribution of residuals over the numerical range of partition coefficients. Figure 12 compares the calculated partition coefficients from eq. (28) against experimentally determined values. To illustrate that chemical functionality does not influence the prediction of partition coefficients, solutes were placed in four groups based on their A_i and B_i^0 descriptors, as weak and/ or strong hydrogen bond donors/ acceptors, and respectively colored in Figure 12. Boundary values for were arbitrarily chosen to be $A_i > 0.09$ for strong hydrogen bond donors and $B_i^0 > 0.6$ for strong hydrogen bond acceptors.

In addition, solutes were allocated to respective chemical groups in Figure 14. Statistical analysis of the system parameters presented in eq. (28) shows that system parameters e, s, b, v and c are all highly significant ($P < 0.001$), while the a system parameter (–0.151) is insignificant ($P = 0.079$). Over the past decades, partition coefficients were often estimated by means of log-linear correlations against the solute's octanol-water partition coefficient, $\log K_{i,O/W}$ [161]. This single-parameter linear energy relationship yields the following equation for the complete data set of experimental $\log K_{i,PS80/W}$ values:

$$\log K_{i,PS80/W} = 0.958 \log K_{i,O/W} - 0.0187$$
$$n = 112,\ R^2 = 0.901,\ SD = 0.394 \quad (29)$$

The linear regression curve for eq. (29) is presented in Figure 13 and Figure 15 (chemical functionalities), allowing a direct comparison to the LSER model regression. Note that experimental $\log K_{i,PS80/W}$ values in regressions against $\log K_{i,O/W}$ are plotted on the ordinate, while in LSER regression plots, they are conventionally placed on the abscissa [169].
Recently, Alvarez-Núñez *et al.* [164] reported a rather similar log-linear model based on $\log K_{i,O/W}$ for a more limited data set:

Alvarez-Núñez *et al.*

$$\log K_{i,PS80/W} = 0.917 \log K_{i,O/W} + 0.0163$$
$$n = 43,\ R^2 = 0.942,\ SD = 0.486 \quad (30)$$

To assess the predictive capability of the presented LSER equation, two thirds of the experimental values from both literature and experiments conducted here were randomly chosen as a calibration set, while the remaining third served as an independent validation set. The regression resulting from the calibration set should contain system parameters close to the complete data set of eq. (28), while the experimental partition coefficients in the validation set should be reasonably well predicted by the smaller calibration set. Multiple linear regression of the calibration set yields the following LSER equation:

Calibration set

$$\log K_{i,PS80/W} = -0.305 + 0.918\, E_i - 0.984\, S_i - 0.279\, A_i - 3.376\, B_i^0 + 3.708\, V_i$$
$$n = 75,\ R^2 = 0.967,\ SD = 0.227 \quad (31)$$

System parameters in the smaller calibration set are equally as significant as the parameters of the complete data set presented in eq. (28), with the a parameter exhibiting a slightly more significant P value of 0.012 in eq. (31).
Solutes grouped in calibration and validation set are tabulated in the appendix (in Table A6 and Table A7), where the predicted partition coefficients from the calibration set are compared to partition coefficients from eq. (28) (complete data set).

Finally, experimental micelle partitioning data was divided into a set with data determined in this work and a set with the data from literature. Both sets were individually regressed against respective LSER solute descriptors to yield separate LSER equations:

Set from this work

$$\log K_{i,PS80/W} = -0.258 + 0.767\,E_i - 0.756\,S_i + 0.048\,A_i - 3.910\,B_i^0 + 3.741\,V_i \quad (32)$$

n = 75, R^2 = 0.976, SD = 0.201

Literature set

$$\log K_{i,PS80/W} = -0.109 + 1.071\,E_i - 0.973\,S_i - 0.290\,A_i - 3.013\,B_i^0 + 3.272\,V_i \quad (33)$$

n = 37, R^2 = 0.969, SD = 0.197

The resulting LSER system parameters in eqs. (32) and (33) are compared to the complete data set in the discussion below.

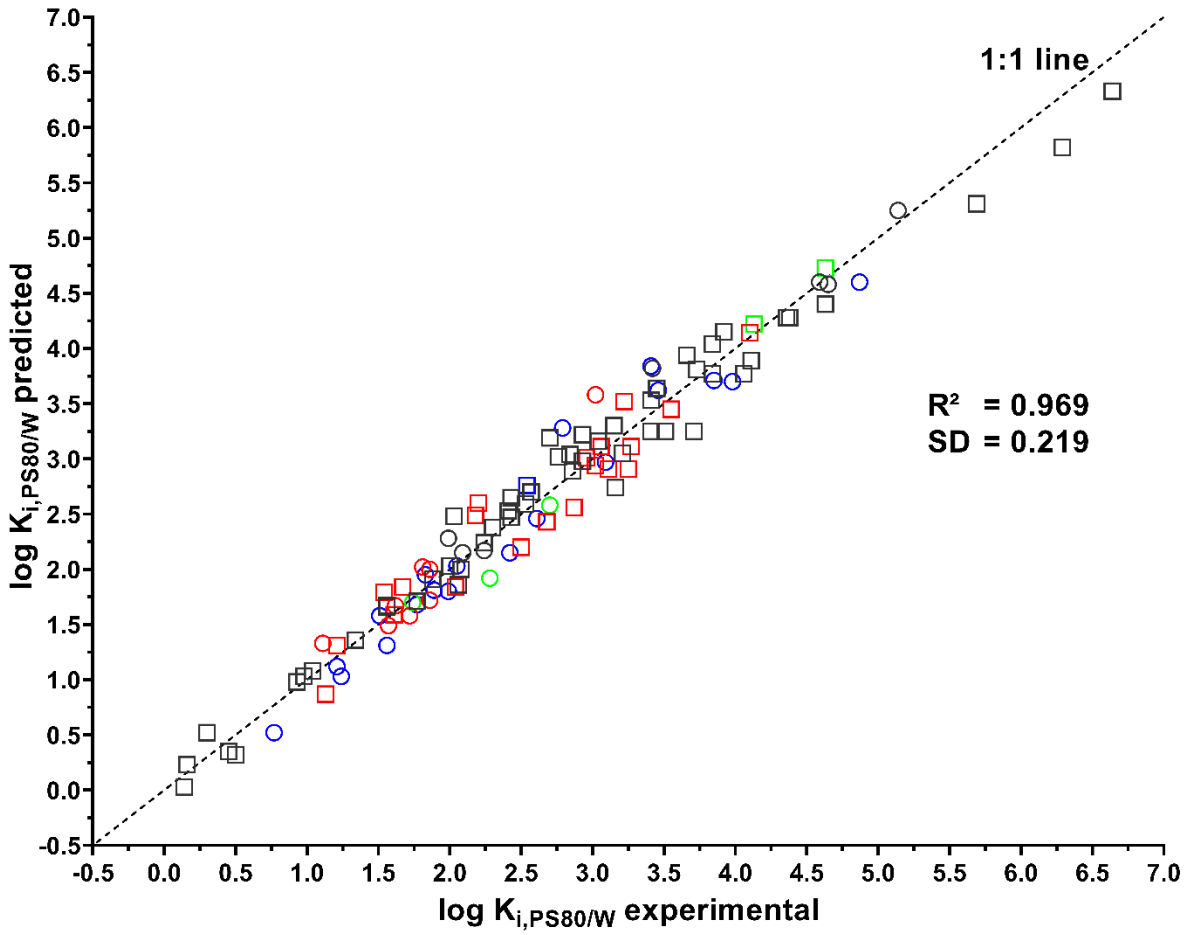

Figure 12. Experimental vs LSER predicted $\log K_{i,PS80/W}$. Squares = partition coefficients from this study. Circles = partition coefficients from literature. Color coding: black = weak hydrogen bond donor and acceptor; red = strong hydrogen bond donor, weak acceptor; green = weak hydrogen bond donor, strong acceptor; blue = strong hydrogen bond donor and acceptor. Predicted $\log K_{i,PS80/W}$ values from eq. (28).

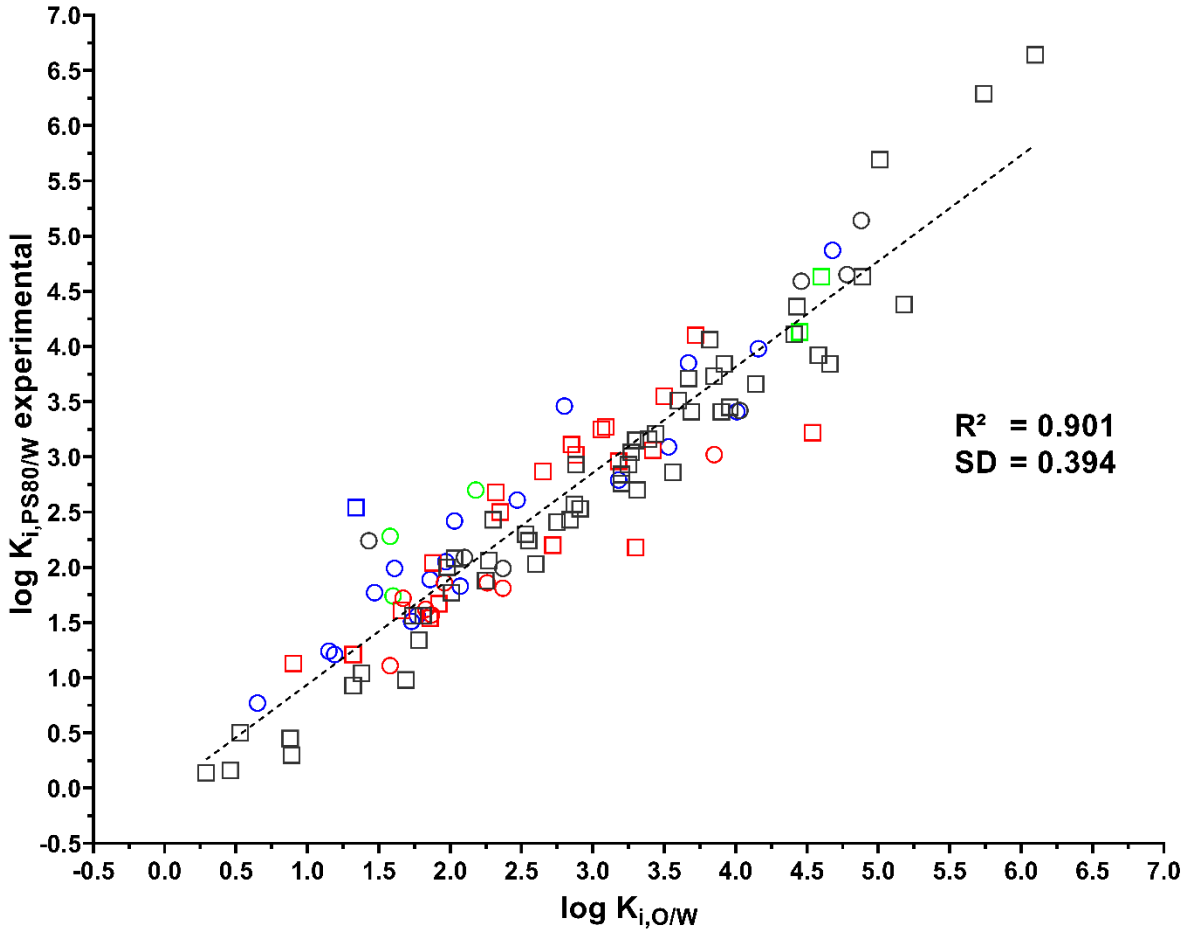

Figure 13. Linear regression of experimental $\log K_{i,PS80/W}$ against $\log K_{i,O/W}$. Squares = partition coefficients from this study. Circles = partition coefficients from literature. Color coding: black = weak hydrogen bond donor and acceptor; red = strong hydrogen bond donor, weak acceptor; green = weak hydrogen bond donor, strong acceptor; blue = strong hydrogen bond donor and acceptor. The dashed line represents the linear regression based on eq. (29).

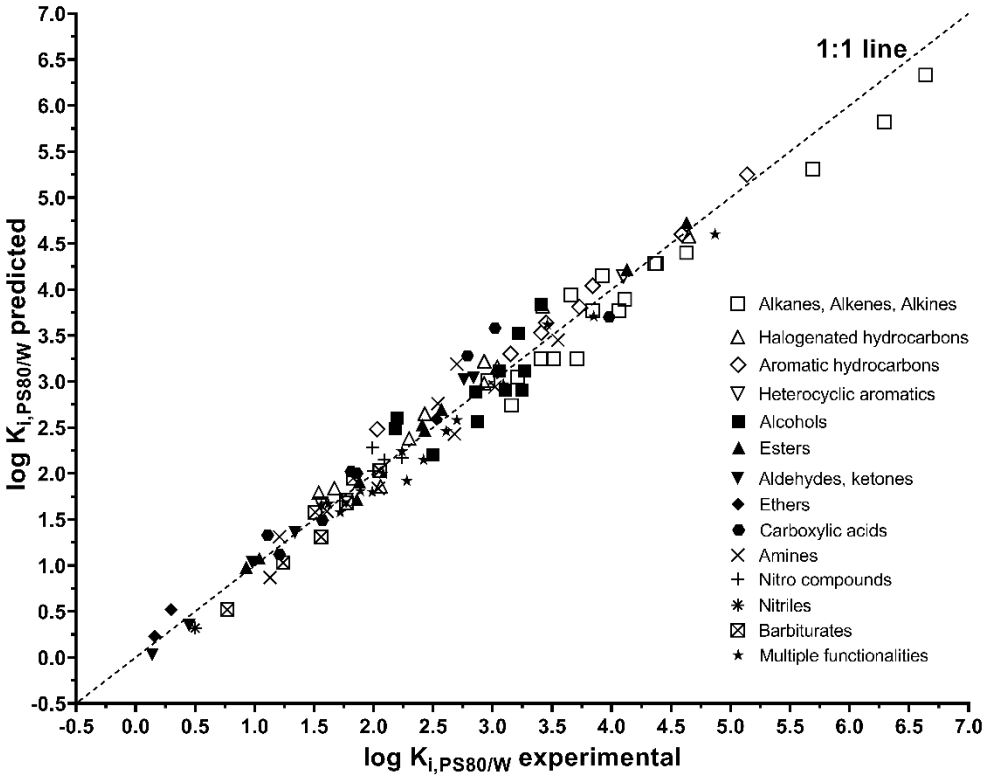

Figure 14. Experimental vs LSER predicted $\log K_{i,PS80/W}$ with solutes allocated to chemical groups. Predicted $\log K_{i,PS80/W}$ values from eq. (28).

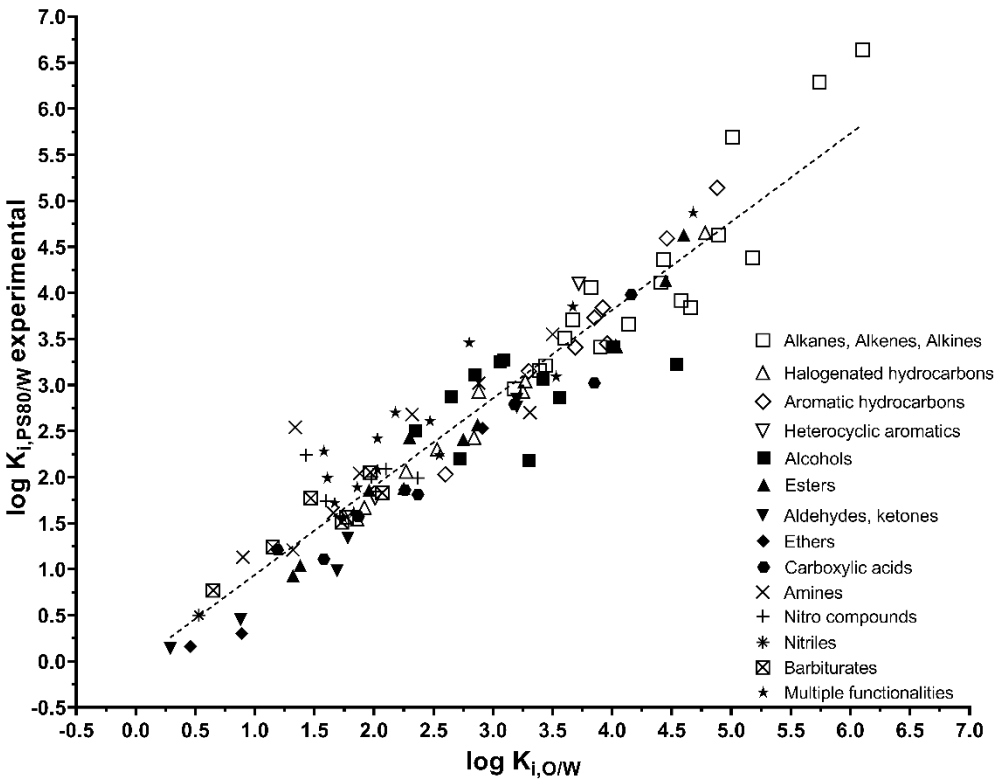

Figure 15. Linear regression against $\log K_{i,O/W}$ with solutes allocated to chemical groups. The dashed line represents the linear regression based on eq. (29).

Table 12. Experimental partitioning data $\log K_{i,PS80/W}$ from this work. Calculated $\log K_{i,PS80/W}$ from equation (28).

Solute	CAS-RN	Exp. $\log K_{i,PS80/W}$	Standard deviation	Calc. $\log K_{i,PS80/W}$	|Diff. exp. – calc.|	Batch ID	$\log K_{i,W/Air}$ or $K_{i,W/Pol}$ [a)]
Butyronitrile	109-74-0	0.50	0.04	0.32	0.18	VOC 1	2.56
Tetrahydrofuran	109-99-9	0.16	0.06	0.23	0.07	VOC 1	2.29
Butyraldehyde	123-72-8	0.45	0.04	0.35	0.10	VOC 1	2.36
Methyl ethyl ketone	78-93-3	0.14	0.07	0.03	0.11	VOC 1	2.76
2-Hexanone	591-78-6	0.98	0.03	1.03	0.05	VOC 1	2.45
Hexanal	66-25-1	1.34	0.02	1.36	0.02	VOC 1	2.09
2-Ethyl-1-hexanol	104-76-7	2.20	0.07	2.60	0.40	VOC 1	2.85
Diethyl ether	60-29-7	0.30	0.04	0.52	0.22	VOC 2	1.19
Thiophene	110-02-1	1.56	0.01	1.67	0.11	VOC 2	1.03
Methyl methacrylate	80-62-6	1.04	0.03	1.08	0.04	VOC 2	1.85
Ethyl acrylate	140-88-5	0.93	0.04	0.98	0.05	VOC 2	2.06
Trichloromethane	67-66-3	1.67	0.02	1.84	0.17	VOC 2	0.64
Isoamyl acetate	123-92-2	1.88	0.08	1.91	0.03	VOC 2	1.75
1-Bromo-2-chloroethane	107-04-0	1.54	0.03	1.79	0.25	VOC 2	1.34
1,2,3-Trichloropropane	96-18-4	2.06	0.02	1.86	0.20	VOC 2	1.82
FTOH 4:2	2043-47-2	2.18	0.02	2.49	0.31	VOC 2	1.77
Toluene	108-88-3	2.03	0.02	2.48	0.45	VOC 3	0.62
Chlorobenzene	108-90-7	2.43	0.01	2.65	0.22	VOC 3	0.69
Diethyl disulfide	110-81-6	2.53	0.01	2.59	0.06	VOC 3	1.16
n-Butyl methacrylate	97-88-1	2.41	0.01	2.53	0.12	VOC 3	1.71
Nonanal	124-19-6	2.86	0.02	2.89	0.03	VOC 3	1.72
Ethyl hexanoate	123-66-0	2.43	0.02	2.47	0.04	VOC 3	1.55
Iodobenzene	591-50-4	2.93	0.00	3.22	0.29	VOC 3	1.52
FTOH 6:2	647-42-7	3.22	0.02	3.52	0.30	VOC 3	1.15
3-Methylpentane	96-14-0	3.51	0.07	3.25	0.26	VOC 4	-1.82
Hept-1-yne	628-71-7	2.96	0.04	3.01	0.05	VOC 4	0.44
2-Chlorotoluene	95-49-8	3.04	0.04	3.16	0.12	VOC 4	0.59
Trichloroethene	79-01-6	2.30	0.04	2.38	0.08	VOC 4	0.08
Tetrachloroethene	127-18-4	2.93	0.03	2.98	0.05	VOC 4	-0.22
Tetralin	119-64-2	3.45	0.03	3.64	0.19	VOC 4	0.73
n-Propylbenzene	103-65-1	3.41	0.04	3.53	0.12	VOC 4	0.12
2,4,4-Trimethylpent-2-ene	107-40-4	3.66	0.03	3.94	0.28	VOC 5	-1.40
Oct-1-ene	111-66-0	4.11	0.02	3.89	0.22	VOC 5	-1.43
Non-1-ene	124-11-8	4.63	0.03	4.40	0.23	VOC 5	-1.56
S-Limonene	5989-54-8	3.92	0.01	4.15	0.23	VOC 5	-0.13

2,2-Dimethylbutane	75-83-2	3.71	0.05	3.25	0.46	VOC 5	-1.82
2,2-Dimethylpentane	590-35-2	4.06	0.03	3.77	0.29	VOC 5	-1.94
2,2,4-Trimethylpentane	540-84-1	4.36	0.03	4.28	0.08	VOC 5	-2.07
Cyclohexane	110-82-7	3.21	0.03	3.05	0.16	VOC 5	-0.90
Pentane	109-66-0	3.16	0.10	2.74	0.42	VOC 6	-1.70
Hexane	110-54-3	3.41	0.09	3.25	0.16	VOC 6	-1.82
Heptane	142-82-5	3.84	0.07	3.77	0.07	VOC 6	-1.94
Octane	111-65-9	4.38	0.03	4.28	0.10	VOC 6	-2.07
Decane	124-18-5	5.69	0.01	5.31	0.38	VOC 6	-2.31
Undecane	1120-21-4	6.29	0.00	5.82	0.47	VOC 6	-2.43
Dodecane	112-40-3	6.64	0.01	6.33	0.31	VOC 6	-2.56
Aniline	62-53-3	1.13	0.08	0.87	0.26	NVOC 1	0.78
N-Methylaniline	100-61-8	1.61	0.04	1.59	0.02	NVOC 1	-0.37
2-Methylaniline	95-53-4	1.21	0.05	1.31	0.10	NVOC 1	0.92
Diphenylamine	122-39-4	3.55	0.02	3.45	0.10	NVOC 1	-2.05
Benzidine	92-87-5	2.54	0.09	2.76	0.22	NVOC 1	1.20
4-Aminobiphenyl	92-67-1	3.02	0.04	2.94	0.08	NVOC 1	-1.10
N,N-Diethylaniline	91-66-7	2.70	0.04	3.19	0.49	NVOC 1	-2.48
2-Chloroaniline	95-51-2	2.04	0.04	1.84	0.20	NVOC 1	-0.41
4-Iodoaniline	540-37-4	2.68	0.03	2.43	0.25	NVOC 1	-0.54
1-Naphthol	90-15-3	3.11	0.02	2.91	0.20	NVOC 2	-0.17
Acetanisole	100-06-1	1.56	0.03	1.66	0.10	NVOC 2	-0.23
2,4-Dinitrotoluene	121-14-2	2.00	0.02	2.03	0.03	NVOC 2	-0.63
2-Iodophenol	533-58-4	2.87	0.01	2.56	0.31	NVOC 2	-0.34
2-Hydroxybiphenyl	90-43-7	3.27	0.01	3.11	0.16	NVOC 2	-0.89
2-Bromophenol	95-56-7	2.50	0.02	2.20	0.30	NVOC 2	-0.19
Benzothiazole	95-16-9	1.77	0.07	1.71	0.06	NVOC 3	-0.69
4-tert-Butylphenol	98-54-4	3.06	0.06	3.11	0.05	NVOC 3	-0.28
Methyl salicylate	119-36-8	2.24	0.08	2.24	0.00	NVOC 3	-1.53
4-Nitroanisole	100-17-4	2.08	0.09	2.00	0.08	NVOC 3	-0.85
Benzophenone	119-61-9	2.76	0.06	3.02	0.26	NVOC 3	-1.86
2,4-Dichlorophenol	120-83-2	3.25	0.05	2.91	0.34	NVOC 3	-0.67
Valerophenone	1009-14-9	2.84	0.10	3.04	0.20	NVOC 3	-2.39
Methyl-4-chlorobenzoate	1126-46-1	2.57	0.04	2.70	0.13	NVOC 3	-2.00
Naphthalene	91-20-3	3.15	0.02	3.30	0.15	NVOC 4	-2.82
Acenaphthene	83-32-9	3.84	0.02	4.04	0.20	NVOC 4	-3.61
Carbazole	86-74-8	4.10	0.04	4.14	0.04	NVOC 4	-2.19
Dibutyl phthalate	84-74-2	4.13	0.01	4.22	0.09	NVOC 4	-3.21
Triphenyl phosphate	115-86-6	4.63	0.01	4.73	0.10	NVOC 4	-2.81

Acenaphthylene	208-96-8	3.73	0.02	3.81	0.08	NVOC 4	-3.26

a) $\mathrm{Log\ K_{i,W/Air}}$ for volatiles (VOC) or $\log \mathrm{K_{i,W/P}}$ for non-volatiles (NVOC).

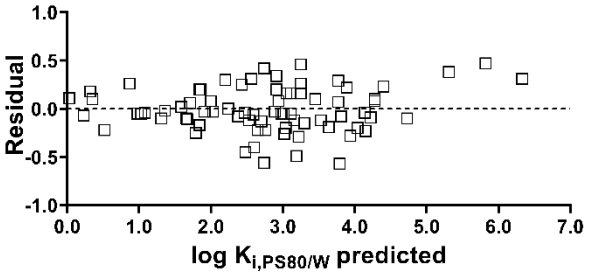

Figure 16. Residual plot of predicted $\log \mathrm{K_{i,PS80/W}}$ values from this work.

Table 13. Literature partitioning data $\log \mathrm{K_{i,PS80/W}}$. Calculated $\log \mathrm{K_{i,PS80/W}}$ from equation (28).

Solute	CAS-RN	Exp. $\log \mathrm{K_{i,PS80/W}}$	Calc. $\log \mathrm{K_{i,PS80/W}}$	|Diff. exp. – calc.|	Literature source
4-Nitrotoluene	99-99-0	1.99	2.28	0.29	[204]
2,3-Dinitrotoluene	602-01-7	2.24	2.17	0.07	[204]
2,6-Dinitrotoluene	606-20-2	2.09	2.15	0.06	[204]
2,4,6-Trinitrotoluene	118-96-7	1.74	1.70	0.04	[204]
Simvastatin	79902-63-9	4.87	4.60	0.27	[205]
Cyclosporin	59865-13-3	3.46	3.62	0.16	[205]
Phenanthrene	85-01-8	4.59	4.60	0.01	[206]
Pyrene	129-00-0	5.14	5.25	0.11	[206]
Phenytoin	57-41-0	2.61	2.46	0.15	[207]
Hydrocortison	50-23-7	1.99	1.80	0.19	[208]
β -Estradiol	50-28-2	3.41	3.84	0.43	[208]
Ethinylestradiol	57-63-6	3.85	3.71	0.14	[208]
Flurbiprofen	5104-49-4	3.98	3.70	0.28	[209]
Hexachloroethane	67-72-1	3.42	3.82	0.40	[210]
Hexachlorobuta-1,3-diene	87-68-3	4.65	4.58	0.07	[210]
Rofecoxib	162011-90-7	2.28	1.92	0.36	[211]
Lorazepam	846-49-1	3.09	2.97	0.12	[212]
Allobarbital	52-43-7	1.24	1.03	0.21	[213]
Barbital	57-44-3	0.77	0.52	0.25	[213]
Butobarbital	77-28-1	1.51	1.58	0.07	[213]
Amobarbital	57-43-2	1.83	1.95	0.12	[213]
Cyclobarbital	52-31-3	1.56	1.31	0.25	[213]
Phenobarbital	50-06-6	1.77	1.68	0.09	[213]

Secobarbital	76-73-3	2.05	2.03	0.02	[213]
4-Hydroxybenzoic acid	99-96-7	1.11	1.33	0.22	[199]
Salicylic acid	69-72-7	1.86	2.00	0.14	[199]
Benzocaine	94-09-7	1.89	1.81	0.08	[214]
Methyl paraben	99-76-3	1.86	1.72	0.14	[215]
Furosemide	54-31-9	2.42	2.15	0.27	[216]
Griseofulvin	126-07-8	2.70	2.58	0.12	[217]
Benzoic acid	65-85-0	1.57	1.49	0.08	[218]
3-Methylbenzoic acid	99-04-7	1.81	2.02	0.21	[218]
3-Nitrobenzoic acid	121-92-6	1.62	1.67	0.05	[218]
4-tert-Butylbenzoic acid	98-73-7	3.02	3.58	0.56	[218]
2,4-Dinitrophenol	51-28-5	1.72	1.58	0.14	[218]
Acetylsalicylic acid	50-78-2	1.21	1.12	0.09	[218]
Naproxen	22204-53-1	2.79	3.28	0.49	[218]

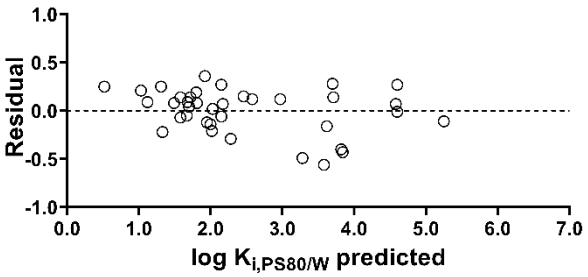

Figure 17. Residual plot of predicted $\log K_{i,PS80/W}$ values from literature.

4.1.2 Discussion

The LSER model regression represented by eq. (28) results in a very good fit for the entire experimental data set. The high chemical diversity of the solutes used for model calibration enables robust predictions of structurally variable neutral organic solutes. With predicted partition coefficients from PS 80 micelles to water at hand, concentration dependent solubilization in a PS 80 solution ($\mathrm{K_{i,f_{PS80/W}}}$) can be estimated based on eq. (12).

Validity of eq. (28) is further supported by nearly identical system parameters obtained from the reduced calibration set specified by eq. (31). $\mathrm{Log\ K_{i,PS80/W}}$ was calculated from eq. (31) for the remaining solutes in the validation set. Resulting calculated values were linearly regressed against experimental partition coefficients of solutes in the validation set. Linear regression yielded a coefficient of determination (R^2) of 0.963 and SD of 0.246, supporting the conformity of calibration and validation sets.

The multi-parameter approach with chemically intuitive and comprehensible solute descriptors underlying the LSER model proved superior over a single-parameter linear free energy relation based on $\log \mathrm{K_{i,O/W}}$. In Figure 13, a higher variability of experimental and predicted $\log \mathrm{K_{i,PS80/W}}$ can be identified in the single-parameter relation. Similar observations were previously made when the model proposed by Alvarez-Núñez *et al.* was used to calculate partition coefficients, showing poor predictability (R^2 of 0.528 and 0.444) [205]. As evident from Figures 12-15, the differences between LSER and $\log \mathrm{K_{i,O/W}}$ regression cannot be ascribed to certain chemical groups that are misrepresented by the octanol-water partition coefficient, but rather, LSER descriptors yield overall improved predictions regardless of chemical identity.

Since LSER parameters evolve from chemically meaningful interactions, eq. (28) allows a discussion of solute affinity to the PS 80 micellar phase. Both e and v model parameters are positive, indicating favorable dispersive interactions within the micellar environment and solute cavity formation requiring less energy than in the highly polar aqueous phase. This is typically the case when organic phases are compared to water, as strong intermolecular hydrogen bond interactions between water molecules require high energy contributions to be separated to form solute cavities. In turn, s and b parameters confirm that the micellar phase, compared to water, offers less hydrogen bond donor moieties and less favorable interactions with dipolar solutes. Although there are three hydroxyl groups per PS 80 molecule, their hydrogen bond donor capacity is outweighed by the high molecular weight of the molecule. Lastly, the a parameter in the LSER model is close to zero, reflecting that both water and the polyethoxylated micelle phase offer abundant hydrogen bond acceptor functions. Therefore, hydrogen bond donor moieties of solutes do not greatly contribute to partitioning into either aqueous or micellar phase, explaining the high (i.e., insignificant) P value of a in comparison to the other system parameters.

Separate LSER models were additionally regressed for the data set from literature (eq. (32)) and for the partition data determined in this work (eq. (33)). Both regressions show overall similar system parameters to the complete data set, supporting that different authors and experimental platforms are able to generate uniform micelle to water partition data. The dispersion- and polarity-related e and s parameters from the literature set, however, display much closer resemblance to the complete set (1.07 to 0.945 and -0.973 to -1.02, respectively) than the same parameters from the data set that contains only values from this work ($\mathrm{e} = 0.767$, $\mathrm{s} = -0.756$). In turn, the solute size-related v parameter in the set from this work coincides closely with the v parameter of the full data set (3.645 to 3.741). LSER system parameters reflect the chemical nature of solutes, and for that reason, the 37 solutes from literature are sufficient to represent relevant dispersive and polar molecular interactions. On the other hand, solutes measured in this work span the relevant

molecular size range of the complete data set, hence v parameters in eq. (28) and eq. (33) align closely.

Table 14 offers an overview of LSER system parameters of other micelle/ water partitioning systems (SDS, CTAB) and the octanol/water system. Parameters generally coincide between all systems, with the a parameter in the CTAB/water and the b parameter in the SDS/water system as notable exceptions. While the other listed phase pairs display almost equal hydrogen bond acceptor functions as water, the negatively charged bromide counterion in CTAB allows strong interaction with solute hydrogen bond donor functions (e.g. hydroxyl, amine, carboxy groups). Similarly, the positively charged sodium counterion in SDS interacts with solute hydrogen bond acceptor functions (e.g. carbonyl, ether groups) and therefore displays a less negative b parameter than other systems. Clearly, surfactant and counterion charge affect hydrogen bonding in the micellar phase. Partitioning of solutes from PS 80 micelles and octanol to water is fairly similar, according to the respective LSER system parameters, yet log-linear single-parameter regressions based on $\log K_{i,Octanol/W}$ (eq. (29)) provide less accurate model equations than multi-parameter LSERs, as shown in Figure 12 and 13.

The similarity between micelle-water and organic solvent-water partitioning has also been acknowledged by the authors of the articles on LSERs for SDS and CTAB to water partitioning [187, 189].

Table 14. Overview of LSER system parameters of comparable systems (at 25°C).

System	LSER system parameters					Reference
	e	**s**	**a**	**b**	**v**	
PS80/water	0.945	-1.021	-0.151	-3.378	3.645	Eq. (28), complete data set
PS80/water	0.918	-0.984	-0.279	-3.376	3.708	Eq. (31), calibration set
SDS/water	0.366	-0.407	-0.126	-1.977	2.981	[189]
CTAB/water	0.679	-0.514	0.913	-2.999	3.110	[187]
Octanol/water	0.562	-1.054	0.034	-3.460	3.814	[219]

4.1.2.1 Inspection of Experimental Data Employed in this Work

In the following, the experimental data constituting the LSER model will be examined more closely. Inspection of Table 12 reveals a disconnect between experimental and predicted partition coefficients of hydrocarbons with equal molecular weight. Branched hydrocarbons partition stronger from water to PS 80 micelles than their linear isomers. As the V_i descriptor is calculated from McGowan's molecular volume, which does not discriminate between constitutional isomers of hydrocarbons, V_i is equal for all hydrocarbons with the same molecular formula. Accordingly, equal $\log K_{i,PS80/W}$ are calculated from eq. (28) in the given scenario. While the difference in experimental $\log K_{i,PS80/W}$ is rather large in hexane isomers (3.41, 3.51, 3.71 for n-hexane, 3-methylpentane, 2,2-dimethylbutane, respectively), the effect diminishes as the carbon number increases (4.38 and 4.36 for n-octane and 2,2,4-trimethylpentane). A reversed trend was observed in the literature for alkane partitioning between hexadecane and water, with linear alkane isomers exhibiting higher partitioning to the organic phase [220]. Conversely, branching of alkanes has no influence on partitioning from water to air [191]. Evidently, the V_i descriptor alone is insufficient at summarizing size-related solute-solvent interactions of constitutional isomers with the influence of branching depending on the nature of the organic phase [170, 194]. As an alternative

size-related molecular descriptor, molecular surface area could more accurately represent the three-dimensional form of solutes but would in turn necessitate new calculation of solute descriptors and system parameters [176].

The accuracy of the deployed experimental micelle partition coefficients can be affirmed by comparison of solutes that were examined by multiple authors. Table 15 shows that micelle to water partition coefficients from different authors are mostly in good agreement, despite different experimental methods, again supporting the idea that precise $\log K_{i,PS80/W}$ can be collected in multiple ways. While missing harmonization of experimental protocols in literature typically lead to differences in absolute solubility values collected for both PS 80 and water [221], the differential solubilities used to derive micelle partition coefficients seem to mitigate potential deviations. A selection between $\log K_{i,PS80/W}$ of identical compounds to include in the LSER model regression was accomplished by identifying the value resulting in the best regression fit. Naphthalene's partition coefficient determined with the reference phase method introduced here exceeds two values from literature by 0.19 and 0.25 log units, respectively. Whether this observation can be attributed to methodical or analytical differences will be elucidated in Chapter 4.1.2.4.

Table 15. Comparison of experimental $\log K_{i,PS80/W}$ recorded in multiple references, values chosen for LSER model in bold text.

Compound	Experimental $\log K_{i,PS80/W}$								
	This study	**Ref. 204**	**Ref. 139**	**Ref. 222**	**Ref. 206**	**Ref. 143**	**Ref. 199**	**Ref. 218**	**Ref. 213**
2,4-Dinitrotoluene	**2.00**	2.04							
Acetylsalicylic acid							1.14	**1.21**	
Naphthalene	**3.15**		2.90	2.96					
Phenanthrene					**4.59**	4.3			
Phenobarbital							1.80		**1.77**
Pyrene			5.01		**5.14**				

4.1.2.2 LSER Model Domain of Applicability

An important aspect of any model equation based on experimental data is its domain of applicability, which in the case of LSER regressions loosely defines the spectrum of compounds that are expected to be well represented, and therefore predicted with sufficient accuracy, by the model equation. A large domain of applicability of an LSER model relies on the diversity of the data set to represent as many chemical groups, structures, and sizes as possible, with experimentally determined partition coefficients distributed over a wide numerical range. Figure 18 shows the distribution of experimental $\log K_{i,PS80/W}$ values that were collected for the LSER model. As evident from the figure, the values center around $\log K_{i,PS80/W} =$ 2.0-4.0, with a mean value of 2.66 ± 1.25. In particular, the range of the retrieved literature values was rather low, contributing half of all values from $\log K_{i,PS80/W} =$ 2.0-3.0. The limited range of literature values was addressed by collecting data of chemicals with both lower and higher PS 80 micelle affinity. Inclusion of many compounds with greater partition coefficients is desired in the context of this work, as leachables often display low water solubility and, in turn, high micelle partition coefficients. However, as illustrated by Figure 18, $\log K_{i,PS80/W}$ values greater than 5.0 are still

underrepresented in the model regression. This stems from the fact that solutes falling into this range are highly hydrophobic – e.g. large, halogenated or polynucleated hydrocarbons. Partitioning of these chemicals, as discussed previously, is difficult to ascertain accurately, with adsorption to glass walls of laboratory equipment becoming relevant. Further, precise polymer to water partition coefficients of the very hydrophobic (non-volatile) organic chemicals would be necessary for a correct calculation of $\log K_{i,PS80/W}$ in the reference phase method, which are only available for selected compounds due to the obstacles encountered in experimental measurement [223]. One successful attempt at determining micelle to water partition coefficients for highly hydrophobic chemicals has been presented in the literature, where a polymer was loaded with chemicals and subsequently depleted by surfactant solutions [224]. This approach, however, is far more elaborate and came with its own difficulties, as e.g. glass adhesion could not be prevented.

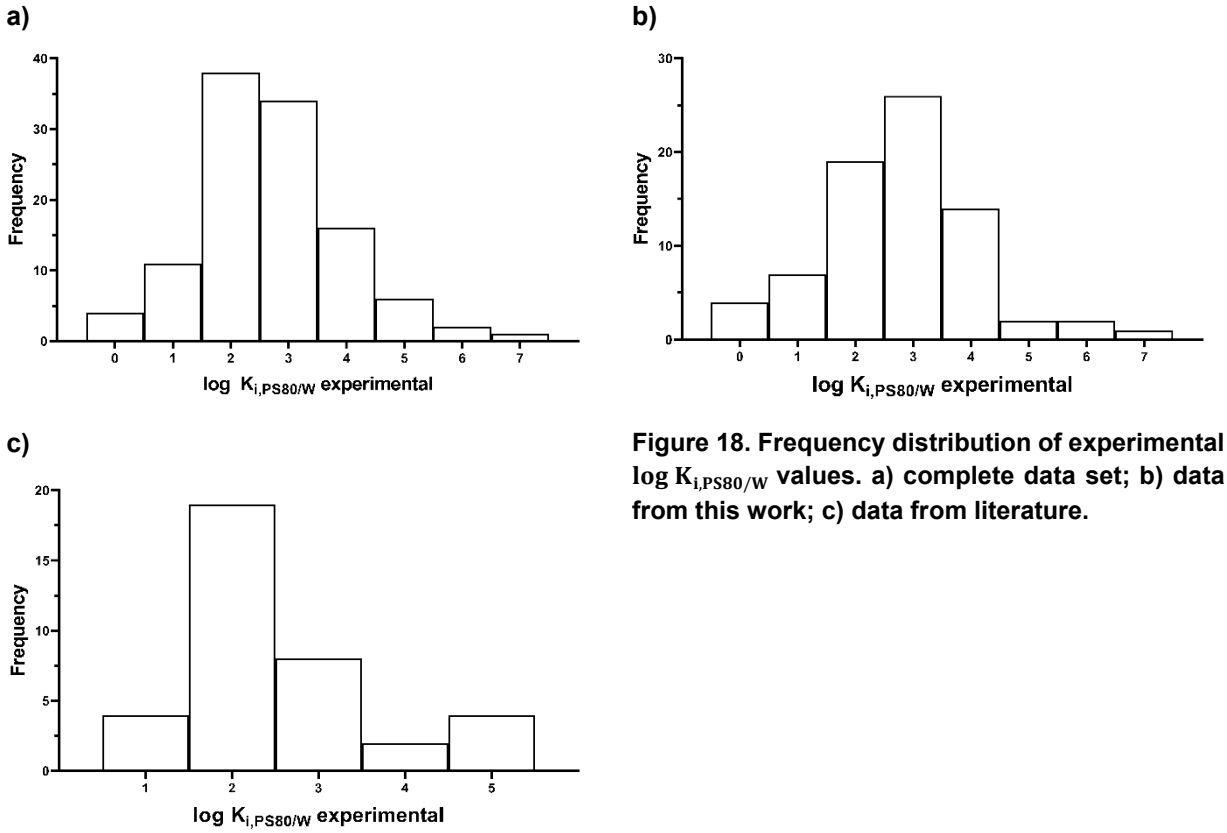

Figure 18. Frequency distribution of experimental $\log K_{i,PS80/W}$ values. a) complete data set; b) data from this work; c) data from literature.

4.1.2.3 Polysorbate 80 Product Source and Quality

As discussed in Chapter 2.3.1, PS 80 is a heterogeneous product. Manufacturing conditions and materials may cause varying compositions of fatty acids and impurities. The limits defined in compendial monographs are broad and allow substantial batch to batch variation. Possible differences in micellar partitioning of polysorbates were evaluated by measuring $\log K_{i,PS80/W}$ of a batch of non-volatile solutes (“NVOC 4”) using polysorbate 80 from various commercial vendors and presented in Table 16.

For the monography grade polysorbate products, detailed certificates of analysis are available, showing distinct differences between the two vendors. Crucially, the fatty acid composition in the

two products differs substantially (67% vs 82% oleic acid, 14% vs 4% palmitic acid). While these differences suggest an effect on the solubilization towards hydrophobic chemicals due to altered interactions with the micellar core, a noteworthy change of $\log K_{i,PS80/W}$ cannot be observed. Moreover, even non-monographed polysorbate 80 products show nearly equal solubilization characteristics (i.e., partition coefficients $\log K_{i,PS80/W}$). As the micellar core constitutes only a small fragment of a micelle, slightly different compositions of fatty acids do not modify solubilization capacity, even for the more hydrophobic compounds listed below.

Table 16. Comparison of partition coefficients ("NVOC 4") of various polysorbate 80 vendors, standard deviations in parentheses.

Compound	$\log K_{i,PS80/W}$			
	Ph. Eur. grade		laboratory grade	
	Vendor 1	Vendor 2	Vendor 3	Vendor 4
Naphthalene	3.15 (0.02)	3.15 (0.02)	3.16 (0.08)	3.12 (0.02)
Acenaphthene	3.84 (0.02)	3.83 (0.01)	3.85 (0.08)	3.82 (0.03)
Carbazole	4.09 (0.05)	4.10 (0.01)	4.17 (0.04)	4.15 (0.01)
Dibutyl phthalate	4.13 (0.01)	4.12 (0.00)	4.16 (0.05)	4.10 (0.02)
Triphenyl phosphate	4.63 (0.01)	4.67 (0.02)	4.67 (0.05)	4.60 (0.04)
Acenaphthylene	3.73 (0.02)	3.72 (0.01)	3.74 (0.06)	3.71 (0.02)

4.1.2.4 Comparison of Solubility Method and Reference Phase Method to Determine Micelle Partition Coefficients

Further data scrutiny ensued by determining $\log K_{i,PS80/W}$ for some crystalline chemicals from the experimental set, demonstrating the viability of both reference phase and solubility method to generate $\log K_{i,PS80/W}$ values (Table 17). While both methods yield similar partition coefficients for most compounds, some discrepancies between the values obtained from solubility and reference phase method can be observed. For example, experimental partition coefficients for carbazole and dibutyl phthalate differ by 0.27 and 0.46 log units, respectively. Without further information on the cause of the differences, values obtained via reference phase method are generally preferable, as the activity of solutes is low in both micellar and aqueous phase, while determination with the solubility method occurs at saturated conditions. The solute's activity coefficient at saturation may deviate from the activity coefficient at diluted concentrations ($\gamma_i^{sat} \neq \gamma_i^{\infty}$), especially in the micellar phase which generally solubilizes more organic solute per volume than water. Here, the assumption that solutes only interact with the surrounding micellar phase may no longer be valid, consequently altering partition equilibria [225].
Experimental solubility values were highly repeatable and had an overall lower standard deviation (Table 17) in comparison to the reference phase approach.

Table 17. $\mathrm{Log\,K_{i,PS80/W}}$ determined with reference phase and solubility method against predicted values from eq. (28). Standard deviations in parentheses.

Compound	$\mathbf{log\ K_{i,PS80/W}}$ predicted eq. (28)	$\mathbf{log\ K_{i,PS80/W}}$ reference phase method	$\mathbf{log\ K_{i,PS80/W}}$ solubility method
2,4-Dinitrotoluene	2.03	2.00 (0.02)	2.10 (0.01)
4-Nitroanisole	2.00	2.08 (0.09)	2.05 (0.04)
Methyl-4-chlorobenzoate	2.70	2.57 (0.04)	2.70 (0.03)
Benzophenone	3.02	2.76 (0.06)	3.00 (0.01)
4-tert-Butylphenol	3.11	3.06 (0.06)	3.06 (0.01)
Naphthalene	3.30	3.15 (0.02)	3.31 (0.00)
Acenaphthylene	3.81	3.73 (0.02)	3.64 (0.01)
Acenaphthene	4.04	3.84 (0.02)	4.10 (0.01)
Carbazole	4.14	4.10 (0.04)	3.83 (0.00)
Dibutyl phthalate	4.22	4.13 (0.01)	4.59 (0.01)

4.1.2.5 Linear Range of Partition Isotherm

A conventional experimental approach comprises determining $S_{i,f_{Surf}}$ at several polysorbate concentrations, plotting the amount of solubilized chemical against surfactant concentration [208, 213, 226]. The resulting slope is used to calculate a partition coefficient or a molar solubilization ratio κ_i. This is possible due to the linear relationship between total solubilization and PS 80 concentration above the CMC. Accordingly, partition coefficients between PS 80 micelles and water remain constant over the so-called linear solubilization range. Solubilization increasing linearly with PS 80 concentrations is expected when micelle formation in water is unaffected by the total surfactant concentration. Nonlinear solubilization behavior would be indicative of altered micellar assembly at increasing concentrations.

Experimental data in this paper confirms micellar solubilization increasing linearly with PS 80 concentration. $\mathrm{Log\,K_{i,PS80/W}}$ of batch “VOC 3” was measured at 10%, 15% and 20% w/v PS 80 to investigate the linear range of solubilization at higher PS 80 concentrations. The resulting partition coefficients and standard deviations are reported in Table 18. The data collected suggest no deviation of partition coefficients at increasing concentrations up to 20% PS 80 in water, supporting that linear solubilization of PS 80 solutions can be presumed up to this concentration.

Table 18. Effect of high PS 80 concentration on $\log K_{i,PS80/W}$. Standard deviation in parentheses.

Compound	$\log K_{i,PS80/W}$		
	10% PS 80	15% PS 80	20% PS 80
Diethyl ether	0.29 (0.09)	0.29 (0.05)	0.32 (0.02)
Thiophene	1.55 (0.02)	1.56 (0.01)	1.57 (0.00)
Methyl methacrylate	1.03 (0.05)	1.04 (0.01)	1.06 (0.01)
Ethyl acrylate	0.93 (0.05)	0.93 (0.01)	0.96 (0.01)
Trichloromethane	1.67 (0.02)	1.67 (0.01)	1.67 (0.01)
1-Bromo-2-chloroethane	1.52 (0.03)	1.54 (0.01)	1.55 (0.01)
1,2,3-Trichloropropane	2.05 (0.03)	2.06 (0.00)	2.07 (0.02)
FTOH 4:2	2.17 (0.03)	2.17 (0.00)	2.18 (0.02)

4.1.2.6 PS 80 Solubilization Strength from Predicted Micelle Partition Coefficients

The application of LSER predicted micelle to water partition coefficients for the calculation of PS 80 solubilization strength is demonstrated in Figure 19 a), where $\log K_{i,PS80/W}$, predicted with eq. (28), was converted to PS 80 solubilization strength, i.e. the logarithmic differential solubilities in a PS 80 solution and pure water ($\log K_{i,f_{PS80}/W} \approx \log \frac{S_{i,f_{PS80}}}{S_{i,W}}$, eq. (12)). Figure 19 b) shows the same data with the logarithm taken from the solubilization strength, i.e. simply $\frac{S_{i,f_{PS80}}}{S_{i,W}}$. Here, $S_{i,f_{PS80}}$ grows linearly with PS 80 and micelle concentration, while $S_{i,W}$ is a constant value.

The evolution of solubilization for three exemplary chemicals from the experimental LSER data set with increasing concentration of PS 80 shows that solubilization in micellar solution depends on solute hydrophobicity. For a branched alkane (2,2,4-trimethylpentane, $\log K_{i,O/W}$ = 4.43) 0.5% PS 80 in water already increases solubility roughly 100-fold (2 log units), while 1-naphthol ($\log K_{i,O/W}$ = 2.85), an anellated phenol, requires 2.0% PS 80 for a 10-fold (1 log unit) increase. In comparison, aniline ($\log K_{i,O/W}$ = 0.90) shows the lowest solubilization in micellar solution, with only a 2-fold (0.3 log units) increase of solubility at 2.0% PS 80. The differences in solubilization are further evidenced by the slope of the connecting lines in Figure 19, implying greater solubilization per micelle for more hydrophobic compounds. It is obvious that hydrophobicity and chemical structure markedly impact solubilization in a PS 80 solution. By applying the presented LSER equation, this solubilization can now be accurately foreseen and applied for calculation of relevant pre-experimental data supporting E & L studies, e.g. as a relevant parameter for simulating solvent alignment.

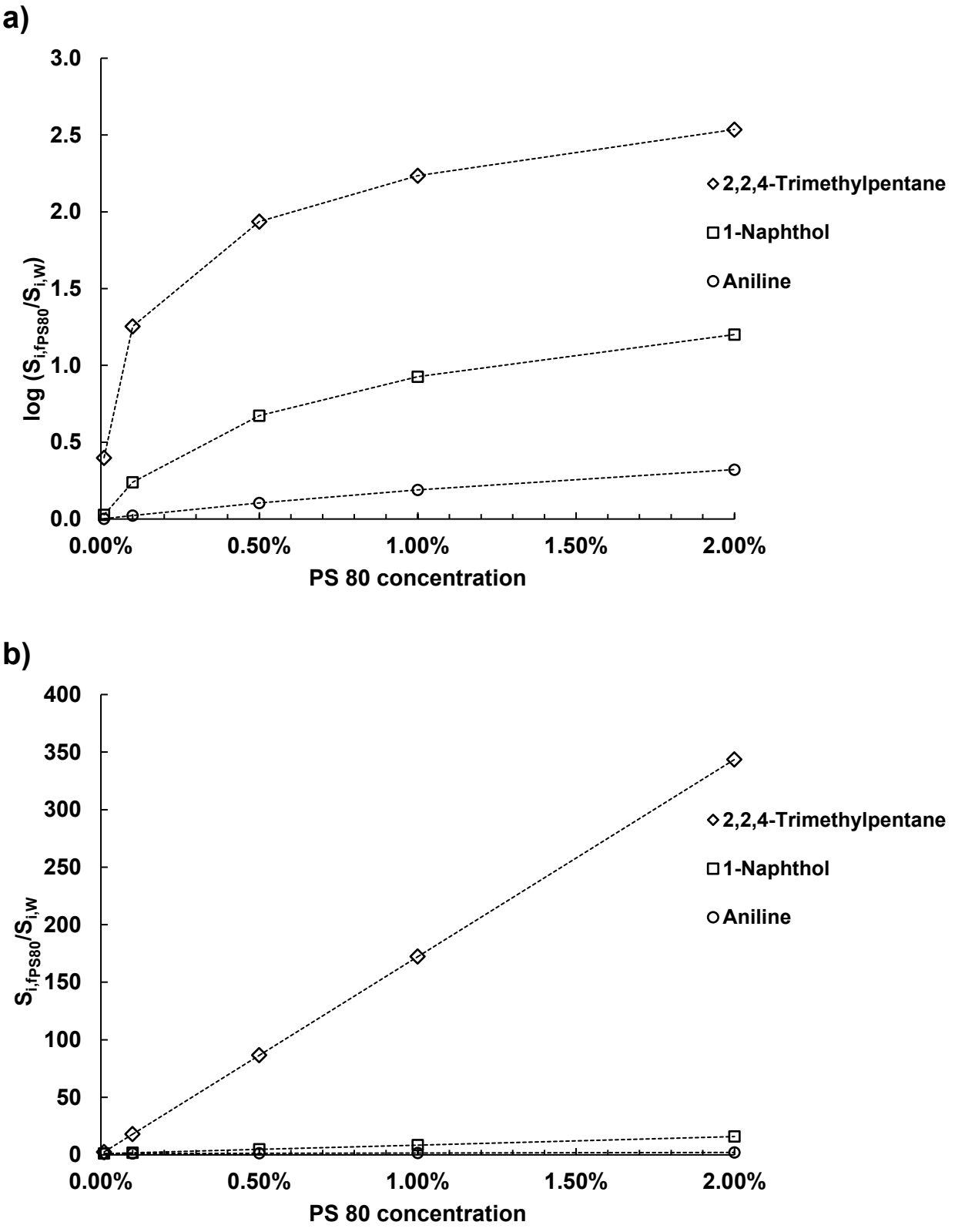

Figure 19. Trend of PS 80 solubilization strength with concentration for three exemplary chemicals from the experimental data set based on predicted micelle to water partition coefficients. a) Standard logarithmic solubilization strength; b) Non-logarithmic solubilization strength.

4.1.2.7 Solubilization in Polysorbate 20 Solutions

Polysorbate 20 (polyoxyethylene (20) sorbitan monolaurate, PS 20) is another commonly formulated surfactant in parenteral preparations, with the fatty acid tail (laurate) as the only molecular difference to the PS 80 lead structure (i.e., polyoxyethylene (20) sorbitan monooleate) [132, 227]. Similar to PS 80, PS 20 is a potent solubilizer in aqueous parenteral formulations requiring inspection [100]. Recently, solubilization characteristics of nonionic surfactants including PS 20 and PS 80 were compared and a strong linear relationship between the molar solubilization ratio κ_i of PS 80 and PS 20 was established [205]:

$$\kappa_{i,PS20} = 1.50 \pm 0.07\ \kappa_{i,PS80} \quad (34)$$

Unlike PS 80 solubilization strength, $\kappa_{i,PS80}$ can only be calculated with knowledge of the equilibrium water solubility $S_{i,W}$ of the solute via eq. (27). In turn, $S_{i,W}$ is then also needed to calculate PS 20 solubilization strength from $\kappa_{i,PS20}$. Experimental $S_{i,W}$ values can be retrieved from many freely accessible databases, e.g. the EPI Suite desktop application [228] or the online tools provided by the Organization for Economic Co-operation and Development (OECD) [229] and the International Union of Pure and Applied Chemistry (IUPAC) [230]. If no experimental value can be found, predictions from physicochemical solute parameters (e.g. LSER or $\log K_{i,O/W}$) or in-silico calculations [231, 232] may be used instead. Naturally, the use of literature or predicted solubility values introduces errors in the calculation of PS 20 solubilization strength from the relation in eq. (34), especially in comparison to a dedicated LSER model as presented for PS 80, where differential concentrations or solubilities in PS 80 and water stem from identical sources for each chemical.

To illustrate the relationship in eq. (34), PS 20 micelle to water partition coefficients for some LSER model solutes, calculated with eqs. (27) and (34) from experimental $\log K_{i,PS80/W}$ and respective aqueous solubilities retrieved from the EPI Suite program, are listed and compared to the original PS 80 micelle to water partition coefficients in Table 19. The linear, solute-independent solubilization relationship of PS 20 and PS 80, as depicted by κ_i in eq. (34), produces $\log K_{i,PS20/W}$ values very closely related to the original, experimental $\log K_{i,PS80/W}$ values. Although the compounds in Table 19 offer sufficient chemical diversity according to their LSER solute descriptors, differences between respective $\log K_{i,PS20/W}$ and $\log K_{i,PS80/W}$ are fairly uniform and range from 0.2 to 0.3 log units. Since most solutes partition to the outer or interfacial regions of the polysorbate micellar phases, such a narrow distribution is comprehensible, as the chemical composition of the micelles in these regions is practically identical (polyethoxylated sorbitan). A linear alkane like octane, however, is expected to penetrate the micellar core region in PS 20 and PS 80 micelles, where the solute experiences distinct molecular interactions from the different fatty acid tails (lauric and oleic acid) that comprise the core region. While respective micelle partition coefficients should accordingly vary from the trend observed in the partition coefficients of more polar solutes, no discrepancy can be observed for octane. As outlined above, a dedicated model equation for PS 20 would likely improve this prediction. Nonetheless, as no physicochemical model predicting solubilization by PS 20 in water has been presented so far, the approach detailed here offers a reasonable alternative to experimental determination.

Table 19. Comparison of calculated $\log K_{i,PS20/W}$ to experimental $\log K_{i,PS80/W}$.

Compound	$\log K_{i,PS20/W}$ calculated (1)	$\log K_{i,PS80/W}$ experimental (2)	(1) – (2)
2-Hexanone	1.30	0.98	0.32
Aniline	1.37	1.13	0.24
Thiophene	1.79	1.56	0.23
Benzocaine	2.13	1.89	0.24
2-Iodophenol	3.12	2.87	0.25
n-Propylbenzene	3.63	3.41	0.22
Octane	4.63	4.38	0.25

4.2 Simulating Solvent Alignment

4.2.1 Results

Simulating solvent alignment was demonstrated for five exemplary leachable compounds at four different PS 80 concentrations for ethanol- and isopropanol-water mixtures. Tables 20, 21, 22, and 23 list the respective solubilization strength, depicted as the hypothetical partition coefficient between a solution with a given fraction f of PS 80 and water, $\log \mathrm{K}_{\mathrm{i,f_{PS80}/W}}$, of each compound. Alongside the solution solubilization strength, the closest alcohol-mixture solubilization strength $\log \mathrm{K}_{\mathrm{i,f_C/W}}$ derived from the LSER equations (Appendix, Chapter 10.5) is listed, together with the corresponding volumetric alcohol fraction in the respective simulating solvent. Figure 20 visually presents PS 80 solubilization strength over the selected concentration range. As a reminder, solubilization strength is defined as the logarithmic differential limiting solubilities in PS 80 solution or alcohol-water mixture ($\mathrm{S}_{\mathrm{i,f_{PS80}}}$ or $\mathrm{S}_{\mathrm{i,f_C}}$) and water ($\mathrm{S}_{\mathrm{i,W}}$). While a calculation of PS 80 solubilization strength, i.e. $\log \mathrm{K}_{\mathrm{i,f_{PS80}/W}}$, was possible at any given concentration, solubilization strength of alcohol-water mixtures $\log \mathrm{K}_{\mathrm{i,f_C/W}}$ could only be calculated in 10% v/v increments with a respective LSER model, as the solubilization in alcohol-water mixtures does not evolve linearly with the alcohol fraction. Hence, the closest alcohol concentration match for a given PS 80 concentration can only be found at said increments ranging from 0 to 100% alcohol in water.

Beside the results presented here, alignment of simulating solvents has also received some attention in literature, particularly for the plasticizer di(2-ethylhexyl) phthalate (DEHP). An empirical equation was derived by Jenke *et al.*, where the experimentally extracted amount of DEHP from polyvinyl chloride resin was utilized to calculate the polarity (as cohesion energy density) of the contact medium [7]. Medium polarity was then taken to find a coinciding EtOH fraction in an ethanol-water simulant. Table 24 shows the resulting EtOH concentrations in simulating solvent for simulation of three PS 80 solutions by Jenke *et al.* and from the method based on LSER equations presented here.

Another simulating solvent alignment was previously carried out for a 1.0% PS 80 solution, where 40% IPA in water were identified to best represent the solubilization strength based on an empirical mathematical function that specifically applies to DEHP [5].

Table 20. Alignment of simulating solvent solubilization strength for five exemplary leachables with a 0.01% PS 80 solution.

Compound	0.01% Polysorbate 80 w/v in water					
	$\log K_{i,PS80/W}$ [a)]	$\log K_{i,f_{PS80=0.01\%}/W}$	$\log K_{i,f_{EtOH}/W}$ [b)]	Aligned EtOH fraction	$\log K_{i,f_{IPA}/W}$ [b)]	Aligned IPA fraction
Pyridine	0.39	0.00	0.00	**0%**	0.00	**0%**
Benzothiazole	1.71	0.00	0.00	**0%**	0.00	**0%**
Ethylbenzene	2.96	0.03	0.00	**0%**	0.00	**0%**
Butylbenzyl phthalate	4.79	0.77	0.54	**10%**	0.51	**10%**
Dodecyl acrylate	6.07	1.97	2.32	**30%**	2.23	**30%**

a) Calculated from LSER eq. (28).
b) See appendix (10.5) for corresponding equations.

Table 21. Alignment of simulating solvent solubilization strength for five exemplary leachables with a 0.1% PS 80 solution.

Compound	0.1% Polysorbate 80 w/v in water					
	$\log K_{i,PS80/W}$	$\log K_{i,f_{PS80=0.1\%}/W}$	$\log K_{i,f_{EtOH}/W}$	Aligned EtOH fraction	$\log K_{i,f_{IPA}/W}$	Aligned IPA fraction
Pyridine	0.39	0.00	0.00	**0%**	0.00	**0%**
Benzothiazole	1.71	0.02	0.00	**0%**	0.00	**0%**
Ethylbenzene	2.96	0.26	0.21	**10%**	0.28	**10%**
Butylbenzyl phthalate	4.79	1.75	1.85	**30%**	1.53	**30%**
Dodecyl acrylate	6.07	3.02	3.26	**40%**	3.13	**40%**

Table 22. Alignment of simulating solvent solubilization strength for five exemplary leachables with a 0.5% PS 80 solution.

Compound	0.5% Polysorbate 80 w/v in water					
	$\log K_{i,PS80/W}$	$\log K_{i,f_{PS80=0.5\%}/W}$	$\log K_{i,f_{EtOH}/W}$	Aligned EtOH fraction	$\log K_{i,f_{IPA}/W}$	Aligned IPA fraction
Pyridine	0.39	0.00	0.00	**0%**	0.00	**0%**
Benzothiazole	1.71	0.09	0.06	**10%**	0.11	**10%**
Ethylbenzene	2.96	0.71	0.54	**20%**	0.60	**20%**
Butylbenzyl phthalate	4.79	2.44	2.56	**40%**	2.59	**50%**
Dodecyl acrylate	6.07	3.72	3.26	**40%**	3.85	**50%**

Table 23. Alignment of simulating solvent solubilization strength for five exemplary leachables with a 1.0% PS 80 solution.

Compound	1.0% Polysorbate 80 w/v in water					
	$\log K_{i,PS80/W}$	$\log K_{i,f_{PS80=1.0\%}/W}$	$\log K_{i,f_{EtOH}/W}$	Aligned EtOH fraction	$\log K_{i,f_{IPA}/W}$	Aligned IPA fraction
Pyridine	0.39	0.01	0.00	**0%**	0.00	**0%**
Benzothiazole	1.71	0.16	0.26	**20%**	0.11	**10%**
Ethylbenzene	2.96	0.96	0.96	**30%**	0.94	**30%**
Butylbenzyl phthalate	4.79	2.74	2.56	**40%**	2.59	**50%**
Dodecyl acrylate	6.07	4.02	4.21	**50%**	3.85	**50%**

Table 24. Alignment of ethanol concentration in simulating solvent for DEHP extraction with three PS 80 concentrations.

PS 80 concentration	DEHP[a)] $\log K_{f_{PS80}/W}$	Aligned EtOH fraction	Proposed EtOH fraction [7]
0.2%	4.87	50%	36%
1.0%	5.57	50%	49%
5.0%	6.27	60%	61%

a) Di(2-ethylhexyl) phthalate

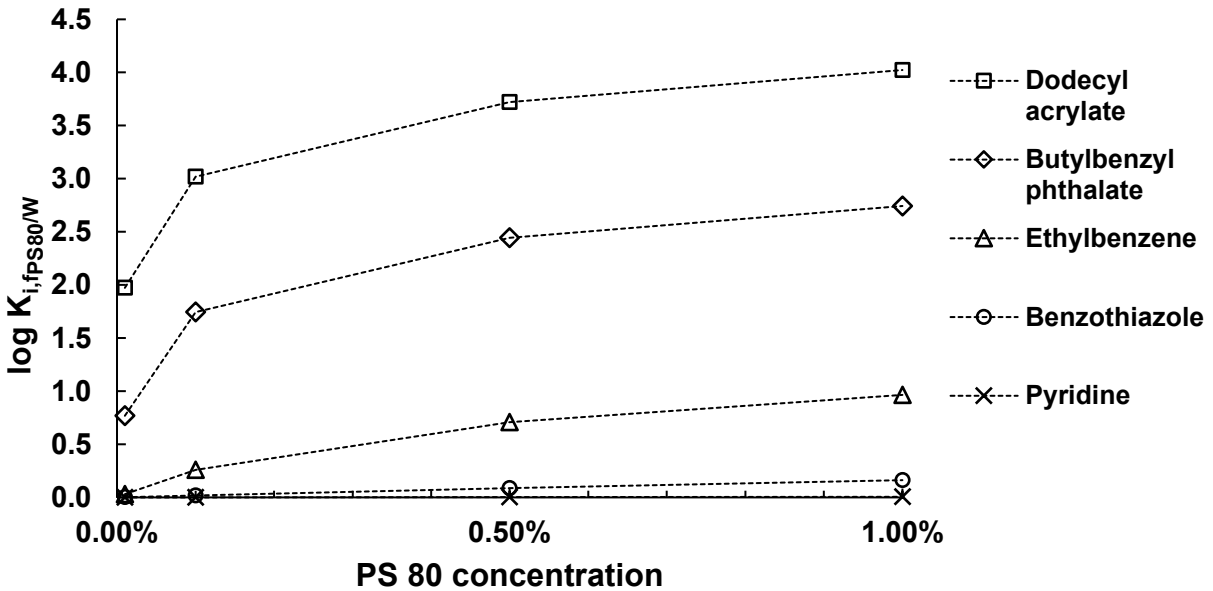

Figure 20. Solubilization strength of PS 80 solutions ranging from 0.01% to 1.0% w/v for the five selected leachables used in simulating solvent alignment.

4.2.2 Discussion

LSER models help establish solubilization of chemical compounds for which no experimental data is available or (easily) accessible. In the LSER system, five comparably scaled system parameters are multiplied with solute descriptors of the desired chemical to yield a partition coefficient for the solute in question. Linear, concentration dependent solubilization in solutions containing PS 80 micelles allow the simple conversion of micelle to water partition coefficients into solubilization strength of a PS 80 solution. The calculations of simulating solvent composition at increasing PS 80 fractions reveal the concentration dependency of PS 80 solubilization. At 0.01% PS 80, even the most hydrophobic model compound dodecyl acrylate is best represented by only 30% v/v alcohol in water. As expected, increasing the PS 80 concentration demands higher alcohol fractions in simulating solvents for four of the five model compounds. The results also clearly demonstrate that solubilization is dependent on the chemical identity of extractables, with suggested alcohol fractions ranging from 0 to 50% at the two higher PS 80 concentrations (0.5% and 1.0%). Pyridine highlights a rather interesting case in this discussion, as even at 1.0% PS 80, the best representative simulating solvent based on solubilization strength of the solution is pure water (i.e., 0% alcohol). As pyridine, used in the production of polymers and rubbers, is a toxic solvent [233], extraction of significant amounts of the chemical from the contact material during a simulation study would be cause for further investigations. Simulating solvents comprising 50% EtOH or IPA would increase the extraction of pyridine twofold compared to water, thereby misrepresenting the actual extraction strength of the PS 80 solution as a surrogate pharmaceutical formulation. This demonstrates the usefulness of aligning simulating solvent compositions with the actual solubilization propensity of a pharmaceutical solution, because scientifically justified focus can be laid on other leachables that more readily partition to the contact solution.

Both IPA and EtOH are proposed components of simulating solvents in chemical safety assessments [7, 46]. The calculated alcohol concentrations allow a direct comparison between the two alcohols. Based on the LSER model calculations for the five compounds presented, solubilization in IPA- and EtOH-water mixtures is quite similar, with alcohol content in simulating solvents for a particular PS 80 solution differing by only 10% v/v at most. An appropriate choice of either alcohol for simulating solvents can thus, according to the simulating solvent alignment of the assigned leachables, be made solely on technical and experimental considerations without severely affecting solubilization properties of the solvent.

Considering the attempts at simulating solvent alignment in literature, a comparison between the empirical equation for DEHP presented by Zdravkovic [5] and the LSER system results in a rather large disconnect between suggested IPA concentrations in simulating solvents. From the LSER system, 70% IPA are suggested as alcohol proportion in water to represent 1.0% PS 80, compared to 40% based on Zdravkovic's equation. The large disconnect between the results could arise from the LSER equations applied for the calculation of solubilization strengths, as none of them incorporated many chemicals as hydrophobic as DEHP in their regression.

A similar approach by Jenke *et al.* (Table 24) offers practically identical forecast EtOH concentrations to simulate DEHP extraction in comparison with the LSER system. For 1% and 5% PS 80, around 50% and 60% EtOH in water were determined as simulating solvent, respectively. For 0.2% PS 80, however, calculations with the LSER equations suggest a greater EtOH concentration compared to the polarity-based equation. In contrast to the literature data, an overall tendency towards overestimation of alcohol content in simulating solvents by the employed LSER equations can be observed, at least for DEHP. This overestimation, however, is generally tolerable when considering the intended use of the models in chemical safety assessments, where safety margins are included to generate worst-case data [20]. Further experimental inspection of

DEHP as a migrant originating from contact polymers will be presented in the case study below, allowing a more nuanced discussion.
LSER-based simulating solvent alignment proves a great opportunity to apply state-of-the-art physicochemical modeling to chemical safety assessments for its straightforward use of thermodynamically orientated LSER equations and solute descriptors, which are easy to retrieve from publicly available sources. A valuable improvement of simulation studies is anticipated through alignment, as the solubilization of the pharmaceutical formulation will be closely resembled by the tailored simulating solvent. Aligned solubilization leads to aligned extraction propensity of the medium towards contact materials if no relevant adsorption of solution constituents to or swelling of the contact material occurs, and accordingly, the quantitative extractable profile found in a simulation study is more representative of the leachable profile ascertained under real-use conditions in the drug product.

4.3 Interactions of Parenteral Excipients Affecting Solubilization

In the previous sections, solubilization in aqueous solution by one of the most formulated parenteral excipients, polysorbate 80, was thoroughly characterized and scrutinized. In the following, solubilization caused by PS 80 and other commonly encountered parenteral excipients is investigated considering potential novel solubilization phenomena arising from simultaneous application of multiple excipients. Model equations predicting solubilization of individual excipients were retrieved from literature or established here.

Interactions of excipients were assessed by experimentally determining the logarithmic differential solubilities in medium and water, $\log \frac{S_{i,M}}{S_{i,W}} \approx \log K_{i,M/W}$ of three model organic chemicals: 2,4-dinitrotoluene (DNT), naphthalene (NAP) and carbazole (CAZ).

If $\log K_{i,M/W}$ is assumed to arise from additive solubilization of individual components in the formulation, it consists of the solubilization strengths of the respective fractions f of the excipients present, i.e. $K_{i,f_{PS80}/W}$, $K_{i,f_{EtOH}/W}$, $K_{i,f_{NaCl}/W}$, $K_{i,f_{Dextrose}/W}$, and $K_{i,f_{EDTA}/W}$. Where available, LSER models were used to calculate $\log K_{i,f_{Excipient}/W}$ (eq. (28) for PS 80 and eq. (A3) for NaCl [111] solutions as well as eq. (A4) for ethanol-water mixtures [96]). $\mathrm{Log}\, K_{i,M/W}$ in mixtures containing PS 80, ethanol, and/ or NaCl was calculated from the respective LSER models assuming additive solubilization behavior according to the following equation:

$$\log K_{i,M/W} = \log \left(K_{i,f_{PS80}/W} + K_{i,f_{EtOH}/W} + K_{i,f_{NaCl}/W} - (n-1) \right) \quad (35)$$

where n is the number of excipients (2 or 3) and f the respective fraction of excipient in the solution.

4.3.1 Results

Table 25 lists the result for 38 different aqueous excipient mixtures. Line 1 represents pure water (no excipients) and accordingly has a $\log K_{i,M/W}$ value of 0 $\left(= \log \frac{S_{i,W}}{S_{i,W}}\right)$, while subsequent lines in bold text (line number 12, 21, and 30) indicate increasing PS 80 concentration in the mixture. As both EDTA and dextrose showed no or only marginal solubilization capacity in all mixtures, the results for mixtures containing these excipients were not as thoroughly reported as for other excipients investigated.

Table 25. Experimental and predicted $\log K_{i,M/W}$ of 2,4-dinitrotoluene (DNT), naphthalene (NAP) and carbazole (CAZ) in aqueous excipient mixtures.

	Excipient[a)]						$\log K_{i,M/W}$					
#	PS (%)	EDTA (%)	NaCl (%)	BzOH (%)	EtOH (%)	Dex (%)	DNT exp.	DNT *pred.*	NAP exp.	NAP *pred.*	CAZ exp.	CAZ *pred.*
1	**-**	**-**	**-**	**-**	**-**	**-**	**0.00**	***0.00***	**0.00**	***0.00***	**0.00**	***0.00***
2	-	-	-	-	10	-	0.08	*0.17*	0.25	*0.21*	0.29	*0.35*
3	-	-	-	1.5	-	-	0.08		0.09		0.09	
4	-	-	0.9	-	-	-	-0.01	*-0.03*	-0.03	*-0.03*	-0.03	*-0.03*
5	-	0.11	-	-	-	-	0.01		0.00		-0.01	
6	-	-	-	-	-	5	0.00		-0.03		0.00	
7	-	-	-	1.5	10	-	0.19		0.22		0.39	
8	-	-	0.9	-	10	-	0.09	*0.15*	0.07	*0.19*	0.27	*0.34*
9	-	-	0.9	1.5	-	-	0.09		0.05		0.08	
10	-	-	0.9	1.5	10	-	0.17		0.16		0.40	
11	-	0.11	0.9	1.5	10	5	0.17		0.13		0.38	
12	**0.01**	**-**	**-**	**-**	**-**	**-**	**0.02**	***0.00***	**0.05**	***0.06***	**0.38**	***0.31***
13	0.01	-	-	-	10	-	0.10	*0.17*	0.28	*0.24*	0.55	*0.52*
14	0.01	-	-	1.5	-	-	0.10		0.16		0.38	
15	0.01	-	0.9	-	-	-	-0.01	*-0.03*	0.04	*0.02*	0.36	*0.30*
16	0.01	-	-	1.5	10	-	0.19		0.32		0.52	
17	0.01	-	0.9	-	10	-	0.07	*0.15*	0.22	*0.22*	0.54	*0.51*
18	0.01	-	0.9	1.5	-	-	0.08		0.04		0.33	
19	0.01	-	0.9	1.5	10	-	0.17		0.31		0.50	
20	0.01	0.11	0.9	1.5	10	5	0.18		0.24		0.49	
21	**0.1**	**-**	**-**	**-**	**-**	**-**	**0.06**	***0.04***	**0.41**	***0.44***	**1.06**	***1.10***
22	0.1	-	-	-	10	-	0.13	*0.20*	0.55	*0.53*	1.08	*1.14*
23	0.1	-	-	1.5	-	-	0.14		0.52		0.95	
24	0.1	-	0.9	-	-	-	0.06	*0.01*	0.41	*0.43*	1.03	*1.10*
25	0.1	-	-	1.5	10	-	0.23		0.67		1.03	
26	0.1	-	0.9	-	10	-	0.12	*0.18*	0.54	*0.52*	1.06	*1.14*
27	0.1	-	0.9	1.5	-	-	0.13		0.54		0.97	
28	0.1	-	0.9	1.5	10	-	0.21		0.63		1.05	
29	0.1	0.11	0.9	1.5	10	5	0.21		0.59		1.04	
30	**0.5**	**-**	**-**	**-**	**-**	**-**	**0.21**	***0.17***	**1.00**	***1.00***	**1.64**	***1.78***
31	0.5	-	-	-	10	-	0.26	*0.29*	1.04	*1.03*	1.65	*1.79*
32	0.5	-	-	1.5	-	-	0.29		1.10		1.56	
33	0.5	-	0.9	-	-	-	0.20	*0.15*	0.96	*1.00*	1.65	*1.78*
34	0.5	-	-	1.5	10	-	0.35		1.15		1.59	
35	0.5	-	0.9	-	10	-	0.26	*0.28*	1.03	*1.02*	1.67	*1.79*
36	0.5	-	0.9	1.5	-	-	0.29		1.12		1.56	
37	0.5	-	0.9	1.5	10	-	0.36		1.16		1.59	
38	0.5	0.11	0.9	1.5	10	5	0.36		1.17		1.61	

a) Abbreviations: PS = polysorbate 80; BzOH = benzyl alcohol; EtOH = ethanol; Dex = dextrose; NaCl = sodium chloride.

4.3.2 Discussion

As shown, LSER predictions for single excipients nearly coincide with the experimentally found values. Even for the lower end of PS 80 concentration, i.e. 0.01% w/v in water, the LSER model equation provides accurate predictions, confirming that solubilization in PS 80 solutions grows linearly with PS 80 concentration above the CMC. In excipient mixtures, further solubilization mechanisms can affect the observed chemical solubility. Particularly, the effect excipients have on micelle formation and micellar solubilization of PS 80 is discussed in the following. The state of PS 80s micellar microenvironment (i.e., average aggregation number or micelle size) in presence of other excipient was not considered here, as only interactions affecting a solution's macroscopic solubilization were of interest.

Depending on their concentration in the formulation, short-chain alcohols like ethanol break some of the strong hydrogen bonds between water molecules [234], leading to higher solubility of surfactant monomers and thus a higher CMC for nonionic surfactants [207]. At 10% v/v ethanol, however, the effect on the CMC is negligible, as the CMC of PS 80 is comparatively low [235]. The increase in CMC and resulting compressed micellar phase therefore has no observable effect on solubilization. Partitioning of hydrophilic solutes (benzaldehyde and benzyl alcohol) into nonionic micelles remained mostly unaffected in the presence of 15% v/v ethanol in one study [186]. Results in Table 25 show that even for the more hydrophobic solutes examined here, the solubilization of micelles (i.e., the partitioning between ethanol-water mixture and micelles) is unaffected by the presence of ethanol. At lower PS 80 concentrations (0.01%), the solubilization effect of 10% ethanol on the bulk aqueous phase dominates (experiment #13, Table 25), whereas at higher PS 80 concentrations (0.5%), $\log \mathrm{K_{i,M/W}}$ is dictated by micellar solubilization (experiment #31). Hence, assuming additive solubilization behavior of PS 80 at the concentrations investigated and 10% ethanol is appropriate, as shown by the conformity of predicted and experimental partition coefficients.

Solubilization behavior of benzyl alcohol in water was found to be complex, despite the small number of chemicals tested. As a not completely water-miscible cosolute, 1.5% benzyl alcohol increased aqueous solubility of all three solutes (experiment #3). In contrast to ethanol, however, solubilization (i.e., $\log \mathrm{K_{i,M/W}}$) did not increase with hydrophobicity of solutes (as indicated by $\log \mathrm{K_{i,O/W}}$). In PS 80 micellar solutions, benzyl alcohol partitions into micelles, as NMR spectroscopy revealed in one study, where it intercalates the polar head groups of surfactant molecules, changing the micellar microenvironment ("mixed micelles") [236], while also slightly lowering the CMC through this mechanism [237]. Partitioning of benzyl alcohol to micelles is also demonstrable by inserting benzyl alcohol's respective solute descriptors in LSER eq. (28), which yields a partition coefficient of $\log \mathrm{K_{i,PS80/W}} = 1.03$. With 1.5% benzyl alcohol in solution, the effect it conveys on PS 80 micelles is somewhat considerable and can be attested to altered solubilization of chemicals in the micellar environment. For DNT and NAP, the presence of benzyl alcohol in micelles increases their solubilization at every PS 80 concentration tested compared to a pure PS 80 solution (experiments #14, 23, and 32). For CAZ, an opposing effect is observed, where solubilization decreased at every PS 80 concentration. The hydrophobic drug itraconazole displayed similar behavior as CAZ in nonionic surfactant solutions containing benzyl alcohol [238]. Change in micellar solubilization through benzyl alcohol seems to depend on whether benzyl alcohol in- or decreases favorable molecular interactions for the solute within the micellar microenvironment. To better understand how the specific interaction between benzyl alcohol and PS 80 as well as other organic excipient/ surfactant micelle interactions affect micellar solubilization, detailed studies of the microscopic micellar environment would be necessary. Even so, a thermodynamic model more sophisticated than the LSER equations presented here would

be needed to forecast chemical solubilization relative to PS 80 and benzyl alcohol concentration. As many organic excipients have potential to interact with micelles in pharmaceutical solutions, such efforts would quickly become futile and would likely not significantly contribute to the determination of a solution's solubilization strength. This is best demonstrated by comparison of chemical solubilization in presence of PS 80 alone and in combination with benzyl alcohol in Table 25. Here, $\log K_{i,M/W}$ values show notable, but minor differences that do not exceed ± 0.1 log units at most, compared to an increase of 1 log unit and more when solubilization in a PS 80 solution and water are contrasted (e.g. experiment #30).

The molecular theory of micellization in presence of salts has received considerable attention in literature, especially pertaining to ionic surfactant micelles [239-246]. Regarding nonionic surfactant micelles, physiological saline (0.9% NaCl) has a negligible effect on the CMC and solubilization, as the hydrophilic ions solvated in the aqueous phase do not penetrate the micelles [247-249]. For polysorbates, one study found no significant influence of NaCl on neither CMC nor micellar solubilization of two dyes, even at concentrations exceeding 0.9% [156]. The three solutes tested here confirm this observation, with 0.9% NaCl slightly decreasing solubility in the bulk aqueous solution (experiment #4), which was excellently predicted by the LSER model, but not affecting micellar solubilization. Likewise, 5% dextrose slightly decreased the bulk aqueous solubility of NAP without influencing the solubilization of other solution components (experiment #6), e.g. PS 80. In fact, since dextrose is highly hydrophilic, prediction of its micelle to water partitioning yields $\log K_{i,PS80/W} = -2.58$ according to eq. (28), reinforcing that virtually no dextrose partitions to and interacts with the micellar phase, unlike e.g. benzyl alcohol as explained above. Furthermore, the chelating agent EDTA, used as a divalent sodium salt, was found to not affect (micellar) solubilization alone or in excipient mixtures at a concentration of 0.11%.

When more than one parenteral excipient is formulated together with PS 80, a combination of the effects detailed above influences solubilization of the three experimental test solutes. Combining PS 80, ethanol, and benzyl alcohol leads to further solubilization of DNT and NAP, as the effect of ethanol on the bulk aqueous phase and benzyl alcohol on the micellar phase merge (experiments #16, 25, and 34). For CAZ, a slight reduction compared to an ethanol/ PS80-mixture is observed, as benzyl alcohol impedes micellar solubilization of CAZ. In mixtures of PS 80, NaCl, ethanol, and/ or benzyl alcohol, NaCl has a minor salting out effect on the bulk water phase, while ethanol/ benzyl alcohol affect (micellar) solubilization at all tested PS 80 concentrations as discussed previously (e.g. experiment #25). Accordingly, assumption of additive solubilization holds true even for more complex excipient mixtures.

NAP displays unexpectedly low solubility in a mixture of 0.01% PS 80, 1.5% benzyl alcohol and 0.9% NaCl (experiment #18). The test protocol was repeated to rule out experimental error. At higher PS 80 concentrations, no similar observation can be made, perhaps suggesting an interaction only in this particular mixture.

Despite the results in Table 25 being internally consistent, they were gathered for only a small number of crystalline chemicals. The three compounds DNT, NAP, and CAZ are of low to moderate aqueous solubility and have high enough micellar partition coefficients to observe changes in the different excipient mixtures containing PS 80. The somewhat limited chemical diversity was further owed to emulsification in excipient mixtures when test compounds contained hydroxyl groups (e.g. phenols), which is a shortcoming of the employed solubility method (3.2.1.3). Although in a reference phase approach with diluted solute concentrations no emulsification would be expected, it lacks the required precision of experimental values compared to direct solubility measurements, as detailed in Chapter 4.1.2.4. This precision was crucial to determine small solubilization effects in the test solutions. Whether further solubilization phenomena outside the chemical sphere of the tested compounds could apply thus remains

unclear. Still, from the results presented here as well as in the literature, no meaningful interaction with micelles was deduced for the majority of incorporated excipients. It is consequently unlikely that chemicals of different polarity, size, or hydrogen bonding would show unexpected solubilization behavior in these mixtures (except PS80/ benzyl alcohol).

When available, LSER models accurately predict solubilization elicited by parenteral excipients. Interaction of excipients, especially with micelle forming solubilizers such as PS 80, must be considered when characterizing the solubilization capacity of a pharmaceutical solution. The addition of excipients to PS 80 solutions can alter micellar solubilization mechanisms, e.g. through incorporation of an excipient into the micellar phase, which was demonstrated by the addition of 1.5% benzyl alcohol to excipient mixtures containing PS 80 micelles. The impact of such interactions on solubilization strength is, however, minor. Therefore, the solubilization of organic chemicals in a mixture of excipients, expressed by $\log K_{i,M/W}$, can be treated as a sum of individual contributions towards solubilization capacity without sacrificing necessary accuracy.

In theory, this allows the application of individual model equations to find the solubilization strength of a complex mixture with eq. (35). To date, however, only few comprehensive models that can predict solubilization exerted by relevant parenteral excipients have been presented, which hinders precise prediction of $\log K_{i,M/W}$. Fortunately, only considering the excipient exerting the greatest solubilization in an aqueous parenteral formulation (e.g. PS 80 ≥ 0.1%) can already yield accurate forecasts of solubilization strength.

4.4 Migration from Polymer to Contact Solutions – Case Study

Quantitative prediction of migration processes of small molecule constituents from polymers to contact solutions is a central objective of mass transport modeling. In the previous sections, the underlying mechanisms supporting the modeling approach were defined and tested, with a particular attention for partitioning and solubilization in parenteral formulations and their simulating solvents. The experimental determination of final leachable concentrations in a drug product is, to this point, an unavoidable step to establish patient exposure to a particular leachable if extractable data cannot demonstrate safety of the material, according to the intended use of the drug product and the toxicological assessment. The prediction of leachable accumulation in a drug product through modeled diffusion in polymers and, more importantly, predicted partitioning of leachables to a drug product could improve experimental designs or replace experimental testing in certain situations.

4.4.1 Results

To test the predictive capability of LSER models that were introduced in this thesis in a realistic scenario, a case study was carried out to investigate migration of five model leachables from loaded polymers to various contact solutions. Resulting migration profiles into all contact solutions are shown in Figure 21 a)–i), with the exception of phosphate buffered water, where after eight weeks equilibration time no leachable was detected. To more easily compare migration of individual model leachables from PDMS into different solutions, corresponding migration curves were plotted in Figure 22 a)–e).
Partitioning between a loaded polymer and a contacting medium $\log K_{P/M}$ was calculated via a thermodynamic cycle from $\log K_{P/W}$ (Table 9) and $\log K_{M/W}$, as expressed by eq. (5):

$$\log K_{i,P/M} = \log K_{i,P/W} - \log K_{i,M/W} \quad (5)$$

Final leachable concentrations in the contact medium were then calculated using eq. (3):

$$C_{i,M} = \frac{C_{i,P}^{0}}{\left(\frac{V_M}{V_P} + K_{i,P/M}\right)} \quad (3)$$

Initial polymer load $C_{i,P}^{0}$ was determined by loading four polymer disks and immediately extracting them according to the experimental protocol (Chapter 3.2.4). Polymer disks are expected to have a uniformly distributed leachable load across the polymer matrix, as leachable concentration in the adjacent loading solution reached equilibrium. From $C_{i,P}^{0}$ and predicted $K_{i,P/M}$, the final leachable concentration $C_{i,M}$ was calculated with eq. (3). Equilibrium concentrations in the three placebo solutions (see Table 10 for details) were forecast only considering PS 80, disregarding the smaller impact other excipients have on solubilization at a PS 80 concentration of 0.5%, as discussed in Chapter 4.3. To the right of the migration profiles in Figure 21, respective predicted equilibrium concentrations are plotted, with error bars representing a range of ±0.5 log units of the predicted partition coefficient, converted to upper and lower limit concentrations. With standard deviations of typical LSER model equations typically ranging from 0.1 to 0.3 log units, 0.5 log units are deemed an acceptable error range when multiple LSER models are combined via eq. (5). The range of error bars is subject to the initial polymer concentration and the predicted partition coefficient between polymer and medium. Predicted and experimental equilibrium

leachable concentrations are listed in the tables below. Corresponding logarithmic polymer to medium partition coefficients $\log K_{i,P/M}$ from final leachable concentrations in polymer and medium and their respective predicted values can be retrieved from the appendix (10.4).

Table 26. Predicted (eq. (3)) and experimental equilibrium concentrations in PS 80 solutions from loaded PDMS disks, standard deviations in parentheses.

	$C_{i,f_{PS80=0.5\%}}$ (µg/mL)		$C_{i,f_{PS80=0.1\%}}$ (µg/mL)		$C_{i,f_{PS80=0.01\%}}$ (µg/mL)	
Compound	Predicted	Experimental	Predicted	Experimental	Predicted	Experimental
1,2-Benzanthraquinone	2.61	1.75 (0.23)	1.94	0.96 (0.04)	0.56	0.14 (0.02)
Di-(2-ethylhexyl) phthalate	2.57	1.59 (0.05)	1.25	0.23 (0.00)	0.19	n.d.[a)]
9-Phenylcarbazole	3.29	2.66 (0.00)	1.86	0.98 (0.01)	0.31	0.10 (0.00)
Oleamide	2.46	2.54 (0.08)	1.20	1.07 (0.06)	0.18	0.04 (0.00)
3,5-Di-tert-butyl-4-hydroxybenzaldehyde	0.14	0.14 (0.03)	0.05	0.06 (0.00)	0.01	0.01 (0.00)

a) not determined

Table 27. Predicted (eq. (3)) and experimental equilibrium concentrations in placebo media containing 0.5% PS 80 from loaded PDMS disks, standard deviations in parentheses.

	$C_{i,Placebo\ 1}$ (µg/mL)		$C_{i,Placebo\ 2}$ (µg/mL)		$C_{i,Placebo\ 3}$ (µg/mL)	
Compound	Predicted	Experimental	Predicted	Experimental	Predicted	Experimental
1,2-Benzanthraquinone	2.61	2.23 (0.31)	2.61	2.12 (0.13)	2.61	1.94 (0.38)
Di-(2-ethylhexyl) phthalate	2.57	1.76 (0.03)	2.57	1.61 (0.06)	2.57	0.77 (0.06)
9-Phenylcarbazole	3.29	2.72 (0.03)	3.29	2.75 (0.05)	3.29	1.63 (0.06)
Oleamide	2.46	4.92 (0.03)	2.46	4.24 (0.07)	2.46	4.36 (0.49)
3,5-Di-tert-butyl-4-hydroxybenzaldehyde	0.14	0.23 (0.00)	0.14	0.19 (0.05)	0.14	0.16 (0.00)

Table 28. Predicted (eq. (3)) and experimental equilibrium concentrations in ethanol-water mixtures and aqueous buffer from loaded PDMS disks, standard deviations in parentheses.

	$C_{i,f_{EtOH=20\%}}$ (µg/mL)		$C_{i,f_{EtOH=50\%}}$ (µg/mL)		$C_{i,W}$ (µg/mL)	
Compound	Predicted	Experimental	Predicted	Experimental	Predicted	Experimental
1,2-Benzanthraquinone	0.76	0.11 (0.00)	2.74	2.64 (0.46)	0.10	n.d.
Di-(2-ethylhexyl) phthalate	0.00	n.d.	2.39	1.20 (0.09)	0.00	n.d.
9-Phenylcarbazole	0.04	0.03 (0.00)	2.91	2.89 (0.07)	0.00	n.d.
Oleamide	0.00	n.d.	2.01	2.53 (0.09)	0.00	n.d.
3,5-Di-tert-butyl-4-hydroxybenzaldehyde	0.08	0.08 (0.00)	0.33	0.37 (0.02)	0.01	n.d.

Table 29. Predicted (eq. (3)) and experimental equilibrium concentrations in 0.5% PS 80 solution from loaded LDPE disks, standard deviations in parentheses.

	$C_{i,f_{PS80=0.5\%}}$ (µg/mL)	
Compound	Predicted	Experimental
1,2-Benzanthraquinone	1.96	0.86 (0.04)
Di-(2-ethylhexyl) phthalate	3.43	2.95 (0.15)
9-Phenylcarbazole	3.44	2.43 (0.02)
Oleamide	0.68	0.57 (0.01)
3,5-Di-tert-butyl-4-hydroxybenzaldehyde	0.08	0.06 (0.00)

a)

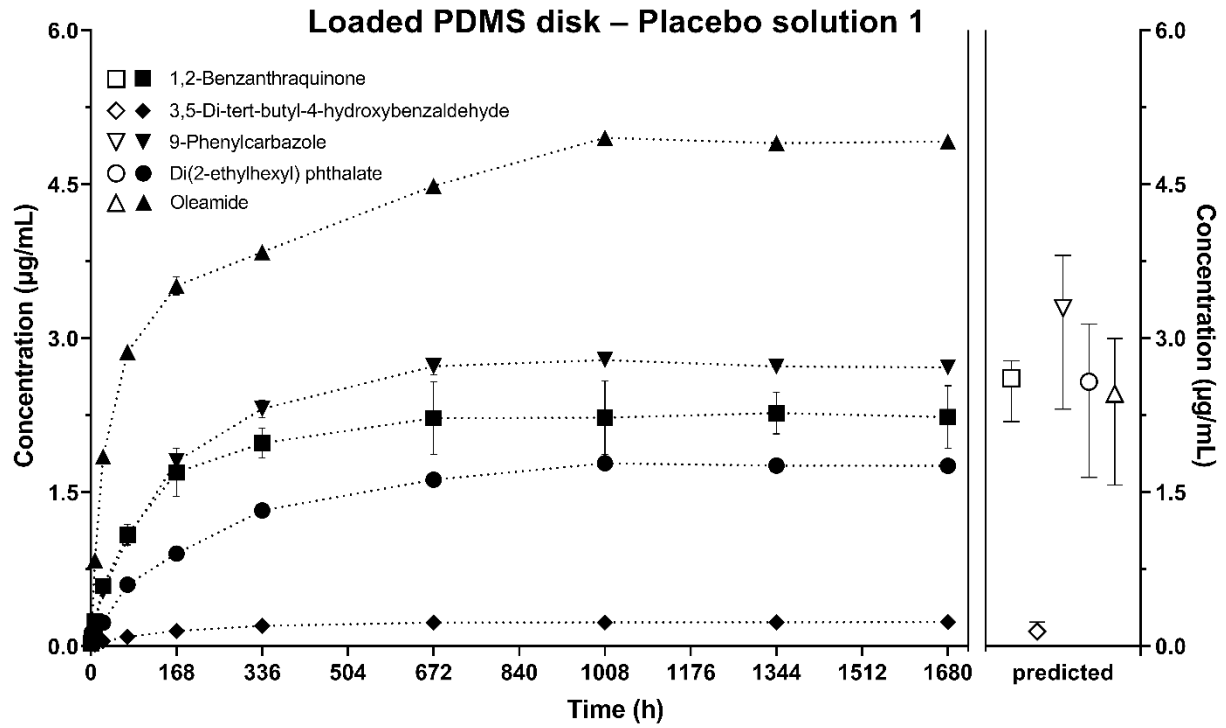

b)

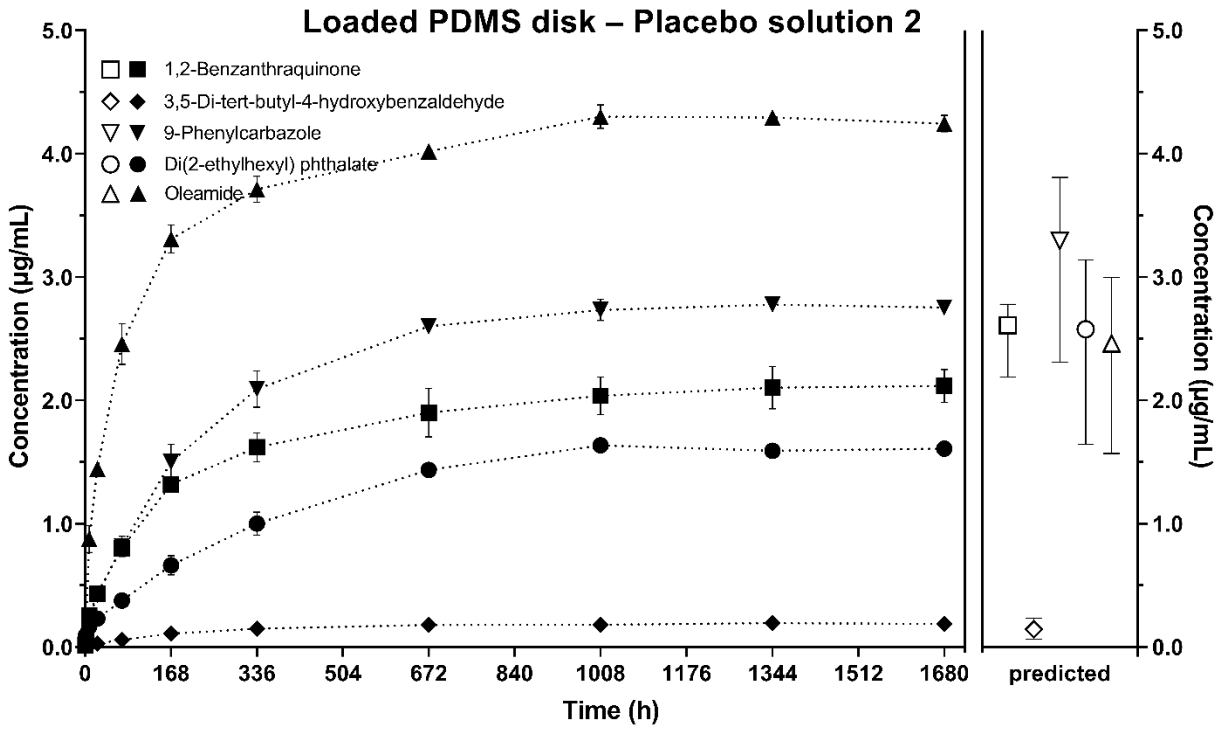
Loaded PDMS disk – Placebo solution 2
1,2-Benzanthraquinone
3,5-Di-tert-butyl-4-hydroxybenzaldehyde
9-Phenylcarbazole
Di(2-ethylhexyl) phthalate
Oleamide
Concentration (µg/mL)
Time (h)
predicted

c)

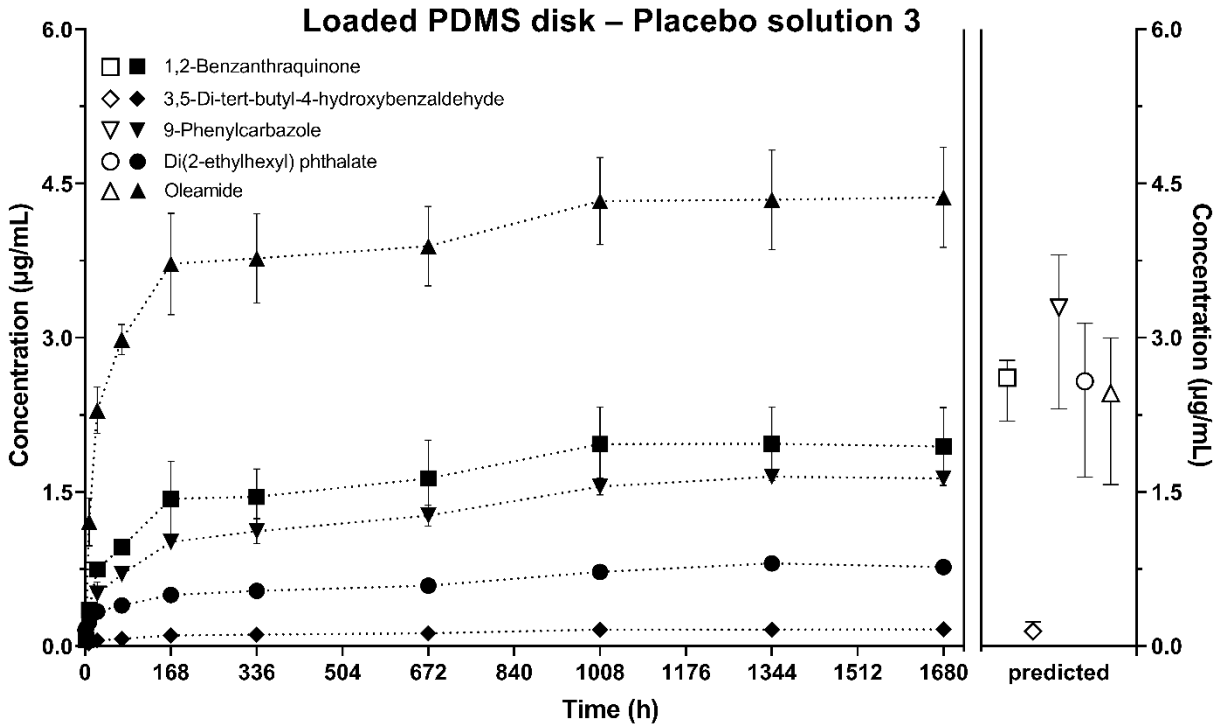
Loaded PDMS disk – Placebo solution 3
1,2-Benzanthraquinone
3,5-Di-tert-butyl-4-hydroxybenzaldehyde
9-Phenylcarbazole
Di(2-ethylhexyl) phthalate
Oleamide
Concentration (µg/mL)
Time (h)
predicted

d)

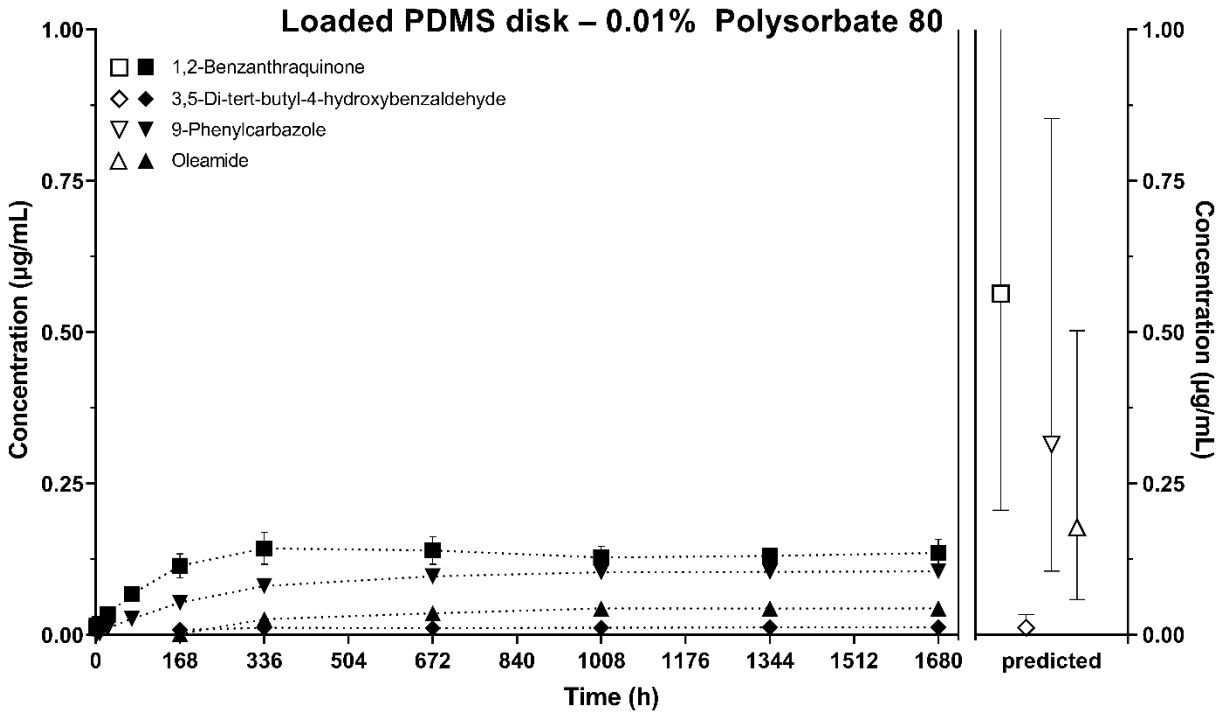
Loaded PDMS disk – 0.01% Polysorbate 80
1,2-Benzanthraquinone
3,5-Di-tert-butyl-4-hydroxybenzaldehyde
9-Phenylcarbazole
Oleamide
Concentration (µg/mL)
1.00
0.75
0.50
0.25
0.00
0
168
336
504
672
840
1008
1176
1344
1512
1680
predicted
Time (h)

e)

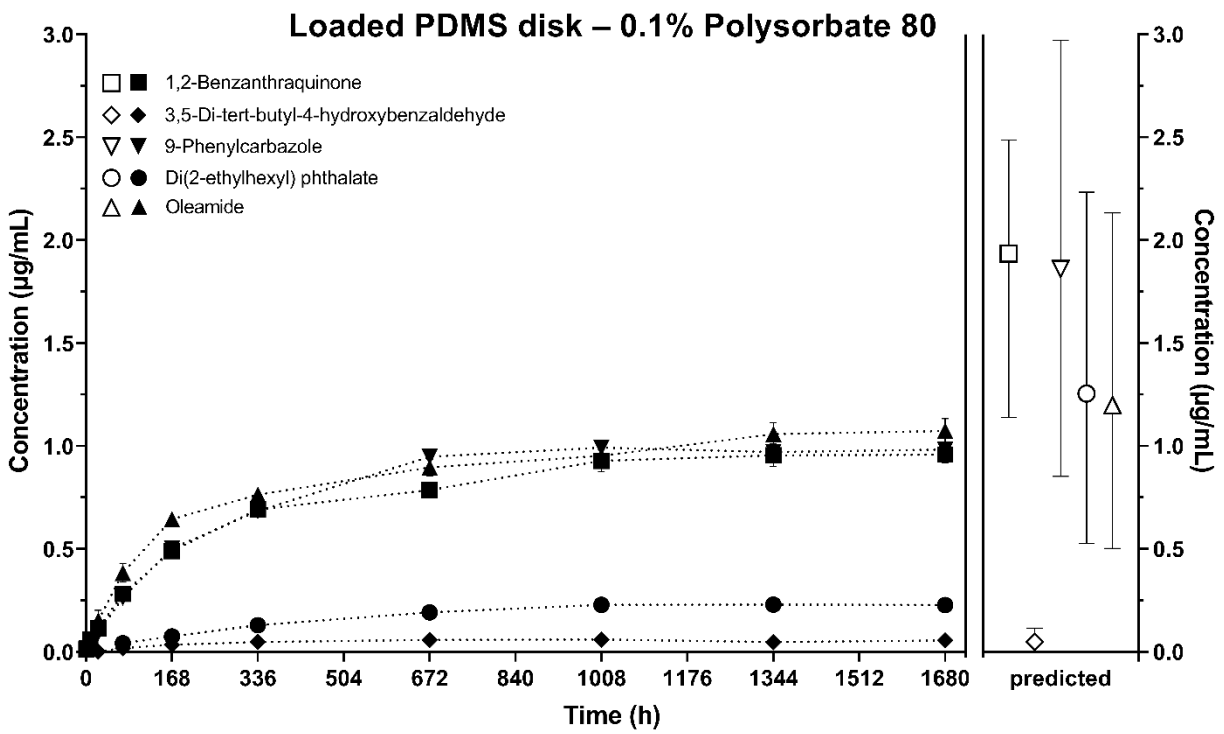
Loaded PDMS disk – 0.1% Polysorbate 80
1,2-Benzanthraquinone
3,5-Di-tert-butyl-4-hydroxybenzaldehyde
9-Phenylcarbazole
Di(2-ethylhexyl) phthalate
Oleamide
Concentration (µg/mL)
3.0
2.5
2.0
1.5
1.0
0.5
0.0
0
168
336
504
672
840
1008
1176
1344
1512
1680
predicted
Time (h)

f)

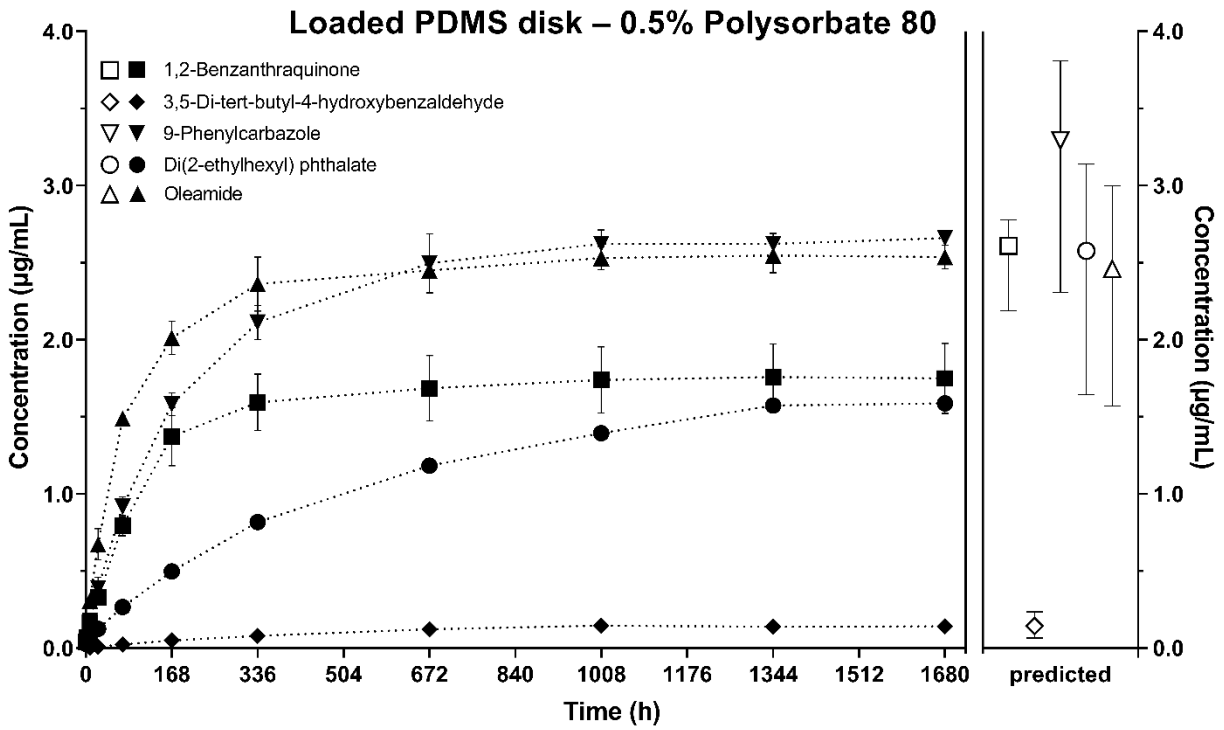
Loaded PDMS disk – 0.5% Polysorbate 80
1,2-Benzanthraquinone
3,5-Di-tert-butyl-4-hydroxybenzaldehyde
9-Phenylcarbazole
Di(2-ethylhexyl) phthalate
Oleamide
Concentration (µg/mL)
Time (h)
0
168
336
504
672
840
1008
1176
1344
1512
1680
predicted
0.0
1.0
2.0
3.0
4.0

g)

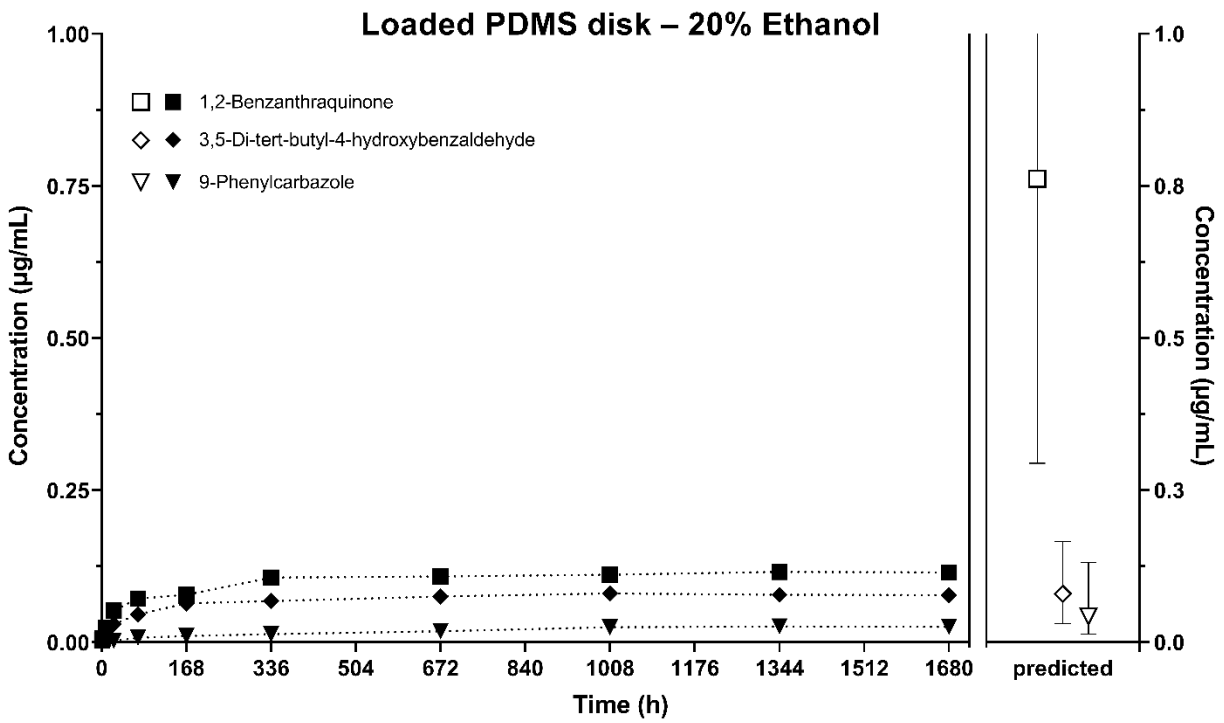
Loaded PDMS disk – 20% Ethanol
1,2-Benzanthraquinone
3,5-Di-tert-butyl-4-hydroxybenzaldehyde
9-Phenylcarbazole
Concentration (µg/mL)
Time (h)
0
168
336
504
672
840
1008
1176
1344
1512
1680
predicted
0.00
0.25
0.50
0.75
1.00
0.0
0.3
0.5
0.8
1.0

h)

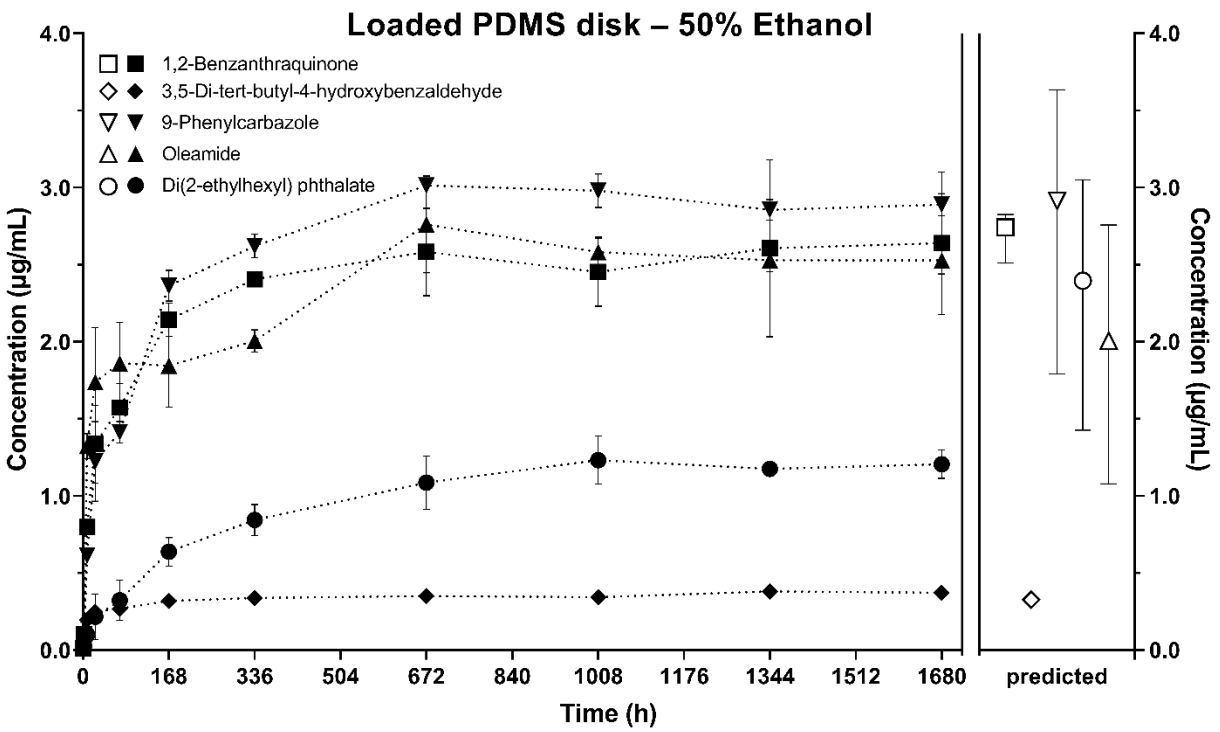
Loaded PDMS disk – 50% Ethanol
1,2-Benzanthraquinone
3,5-Di-tert-butyl-4-hydroxybenzaldehyde
9-Phenylcarbazole
Oleamide
Di(2-ethylhexyl) phthalate
Concentration (µg/mL)
Time (h)
0
168
336
504
672
840
1008
1176
1344
1512
1680
predicted
0.0
1.0
2.0
3.0
4.0

i)

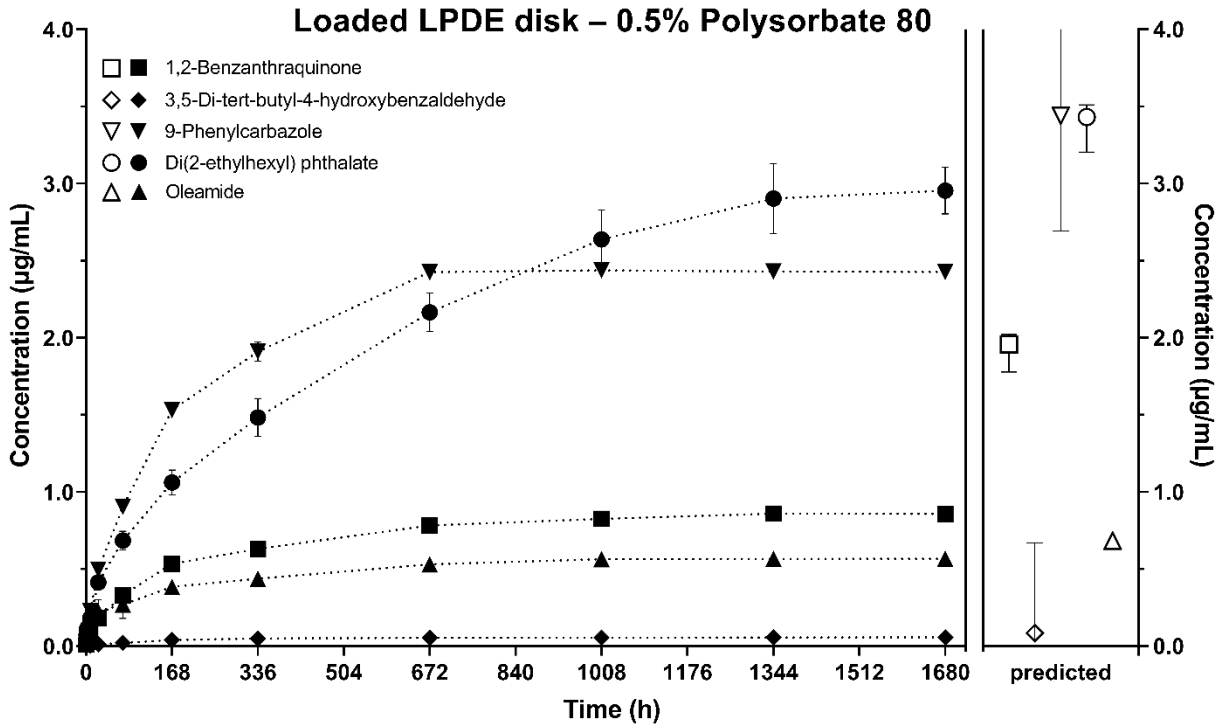

Figure 21. Migration plots from loaded polymer disks into contact solutions. Filled symbols = experimental values. Empty symbols = predicted values. Error bars of predicted equilibrium concentrations were calculated with upper and lower limits of ±0.5 log units of the partition coefficient. Migration from PDMS to a) placebo solution 1; b) placebo solution 2; c) placebo solution 3; d) 0.01% PS 80; e) 0.1% PS 80;f) 0.5% PS 80; g) 20% ethanol-water mixture and h) 50% ethanol-water mixture. Migration from loaded LDPE into 0.5% PS 80 in plot i). Error bars not shown if they do not extend the size of the respective symbol.

a)

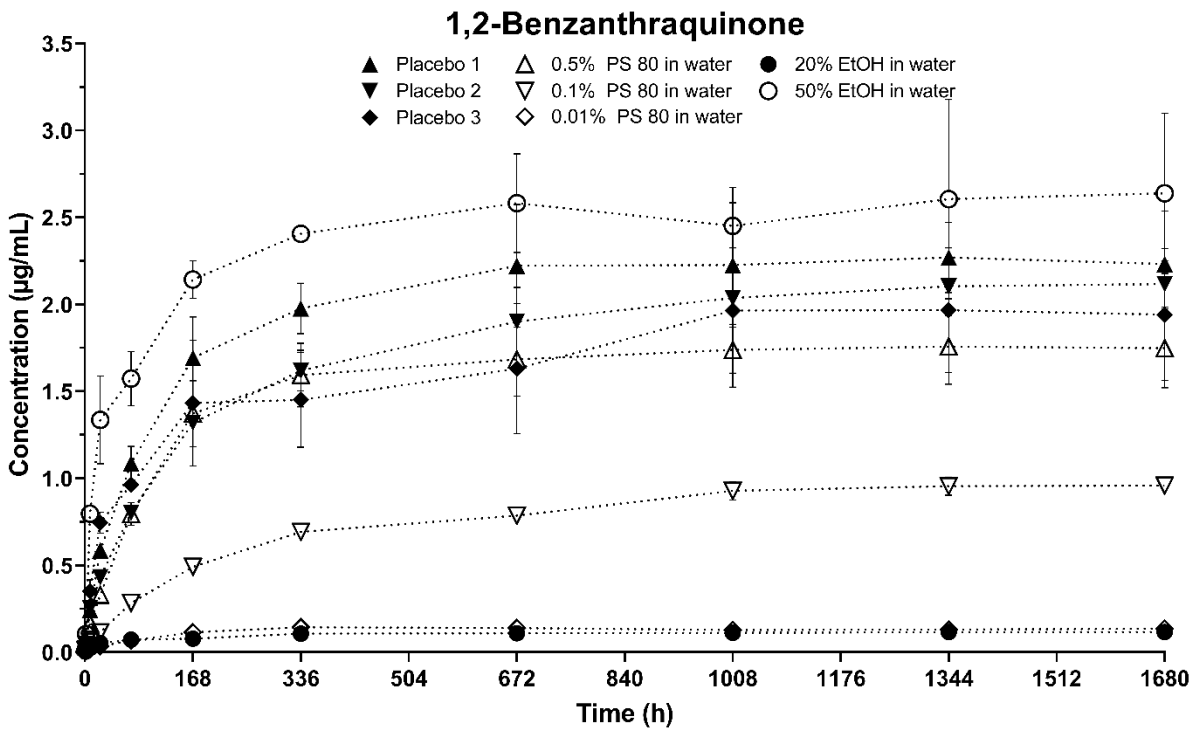
1,2-Benzanthraquinone
Placebo 1
Placebo 2
Placebo 3
0.5% PS 80 in water
0.1% PS 80 in water
0.01% PS 80 in water
20% EtOH in water
50% EtOH in water
Concentration (µg/mL)
Time (h)
0.0
0.5
1.0
1.5
2.0
2.5
3.0
3.5
0
168
336
504
672
840
1008
1176
1344
1512
1680

b)

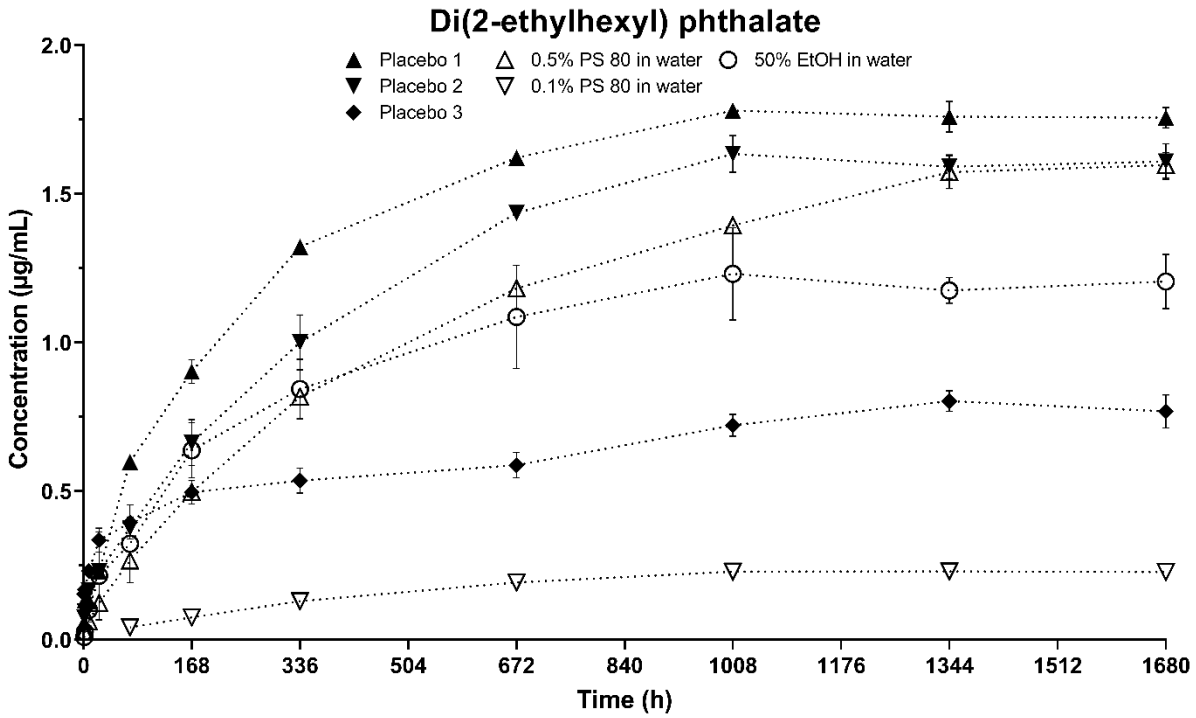
Di(2-ethylhexyl) phthalate
Placebo 1
Placebo 2
Placebo 3
0.5% PS 80 in water
0.1% PS 80 in water
50% EtOH in water
Concentration (µg/mL)
Time (h)
0.0
0.5
1.0
1.5
2.0
0
168
336
504
672
840
1008
1176
1344
1512
1680

c)

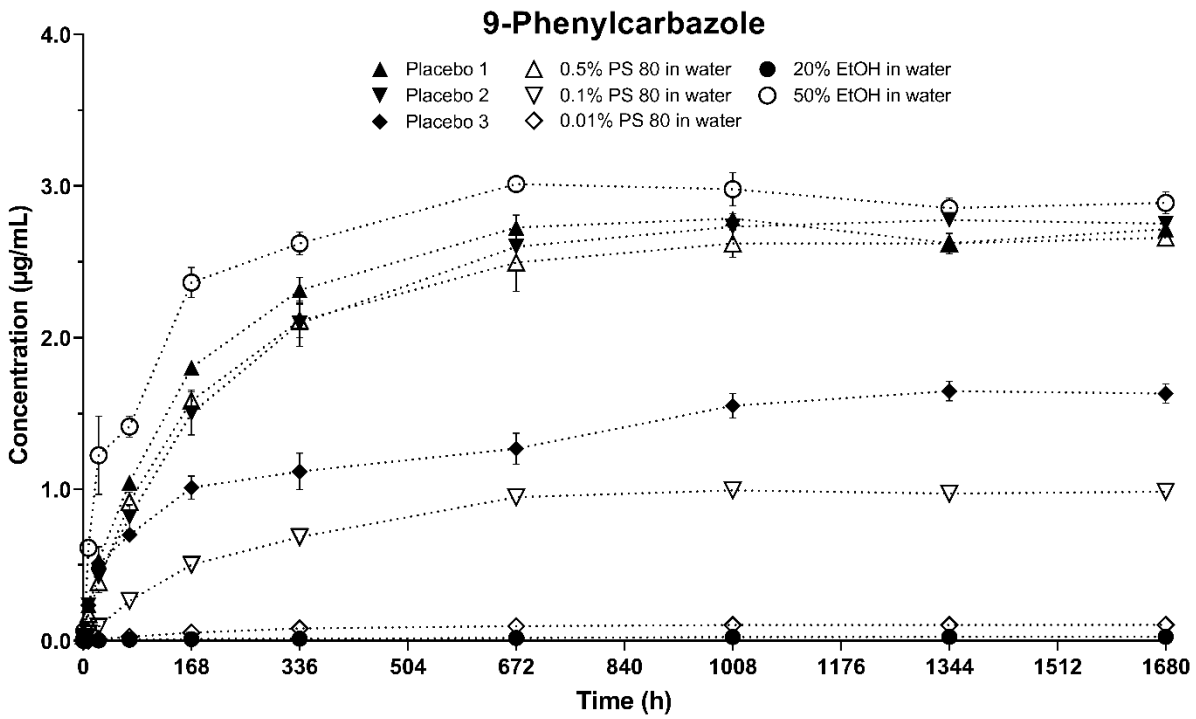
9-Phenylcarbazole
Placebo 1
Placebo 2
Placebo 3
0.5% PS 80 in water
0.1% PS 80 in water
0.01% PS 80 in water
20% EtOH in water
50% EtOH in water
Concentration (µg/mL)
4.0
3.0
2.0
1.0
0.0
0
168
336
504
672
840
1008
1176
1344
1512
1680
Time (h)

d)

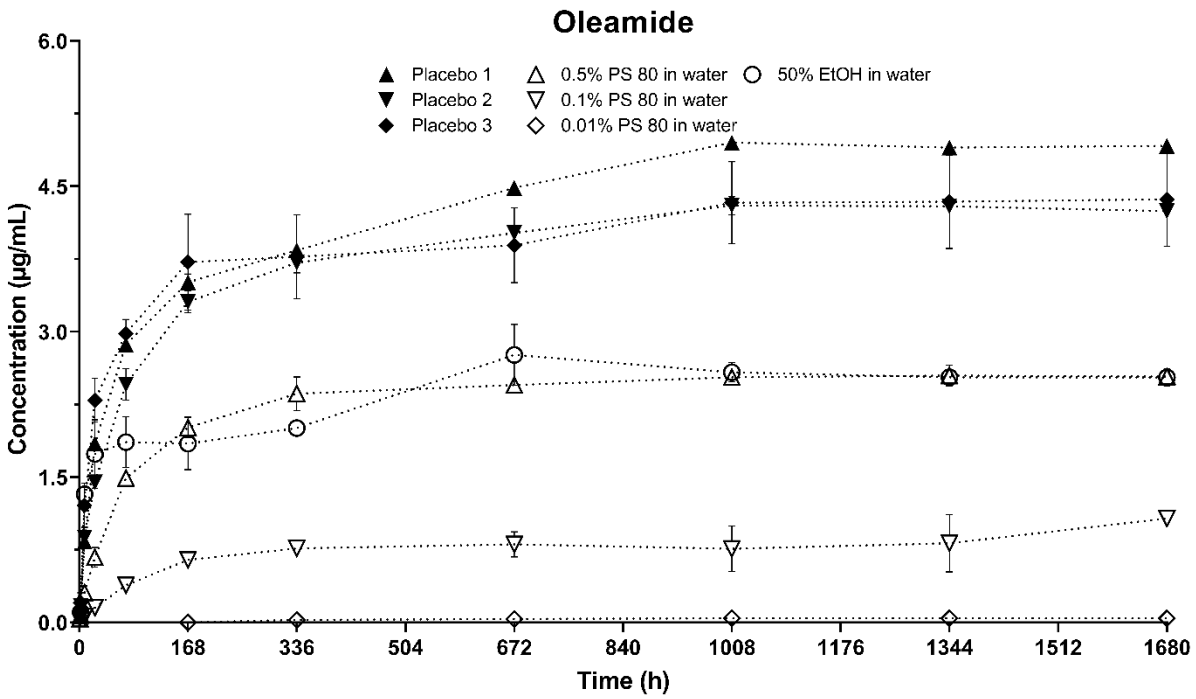
Oleamide
Placebo 1
Placebo 2
Placebo 3
0.5% PS 80 in water
0.1% PS 80 in water
0.01% PS 80 in water
50% EtOH in water
Concentration (µg/mL)
6.0
4.5
3.0
1.5
0.0
0
168
336
504
672
840
1008
1176
1344
1512
1680
Time (h)

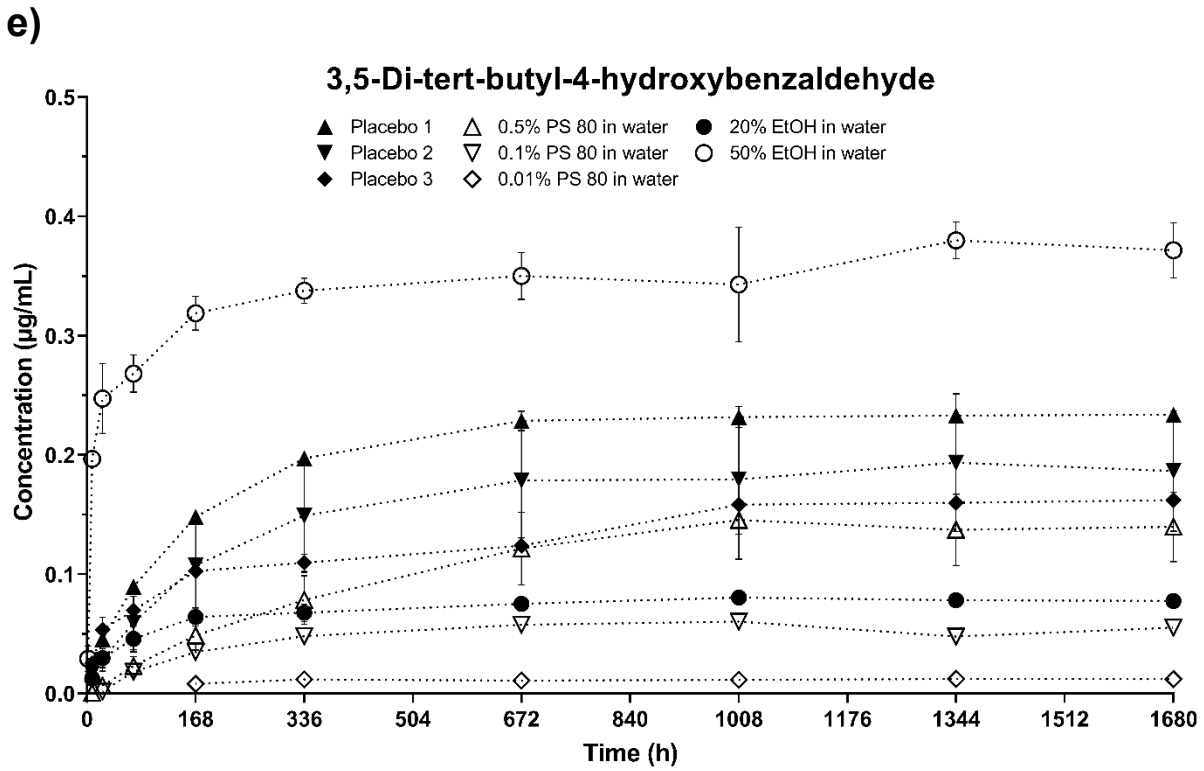

Figure 22. Individual migration plots for the five model leachables from PDMS into different contact solutions. a) 1,2-benzanthraquinone, b) di(2-ethylhexyl) phthalate, c) 9-phenylcarbazole, d) oleamide and e) 3,5-di-tert-butyl-4-hydroxybenzaldehyde.

4.4.2 Discussion

The observed accumulation of leachables that migrated from PDMS and LDPE disks is generally in good agreement with the predicted amount $C_{i,M}$ from eq. (3) considering an error range of ±0.5 log units around the predicted partition coefficient $\log K_{i,P/M}$, substantiating that a thermodynamic cycle, as presented in eq. (5), is an appropriate way to calculate partition coefficients for novel systems from existing LSER equations, e.g. polymer to pharmaceutical medium from predicted $\log K_{i,P/W}$ and $\log K_{i,M/W}$. Migration to all contact media (i.e., $C_{i,M}$) was overestimated for 1,2-benzanthraquinone (from PDMS and LDPE) and di(2-ethylhexyl) phthalate (DEHP) (only from PDMS), except for 1,2-benzanthraquinone in 50% ethanol-water. This coincides with the observations made in Chapter 4.2, where DEHP extraction was often overestimated by the LSER equations in comparison with calculations presented in two published articles [5, 7]. In one of those papers, Zdravkovic found that migration behavior of leachables from loaded polymer bags and bottles into 0.01% PS 80 and 20% isopropanol in water is comparable [5], which is in line with the results of this case study (Table 26, 28). Similar solubilization in isopropanol- and ethanol-water mixtures was established in the discussion of simulating solvents.

In Figure 22, the trend of the migration curve with different polymer to medium partition coefficients for the same compound with equal initial polymer load can be observed. With higher $\log K_{i,P/M}$, e.g. when the polymer is in contact with 0.01% PS 80 solutions or 20% ethanol in water mixtures, equilibrium between polymer and contact medium is reached more rapidly. Calculated migration curves from food contact plastics confirm this observation, where under equal conditions with

$\log K_{i,P/M} < 2$, the curves closely resemble one another, but with $\log K_{i,P/M} \geq 2$, equilibrium concentrations are obtained earlier and migration curves plateau comparatively sooner [250].

The presence of 1.5% benzyl alcohol in combination with 0.5% PS 80 (placebo 1 and 2) markedly increased leachable concentration overall compared to PS 80 alone, especially for oleamide (Figure 22d, Table 27). As discussed previously, benzyl alcohol alone is a weak solubilizer for organic chemicals at 1.5% w/v in water. However, it modifies the PS 80 micellar phase through insertion between aggregated surfactant molecules, introducing new potential molecular interactions for organic molecules solubilized in micelles. Whether these interactions in- or decrease micellar solubilization depends on the potential molecular interactions of the solute.

Placebo solution 1 and 2 accumulated nearly identical amounts of leachables, corroborating that dextrose and EDTA have a negligible effect on solubilization at pharmaceutically relevant concentrations. However, through the addition of a cosolvent (10% v/v ethanol), final leachable concentrations in placebo solution 3 were considerably lower for DEHP and 9-phenylcarbazole (Table 27) compared to placebo 1 and 2, although $C_{i,P}^{0}$ was similar, based on the remaining amount of leachables found in the extracted polymers. Equilibrium leachable concentrations were expected to increase in presence of 10% ethanol based on the solubility experiments in Chapter 4.3, especially for more hydrophobic compounds. While no significant increase of PDMS disk weight after equilibration was found in the case study ($P > 0.1$, t-test), potential swelling as cause of this observation was further investigated. Extracted, unloaded PDMS disks were submersed at room temperature for 48 h in 20% ethanol, 50% ethanol and placebo formulation 3. With a recorded weight increase of 0.18%, 0.48% and 0.34%, respectively, swelling of the polymer matrix by ethanol could have contributed to reduced migration out of the polymer matrix [98, 251, 252].

The polymer loading technique utilized here is subject to the partition coefficient of the chemical between polymer and loading solution, which was sufficiently high for the five test compounds. As a result, the model leachables spiked to the loading solution nearly quantitatively migrated to the polymer. However, more hydrophilic solutes would require immense concentrations in the loading solution to be appreciably loaded. Another avenue to generate a leachable loaded polymer is the in situ manufacture of the desired polymer from liquid components, where leachables are compounded together with the polymer reagents. Here, the load of leachables can be conveniently adjusted to a polymer regardless of their hydrophobicity, as detailed elsewhere [253].

This case study was successful at reliably verifying projected partition coefficients. It was further shown that, in principle, a quantitative correlation of extractable (here: the initial substance load in the polymer) and leachable data can be established by means of LSER predicted partition coefficients without further experimental input. However, in complex pharmaceutical contact solutions where the solubilizing mechanisms of excipients do not show additive behavior (e.g. PS 80 + benzyl alcohol), both under- and overestimations of equilibrium leachable levels are possible, as demonstrated by the comparatively high extraction of oleamide by the placebo solutions.

5. Conclusion and Outlook

In this work, a linear solvation energy relationship (LSER) model was established, enabling the accurate calculation of partitioning between micelles of polysorbate 80 (PS 80) and water for given solutes. LSER modeling is a chemically intuitive and user-friendly approach to predict numerous physicochemical processes and has therefore been applied here. The multi-parameter PS 80 LSER model was found to improve predictability of partitioning over a single-parameter model based on a solute's octanol-water partition coefficient and is applicable to all pharmaceutically relevant PS 80 concentrations above the critical micelle concentration and for compendial grade PS 80 products from different manufacturers. From a forecast micelle to water partition coefficient, calculation of the solubilization strength of a given concentration of PS 80 in water is straightforward.

In conjunction with previously published LSER models, equilibrium solubilization in complex parenteral formulations containing different excipients can be characterized using predicted partition coefficients. While virtually every excipient contributes to the solubilization of chemicals in water, it is important to realize that solubilization in aqueous formulations is typically driven by few excipients. Based on this finding, the complexity of identifying, describing, and calculating solubilization in pharmaceutical media can be limited and broken down to the application of a few model equations. The assumption of additive solubilizing effects could be confirmed for most of the excipient combinations tested.

Knowledge of the solubilization characteristics of a given formulation is important to find suitable experimental protocols in extractable and leachable (E & L) testing for chemical safety assessments. For instance, a useful application of modeled solubilization is the preparation of simulating solvents that accurately mimic the extraction propensity of the clinically relevant solution. The alignment of solubilization between a simulating solvent and a pharmaceutical medium was successfully demonstrated by calculation of solubilization strength for five different potential leachables in various PS 80 solutions. It could be shown that alignment can be easily implemented based on linear equations with freely retrievable chemical descriptors. A comprehensible approach to simulating solvent preparation is paramount in the tightly regulated field of pharmaceutical E & L, especially when, ultimately, experimental data is still demanded by regulatory authorities.

Notwithstanding, meaningful application of LSER models in E & L can go beyond the improvement of experimental protocols. As plastic materials are a major source of leachables, the partitioning between a plastic and contact solutions was investigated to determine final leachable concentrations in solution. Again, LSER partition models can be retrieved that enable the calculation of relevant partition coefficients. Thermodynamic cycles were utilized to derive appropriate partition coefficients from the LSER model predictions that apply to the novel systems, making predictions of leachable partitioning between polymers and pharmaceutical solutions or alcohol mixtures possible. Despite employing multiple model equations in the thermodynamic cycles, experimental values of equilibrium leachable concentrations could be accurately predicted, demonstrating their suitability in an advanced, practically orientated setting. Together with a description of leachable diffusion within contact polymers, quantitative mass transport modeling can be conducted, elucidating the fate of extractable compounds that may migrate into the final drug product as leachables by providing precise migration curves based on predicted diffusion and partition coefficients. To summarize, a key element of E & L analytical techniques, namely polarity-driven extraction of compounds from a contact material, can be augmented beyond the conventional chemical concepts of solvent polarity and compound hydrophobicity towards more quantitative, science-based methods.

Within the limited scope of this work, the focus was on PS 80 as a solubilizing parenteral excipient. Nevertheless, it is not the only excipient capable of strong solubilization in aqueous medium. Future models could encompass more excipients promoting leachable accumulation in drug products, e.g. polyethylene glycol or poloxamer 188. Absence of experimental solubility or partition data is typically the largest obstacle in obtaining sound physicochemical models for the prediction of solubilization in media containing these excipients, therefore necessitating further investment into research in this field. While ab initio models could provide the necessary data, they lack the simple utilization and derivation associated with e.g. LSER models.

Another issue of solubilization modeling in complex pharmaceutical solutions pertains to the interactions of excipient solubilization mechanisms. From the restricted amount of excipient combinations that could be investigated here, one combination (PS 80 and the antimicrobial benzyl alcohol) was found to distinctly change micellar solubilization in solution, which could not be accounted for in the calculations. Without a doubt, more such interactions are bound to be revealed if additional, reasonable combinations of excipients in parenteral formulations are probed. Under the assumption that these interactions will be of comparable magnitude, predicted micelle-water partition coefficients are nonetheless cornerstones of quantitative solubilization description in formulations containing surfactants. Still, it remains the task of the user of solubilization models (and physicochemical models in general) to identify, based on the mechanisms involved, potential limits of a modeling approach.

Methods for the determination of pre-experimental data supporting chemical safety assessments were successfully developed and utilized in this work, offering science-based tools for mass transport modeling to practitioners in the field of E & L. Crucially, the solubilization strength of aqueous based parenteral solutions containing the prominent solubilizer polysorbate 80 can now be characterized.

6. Abstract

Leaching of chemical constituents from pharmaceutical polymeric contact materials to clinically relevant solutions including process streams, drug products, or body compartments, is a physicochemical process demanding expert analysis to ensure the safety and efficacy of a medicinal or medical product. Regulatory agencies require information generated by safety assessment that typically include experimental data supporting the suitability of a given contact material for the marketing authorization of a product.

The extraction propensity of a parenteral solution towards polymers, and hence the profile of leachables in e.g. a drug product at the end of its shelf life, depends on its qualitative and quantitative composition of excipients. Thermodynamic partition coefficients describe the extraction propensity of a contact solution through equilibrium concentrations in solution and polymer. Simulating solvent mixtures containing a fixed amount of alcohol and water are regularly employed in experimental studies supporting authorization to facilitate experimental procedures when collecting data on extractable (i.e., potential leachable) and leachable compounds. Here, simulating solvent mixtures are utilized with the intention of mimicking the extraction propensity of a drug product.

In this work, a linear solvation energy relationship (LSER) was established to calculate the solubilization strength of polysorbate 80 (PS 80), a frequently formulated solubilizing excipient, in water. The system parameters of the LSER model were reported, discussed, and a critical examination of data sourced from the literature and determined here was provided.

The individual solubilizing mechanism of other relevant excipients, as well as their effect on aqueous solubilization in combination with each other and PS 80, was explored. It was found that solubilizing excipients such as PS 80 dominate aqueous solubilization in drug product solutions, and therefore dominate a drug product’s extraction propensity.

In an exercise to generate appropriate simulating solvent compositions for individual drug products, the solubilization strength of simulating solvent mixtures containing either ethanol or isopropanol were aligned with the solubilization strength of PS 80 solutions representing drug products by applying LSER equations from literature and this work. Chemical identity of a leachable and PS 80 concentration in solution were shown to dictate the suitable alcohol concentration in the simulating solvent. By utilizing simulating solvents with aligned solubilization, a better representation of drug product solutions and, consequently, a more representative extraction profile in simulation studies is expected.

Finally, migration of model leachables from loaded polymer disks into pharmaceutically relevant solutions was determined in a case study. By means of LSER predicted partition coefficients and a thermodynamic cycle, equilibrium leachable concentrations in solution were successfully forecast. Predictions were solely based on the total amount of loaded leachable, volume of contact phases, and calculated partition coefficients between polymer and solution.

This thesis demonstrated the practicability of LSER predictions to align the solubilization strength of simulating solvents with drug products and to determine equilibrium leachable concentrations in a drug product from chemical extraction data.

7. Zusammenfassung

Die Herauslösung (Leaching) chemischer Bestandteile aus pharmazeutischen polymerbasierten Kontaktmaterialien durch klinisch relevant Lösungen, zu denen Prozessströme, Arzneimittel und Körperkompartimente gehören, ist ein physikochemischer Prozess, welcher fachkundige Bewertung benötigt, um die Sicherheit und Wirksamkeit eines Arzneimittels oder Medizinprodukts zu gewährleisten. Die jeweiligen Aufsichtsbehörden verlangen Sicherheitsbewertungen, meist basierend auf experimentell ermittelten Daten, welche die Eignung eines gegebenen Kontaktmaterials für die Zulassung eines Medizinprodukts oder Arzneimittels belegen.
Die Extraktionskraft einer parenteralen Lösung gegenüber Polymeren, und, daraus folgend, das Leachable-Profil in beispielsweise einem Arzneimittel am Ende seiner Laufzeit, ist abhängig von der qualitativen und quantitativen Zusammensetzung der Hilfsstoffe. Thermodynamische Verteilungskoeffizienten beschreiben die Extraktionskraft einer Kontaktlösung durch Gleichgewichtskonzentrationen in Lösung und Polymer. Simulanzlösungen, welche eine definierte Menge Alkohol und Wasser enthalten, werden regelmäßig in experimentellen Studien verwendet, um experimentelle Abläufe bei der Datenerhebung extrahierbarer (und damit potentiell leachender) und leachender Substanzen zu vereinfachen. Durch Einsatz der Simulanzlösungen wird eine Nachahmung der Extraktionskraft eines Arzneimittels beabsichtigt.
In dieser Arbeit wurde eine Linear Solvation Energy Relationship (LSER) etabliert, mit der die Lösungskraft von Polysorbat 80 (PS 80), einem häufig formulierten löslichkeitsvermittelnden Hilfsstoffs, in Wasser errechnet werden kann. Die Systemparameter des LSER-Modells wurden berichtet, diskutiert und eine kritische Begutachtung der Daten aus Literatur und eigener Experimente wurde durchgeführt.
Die individuellen Solubilisierungsmechanismen anderer relevanter Hilfsstoffe, sowie deren Effekt auf die Solubilisierung im Wässrigen in Kombination miteinander und mit PS 80, wurde untersucht. Es wurde festgestellt, dass löslichkeitsvermittelnde Hilfsstoffe wie PS 80 vornehmlich für die Solubilisierung im wässrigen Milieu von Arzneimittellösungen verantwortlich sind und demnach gleichzeitig die Extraktionskraft des Arzneimittels bestimmen.
In einer Übung zur Bestimmung angemessener Zusammensetzungen einer Simulanzlösung für individuelle Arzneimittel wurden die Lösungskraft von Simulanzlösungen, welche entweder Ethanol oder Isopropanol enthalten, der Lösungskraft von PS 80 Lösungen mit Hilfe von LSER-Modellgleichungen aus Literatur und dieser Arbeit angepasst. Hierbei konnte gezeigt werden, dass die chemische Identität eines Leachable und die PS 80 Konzentration in Lösung die passende Alkoholkonzentration in der Simulanzlösung bestimmen. Durch Verwendung von Simulanzlösungen mit angepasster Solubilisierung wird eine bessere Abbildung der Arzneimittellösung und, daraus folgend, ein repräsentativeres Extraktionsprofil in Simulationsstudien erwartet.
Zuletzt wurde die Migration von Modell-Leachables aus beladenen Polymerscheiben in pharmazeutisch relevante Lösungen in einer Fallstudie bestimmt. Mit Hilfe von LSER-vorhergesagten Verteilungskoeffizienten und eines thermodynamischen Kreisprozesses wurde die Gleichgewichtskonzentration der Leachables in Lösung erfolgreich vorhergesagt. Die Vorhersagen basierten lediglich auf der Gesamtmenge der beladenen Leachables, den Volumina der Kontaktphasen und den errechneten Verteilungskoeffizienten zwischen Polymer und Lösung. Diese Dissertation demonstrierte die Praktikabilität von LSER-Vorhersagen, um die Lösungskraft von Simulanzlösungen mit der von Arzneimitteln anzugleichen, und um Gleichgewichtskonzentrationen von Leachables in einem Arzneimittel anhand chemischer Extraktionsdaten vorauszusagen.

8. Curriculum Vitae

[redacted]

9. References

1. Jahn, M., 2018. Leachables and Extractables: From Regulatory Expectations to Laboratory Assessment, in: Warne, N.W., Mahler, H.-C. (Eds.), Challenges in Protein Product Development. Springer International Publishing, pp. 337-351.
2. Jenke, D., 2002. Extractable/leachable substances from plastic materials used as pharmaceutical product containers/devices. PDA Journal of Pharmaceutical Science and Technology 56, pp. 332-371.
3. Guidance for Industry: Container Closure System for Packaging Human Drugs and Biologics (Chemistry, Manufacturing, and Controls Documentation), 1999, U.S. Food and Drug Administration.
4. Jenke, D., 2018. Identification, analysis and safety assessment of leachables and extractables. TrAC - Trends in Analytical Chemistry 101, pp. 56-65.
5. Zdravkovic, S.A., 2016. Comparison of the Solubilization Properties of Polysorbate 80 and Isopropanol/Water Solvent Systems for Organic Compounds Extracted from Three Pharmaceutical Packaging Configurations. European Journal of Pharmaceutical Sciences 93, pp. 475-483.
6. Singh, G., Lu, D., Liu, C., Hower, D., 2021. Analytical challenges and recent advances in the identification and quantitation of extractables and leachables in pharmaceutical and medical products. TrAC - Trends in Analytical Chemistry 141. doi:10.1016/j.trac.2021.116286.
7. Jenke, D., Liu, N., Hua, Y., Swanson, S., Bogseth, R., 2015. A Means of Establishing and Justifying Binary Ethanol/Water Mixtures as Simulating Solvents in Extractables Studies. PDA journal of pharmaceutical science and technology 69, pp. 366-382.
8. Yu, X., Decou, D., Wood, D., Zdravkovic, S., Schmidt, H., Stockmeier, L., Piccoli, R., Rude, D., Ding, X., 2010. A study of leachables for biopharmaceutical formulations stored in rubber-stoppered glass vials. BioPharm Int 23, pp. 26-36.
9. Jenke, D., 2011. A general assessment of the physiochemical factors that influence leachables accumulation in pharmaceutical drug products and related solutions. PDA journal of pharmaceutical science and technology 65, pp. 166-176.
10. Rowe, R.C., Sheskey, P., Quinn, M., 2009. Handbook of pharmaceutical excipients. Libros Digitales-Pharmaceutical Press.
11. Gervasi, V., Dall Agnol, R., Cullen, S., McCoy, T., Vucen, S., Crean, A., 2018. Parenteral protein formulations: An overview of approved products within the European Union. European Journal of Pharmaceutics and Biopharmaceutics 131, pp. 8-24.
12. Zdravkovic, S.A., 2021. Assessment of Extractable and Leachable Substances from Pharmaceutical Contact Materials: Where Are We and Where Do We Go from Here? PDA journal of pharmaceutical science and technology 75, pp. 1-3.
13. Jenke, D., Couch, T., Gillum, A., Sadain, S., 2009. Modeling of the solution interaction properties of plastic materials used in pharmaceutical product container systems. PDA Journal of Pharmaceutical Science and Technology 63, pp. 294-306.
14. Feenstra, P., Brunsteiner, M., Khinast, J., 2014. Investigation of migrant-polymer interaction in pharmaceutical packaging material using the linear interaction energy algorithm. Journal of Pharmaceutical Sciences 103, pp. 3197-3204.
15. Paskiet, D., Jenke, D., Ball, D., Houston, C., Norwood, D.L., Markovic, I., 2013. The product quality research institute (PQRI) leachables and extractables working group initiatives for parenteral and ophthalmic drug product (PODP). PDA Journal of Pharmaceutical Science and Technology 67, pp. 430-447.
16. Fliszar, K.A., Walker, D., Allain, L., 2006. Profiling of metal ions leached from pharmaceutical packaging materials. PDA Journal of Pharmaceutical Science and Technology 60, pp. 337-342.
17. Allmendinger, A., Lebouc, V., Bonati, L., Woehr, A., Kishore, R.S.K., Abstiens, K., 2021. Glass Leachables as a Nucleation Factor for Free Fatty Acid Particle Formation in Biopharmaceutical Formulations. Journal of Pharmaceutical Sciences 110, pp. 785-795.

18. Groh, K.J., Backhaus, T., Carney-Almroth, B., Geueke, B., Inostroza, P.A., Lennquist, A., Leslie, H.A., Maffini, M., Slunge, D., Trasande, L., Warhurst, A.M., Muncke, J., 2019. Overview of known plastic packaging-associated chemicals and their hazards. Science of The Total Environment 651, pp. 3253-3268.
19. Guideline on Plastic Immediate Packaging Materials (CPMP/QWP/4359/03), 2005, European Medicines Agency.
20. Jenke, D., 2008. Compatibility of Pharmaceutical Products and Contact Materials: Safety Considerations Associated with Extractables and Leachables.
21. Bee, J.S., Randolph, T.W., Carpenter, J.F., Bishop, S.M., Dimitrova, M.N., 2011. Effects of surfaces and leachables on the stability of biopharmaceuticals. Journal of Pharmaceutical Sciences 100, pp. 4158-4170.
22. Li, K., Rogers, G., Nashed-Samuel, Y., Lee, H., Mire-Sluis, A., Cherney, B., Forster, R., Yeh, P., Markovic, I., 2015. Creating a holistic extractables and leachables (E&L) program for biotechnology products. PDA Journal of Pharmaceutical Science and Technology 69, pp. 590-619.
23. Markovic, I., 2009. Risk management strategies for safety qualification of extractable and leachable substances in therapeutic biologic protein products. American Pharmaceutical Review 12, Issue 4.
24. Dorey, S., Pahl, I., Uettwiller, I., Priebe, P., Hauk, A., 2018. Theoretical and Practical Considerations When Selecting Solvents for Use in Extractables Studies of Polymeric Contact Materials in Single-Use Systems Applied in the Production of Biopharmaceuticals. Industrial and Engineering Chemistry Research 57, pp. 7077-7089.
25. Hauk, A., Jurkiewicz, E., Pahl, I., Loewe, T., Menzel, R., 2018. Filtration membranes - Scavengers for leachables? Eur J Pharm Sci 120, pp. 191-198.
26. Paudel, K., Hauk, A., Maier, T.V., Menzel, R., 2020. Quantitative characterization of leachables sinks in biopharmaceutical downstream processing. European Journal of Pharmaceutical Sciences 143. doi:10.1016/j.ejps.2019.105069.
27. Arbin, A., Jacobsson, S., Hänninen, K., Hagman, A., Östelius, J., 1986. Studies on contamination of intravenous solutions from PVC-bags with dynamic headspace GC-MS and LC-diode array techniques. International Journal of Pharmaceutics 28, pp. 211-218.
28. Kang, J.H., Kondo, F., Katayama, Y., 2006. Human exposure to bisphenol A. Toxicology 226, pp. 79-89.
29. Haverkamp, J.B., Lipke, U., Zapf, T., Galensa, R., Lipperheide, C., 2008. Contamination of semi-solid dosage forms by leachables from aluminium tubes. European Journal of Pharmaceutics and Biopharmaceutics 70, pp. 921-928.
30. Boven, K., Stryker, S., Knight, J., Thomas, A., Van Regenmortel, M., Kemeny, D.M., Power, D., Rossert, J., Casadevall, N., 2005. The increased incidence of pure red cell aplasia with an Eprex formulation in uncoated rubber stopper syringes. Kidney International 67, pp. 2346-2353.
31. Jacobson-Kram, D., Snyder, R.D., 2012. Concept and Application of Safety Thresholds in Drug Development, Leachables and Extractables Handbook: Safety Evaluation, Qualification, and Best Practices Applied to Inhalation Drug Products, pp. 37-44.
32. Norwood, D.L., Paskiet, D., Ruberto, M., Feinberg, T., Schroeder, A., Poochikian, G., Wang, Q., Deng, T.J., Degrazio, F., Munos, M.K., Nagao, L.M., 2008. Best practices for extractables and leachables in orally inhaled and nasal drug products: An overview of the PQRI recommendations. Pharmaceutical Research 25, pp. 727-739.
33. Teasdale, A., Jahn, M., Bailey, S., Feilden, A., Taylor, G., Corcoran, M.L., Malick, R., Jenke, D., Stults, C.L.M., Nagao, L.M., 2015. Controlled Extraction Studies Applied to Polyvinyl Chloride and Polyethylene Materials: Conclusions from the ELSIE Controlled Extraction Pilot Study. AAPS PharmSciTech 16, pp. 664-674.
34. Christiaens, P., Beusen, J.M., Verlinde, P., Baeten, J., Jenke, D., 2020. Identifying and Mitigating Errors in Screening for Organic Extractables and Leachables: Part 1-Introduction to Errors in Chromatographic Screening for Organic Extractables and Leachables and Discussion

of the Errors of Omission. PDA journal of pharmaceutical science and technology 74, pp. 90-107.
35. Jenke, D., Couch, T., 2006. A consideration of the impact of solution composition on the accumulation of organic substances leached from plastics used in container/closure systems. PDA Journal of Pharmaceutical Science and Technology 60, pp. 60-71.
36. Jenke, D.R., 2001. Evaluation of model solvent systems for assessing the accumulation of container extractables in drug formulations. International Journal of Pharmaceutics 224, pp. 51-60.
37. Jenke, D., 2020. Identification and Quantitation Classifications for Extractables and Leachables. PDA Journal of Pharmaceutical Science and Technology 74, pp. 275-285.
38. Jenke, D., 2006. Extractable substances from plastic materials used in solution contact applications: An updated review. PDA Journal of Pharmaceutical Science and Technology 60, pp. 191-207.
39. Vogel, W.M., 2012. The Development of Safety Thresholds for Leachables in Orally Inhaled and Nasal Drug Products, Leachables and Extractables Handbook: Safety Evaluation, Qualification, and Best Practices Applied to Inhalation Drug Products, pp. 45-58.
40. Jenke, D., 2020. Correcting the Analytical Evaluation Threshold (AET) and Reported Extractable's Concentrations for Analytical Response Factor Uncertainty Associated with Chromatographic Screening for Extractables/Leachables. PDA journal of pharmaceutical science and technology 74, pp. 348-358.
41. Jenke, D., Heise, T., 2021. The Implications of Chromatographically Screening Medical Products for Organic Leachables Down to the Analytical Evaluation Threshold Adjusted for Response Factor Variation. PDA journal of pharmaceutical science and technology 75, pp. 273-288.
42. Ball, D.J., Norwood, D.L., Stults, C.L.M., Nagao, L.M., 2012. Leachables and Extractables Handbook: Safety Evaluation, Qualification, and Best Practices Applied to Inhalation Drug Products. John Wiley & Sons, Inc.
43. U.S. Pharmacopeia. 2020. <1664> Assessment of extractables associated with pharmaceutical packaging/delivery systems.
44. Jenke, D., 2012. A general strategy for the chemical aspects of the safety assessment of extractables and leachables in pharmaceutical drug products: The chemical assessment triad. PDA Journal of Pharmaceutical Science and Technology 66, pp. 168-183.
45. Jenke, D.R., 2005. Linking extractables and leachables in container/closure applications. PDA Journal of Pharmaceutical Science and Technology 59, pp. 265-281.
46. U.S. Pharmacopeia. 2020. <1663> Assessment of extractables associated with pharmaceutical packaging/delivery systems.
47. Broschard, T.H., Glowienke, S., Bruen, U.S., Nagao, L.M., Teasdale, A., Stults, C.L.M., Li, K.L., Iciek, L.A., Erexson, G., Martin, E.A., Ball, D.J., 2016. Assessing safety of extractables from materials and leachables in pharmaceuticals and biologics – Current challenges and approaches. Regulatory Toxicology and Pharmacology 81, pp. 201-211.
48. ICH Mission Statement, 2021. International Council for Harmonisation of Technical Requirements for Pharmaceuticals for Human Use. [Retrieved on 30.06.2021]: https://www.ich.org/page/mission.
49. Elder, D., Creasey, J., Waine, C., Feilden, A., Worsøe, C., Teasdale, A., 2020. ICH Q3E (Extractables and leachables): Setting the scene – part 1. Regulatory Rapporteur 17, pp. 22-27.
50. Franz, R., 2005. Migration modeling from food-contact plastics into foodstuffs as a new tool for consumer exposure estimation. Food Additives and Contaminants 22, pp. 920-937.
51. Begley, T., Castle, L., Feigenbaum, A., Franz, R., Hinrichs, K., Lickly, T., Mercea, P., Milana, M., O'Brien, A., Rebre, S., Rijk, R., Piringer, O., 2005. Evaluation of migration models that might be used in support of regulations for food-contact plastics. Food Additives and Contaminants 22, pp. 73-90.

52. Poças, M.F., Oliveira, J.C., Oliveira, F.A.R., Hogg, T., 2008. A critical survey of predictive mathematical models for migration from packaging. Critical Reviews in Food Science and Nutrition 48, pp. 913-928.
53. Castillo, M., Borrell, A., 2018. General european legislation for food contact materials. Current Analytical Chemistry 14, pp. 358-366.
54. Pearson, S.D., Trissel, L.A., 1993. Leaching of diethylhexyl phthalate from polyvinyl chloride containers by selected drugs and formulation components. American Journal of Hospital Pharmacy 50, pp. 1405-1409.
55. European Pharmacopoeia, 10th Edition. Strasbourg: European Directorate for the Quality of Medicines & HealthCare of the Council of Europe (EDQM), 2019. Parenteral Preparations, pp. 923-925.
56. Abrantes, C.G., Duarte, D., Reis, C.P., 2016. An Overview of Pharmaceutical Excipients: Safe or Not Safe? Journal of Pharmaceutical Sciences 105, pp. 2019-2026.
57. Buggins, T.R., Dickinson, P.A., Taylor, G., 2007. The effects of pharmaceutical excipients on drug disposition. Advanced Drug Delivery Reviews 59, pp. 1482-1503.
58. Zhang, W., Li, Y., Zou, P., Wu, M., Zhang, Z., Zhang, T., 2016. The Effects of Pharmaceutical Excipients on Gastrointestinal Tract Metabolic Enzymes and Transporters—an Update. The AAPS Journal 18, pp. 830-843.
59. Pond, S.M., Tozer, T.N., 1984. First-Pass Elimination Basic Concepts and Clinical Consequences. Clinical Pharmacokinetics 9, pp. 1-25.
60. Powell, M.F., Nguyen, T., Baloian, L., 1998. Compendium of excipients for parenteral formulations. PDA Journal of Pharmaceutical Science and Technology 52, pp. 238-239.
61. Nema, S., Brendel, R.J., 2011. Excipients and their role in approved injectable products: Current usage and future directions. PDA Journal of Pharmaceutical Science and Technology 65, pp. 287-332.
62. Strickley, R.G., 1999. Parenteral formulations of small molecules therapeutics marketed in the United States (1999) - Part I. PDA Journal of Pharmaceutical Science and Technology 53, pp. 324-349.
63. Strickley, R.G., 2000. Parenteral formulations of small molecules therapeutics marketed in the United States (1999) Part III. PDA Journal of Pharmaceutical Science and Technology 54, pp. 152-169.
64. Strickley, R.G., 2000. Parenteral formulations of small molecules therapeutics marketed in the United States of America (1999): Part II. PDA Journal of Pharmaceutical Science and Technology 54, pp. 69-96.
65. Rayaprolu, B.M., Strawser, J.J., Anyarambhatla, G., 2018. Excipients in parenteral formulations: selection considerations and effective utilization with small molecules and biologics. Drug Development and Industrial Pharmacy 44, pp. 1565-1571.
66. Ironside, J.W., 2004. Variant Creutzfeldt-Jakob disease: Risk of transmission by blood and blood products. Haemophilia, Supplement 10, pp. 64-69.
67. Colvin, R.R., Dubin, C.C., Haas, G.G., 1994. Creutzfeld-Jacob disease and blood product recalls. Common factor (Stoughton, Mass.). p. 23.
68. Haag-Weber, M., Eckardt, K.-U., Hörl, W.H., Roger, S.D., Vetter, A., Roth, K., 2012. Safety, immunogenicity and efficacy of subcutaneous biosimilar epoetin-α (HX575) in non-dialysis patients with renal anemia: a multi-center, randomized, double-blind study. Clinical Nephrology 77, pp. 8-17.
69. Seidl, A., Hainzl, O., Richter, M., Fischer, R., Böhm, S., Deutel, B., Hartinger, M., Windisch, J., Casadevall, N., London, G.M., Macdougall, I., 2012. Tungsten-Induced Denaturation and Aggregation of Epoetin Alfa During Primary Packaging as a Cause of Immunogenicity. Pharmaceutical Research 29, pp. 1454-1467.
70. Richter, C., Lipperheide, C., Lipke, U., Lamprecht, A., 2018. Impact of extractables from rubber closures on protein stability under heat stress. European Journal of Pharmaceutics and Biopharmaceutics 130, pp. 22-29.

71. Sharma, B., Bader, F., Templeman, T., Lisi, P., Ryan, M., Heavner, G., 2004. Technical investigation into the cause of the increased incidence of anti-body-mediated pure red cell aplasia associated with EPREX®. European Journal of Hospital Pharmacy 5, pp. 86-91.
72. Locatelli, F., Del Vecchio, L., Pozzoni, P., 2007. Pure red-cell aplasia "epidemic" - Mystery completely revealed? Peritoneal Dialysis International 27, pp. S303-S307.
73. Hartley, G.S., Crank, J., 1949. Some fundamental definitions and concepts in diffusion processes. Transactions of the Faraday Society 45, pp. 801-818.
74. Piringer, O.G., Baner, A.L., 2008. Plastic packaging: interactions with food and pharmaceuticals. John Wiley & Sons.
75. Till, D.E., Ehntholt, D.J., Reid, R.C., Schwartz, P.S., Sidman, K.R., Schwope, A.D., Whelan, R.H., 1982. Migration of BHT antioxidant from high density polyethylene to foods and food simulants. Industrial & Engineering Chemistry Product Research and Development 21, pp. 106-113.
76. Piringer, O., 2008. A Uniform Model for Prediction of Diffusion Coefficients with Emphasis on Plastic Materials, Plastic Packaging, pp. 163-193.
77. Welle, F., 2013. A new method for the prediction of diffusion coefficients in poly(ethylene terephthalate). Journal of Applied Polymer Science 129, pp. 1845-1851.
78. Welle, F., 2014. Activation energies of diffusion of organic migrants in cyclo olefin polymer. International Journal of Pharmaceutics 473, pp. 510-517.
79. Brandsch, R., 2017. Probabilistic migration modelling focused on functional barrier efficiency and low migration concepts in support of risk assessment. Food Additives & Contaminants: Part A 34, pp. 1743-1766.
80. Fang, X., Vitrac, O., 2017. Predicting diffusion coefficients of chemicals in and through packaging materials. Critical Reviews in Food Science and Nutrition 57, pp. 275-312.
81. Roduit, B., Borgeat, C., Cavin, S., Fragnière, C., Dudler, V., 2005. Application of Finite Element Analysis (FEA) for the simulation of release of additives from multilayer polymeric packaging structures. Food additives and contaminants 22, pp. 945-955.
82. Hauk, A., Pahl, I., Dorey, S., Menzel, R., 2021. Using extractables data from single-use components for extrapolation to process equipment-related leachables: The toolbox and justifications. European Journal of Pharmaceutical Sciences 163. doi:10.1016/j.ejps.2021.105841.
83. Commission Regulation (EU) No 10/2011 of 14 January 2011 on plastic materials and articles intended to come into contact with food, European Commission. http://data.europa.eu/eli/reg/2011/10/oj.
84. Brandsch, R., Dequatre, C., Mercea, P., Milana, M., Stoermer, A., Trier, X., Vitrac, O., Schaefer, A., Simoneau, C., 2015. Practical guidelines on the application of migration modelling for the estimation of specific migration. EUR 27529. Publications Office of the European Union, Luxembourg.
85. Schlotter, N.E., Furlan, P.Y., 1992. A review of small molecule diffusion in polyolefins. Polymer 33, pp. 3323-3342.
86. Jenke, D.R., Kenley, R.A., Hayward, D.S., 1991. Interactions between polymeric containers and their contained solution: Modeling of polymer-water solute partitioning via coupled solvent-water partition coefficients. Journal of Applied Polymer Science 43, pp. 1475-1482.
87. Franz, R., Brandsch, R., 2013. Migration of acrylic monomers from methacrylate polymers - Establishing parameters for migration modelling. Packaging Technology and Science 26, pp. 435-451.
88. Schwarzenbach, R.P., Gschwend, P.M., Imboden, D.M., 2016. Environmental Organic Chemistry, 3rd Edition. Wiley.
89. Asgarpour Khansary, M., Shirazian, S., Asadollahzadeh, M., 2017. Polymer-water partition coefficients in polymeric passive samplers. Environmental Science and Pollution Research 24, pp. 2627-2631.

90. Zhu, T., Wu, J., He, C., Fu, D., Wu, J., 2018. Development and evaluation of MTLSER and QSAR models for predicting polyethylene-water partition coefficients. Journal of Environmental Management 223, pp. 600-606.
91. Zhu, T., Chen, W., Cheng, H., Wang, Y., Singh, R.P., 2019. Prediction of polydimethylsiloxane-water partition coefficients based on the pp-LFER and QSAR models. Ecotoxicology and Environmental Safety 182. doi:10.1016/j.ecoenv.2019.109374
92. Li, A., 1998. Predicting cosolvency. 1. Solubility ratio and solute log K(ow). Industrial and Engineering Chemistry Research 37, pp. 4470-4475.
93. Li, A., 1998. Predicting cosolvency. 2. Correlation with solvent physicochemical properties. Industrial and Engineering Chemistry Research 37, pp. 4476-4480.
94. Jouyban, A., 2008. Review of the cosolvency models for predicting solubility of drugs in water-cosolvent mixtures. Journal of Pharmacy and Pharmaceutical Sciences 11, pp. 32-58.
95. Jouyban, A., 2019. Review of the cosolvency models for predicting drug solubility in solvent mixtures: an update. Journal of Pharmacy & Pharmaceutical Sciences 22, pp. 466-485.
96. Abraham, M.H., Acree, W.E., 2012. Equations for the Partition of Neutral Molecules, Ions and Ionic Species from Water to Water–Ethanol Mixtures. Journal of Solution Chemistry 41, pp. 730-740. doi:10.1007/s10953-021-01063-w.
97. Abraham, M.H., Acree, W.E., Jr., Rafols, C., Roses, M., 2021. Equations for the Correlation and Prediction of Partition Coefficients of Neutral Molecules and Ionic Species in the Water–Isopropanol Solvent System. Journal of Solution Chemistry.
98. Gelotte, K.M., Lostritto, R.T., 1990. Solvent Interaction with Polydimethylsiloxane Membranes and Its Effects on Benzocaine Solubility and Diffusion. Pharmaceutical Research: An Official Journal of the American Association of Pharmaceutical Scientists 7, pp. 523-529.
99. Bhuiyan, A.K.M.M.H., Waters, L.J., 2017. Permeation of pharmaceutical compounds through silicone membrane in the presence of surfactants. Colloids and Surfaces A: Physicochemical and Engineering Aspects 516, pp. 121-128.
100. Cheung, J.K., Sharma, M., Dabbara, A., Petersen, J., 2012. The effect of formulation excipients on leachables for IV-administered products. Pharmaceutical Outsourcing 13. Published online: https://www.pharmoutsourcing.com/Featured-Articles/125938-The-Effect-of-Formulation-Excipients-on-Leachables-for-IV-Administered-Products [Retrieved on 30.08.2021].
101. Bergström, C.A.S., Larsson, P., 2018. Computational prediction of drug solubility in water-based systems: Qualitative and quantitative approaches used in the current drug discovery and development setting. International journal of pharmaceutics 540, pp. 185-193.
102. Rubino, J.T., Yalkowsky, S.H., 1987. Cosolvency and cosolvent polarity. Pharmaceutical research 4, pp. 220-230.
103. Munz, C., Roberts, P.V., 1986. Effects of solute concentration and cosolvents on the aqueous activity coefficient of halogenated hydrocarbons. Environmental Science & Technology 20, pp. 830-836.
104. Li, A., Doucette, W.J., Andren, A.W., 1992. Solubility of polychlorinated biphenyls in binary water/organic solvent systems. Chemosphere 24, pp. 1347-1360.
105. Grover, P.K., Ryall, R.L., 2005. Critical appraisal of salting-out and its implications for chemical and biological sciences. Chemical Reviews 105, pp. 1-10.
106. Ni, N., El-Sayed, M.M., Sanghvi, T., Yalkowsky, S.H., 2000. Estimation of the effect of NaCl on the solubility of organic compounds in aqueous solutions. Journal of Pharmaceutical Sciences 89, pp. 1620-1625.
107. Xie, W.H., Shiu, W.Y., Mackay, D., 1997. A review of the effect of salts on the solubility of organic compounds in seawater. Marine Environmental Research 44, pp. 429-444.
108. Görgényi, M., Dewulf, J., Van Langenhove, H., Héberger, K., 2006. Aqueous salting-out effect of inorganic cations and anions on non-electrolytes. Chemosphere 65, pp. 802-810.
109. Kunz, W., Henle, J., Ninham, B.W., 2004. 'Zur Lehre von der Wirkung der Salze' (about the science of the effect of salts): Franz Hofmeister's historical papers. Current Opinion in Colloid and Interface Science 9, pp. 19-37.

110. Hribar, B., Southall, N.T., Vlachy, V., Dill, K.A., 2002. How ions affect the structure of water. Journal of the American Chemical Society 124, pp. 12302-12311.
111. Endo, S., Pfennigsdorff, A., Goss, K.U., 2012. Salting-out effect in aqueous NaCl solutions: Trends with size and polarity of solute molecules. Environmental Science and Technology 46, pp. 1496-1503.
112. Janado, M., Nishida, T., 1981. Effect of sugars on the solubility of hydrophobic solutes in water. Journal of Solution Chemistry 10, pp. 489-500.
113. Etman, M.A., Naggar, V.F., 1990. Thermodynamics of paracetamol solubility in sugar-water cosolvent systems. International Journal of Pharmaceutics 58, pp. 177-184.
114. Hansson, A., Andersson, J., Leufvén, A., 2001. The effect of sugars and pectin on flavour release from a soft drink-related model system. Food Chemistry 72, pp. 363-368.
115. Nango, M., Yamamoto, H., Joukou, K., Ueda, M., Katayama, A., Kuroki, N., 1980. Solubility of aromatic hydrocarbons in water and aqueous solutions of sugars. Journal of the Chemical Society, Chemical Communications. pp. 104-105.
116. Mani, N., Jun, H.W., Beach, J.W., Nerurkar, J., 2003. Solubility of Guaifenesin in the Presence of Common Pharmaceutical Additives. Pharmaceutical Development and Technology 8, pp. 385-396.
117. Covarrubias-Cervantes, M., Bongard, S., Champion, D., Voilley, A., 2005. Effects of the nature and concentration of substrates in aqueous solutions on the solubility of aroma compounds. Flavour and Fragrance Journal 20, pp. 265-273.
118. Kim, K., Kwon, T., Sung, B.J., Kim, C., 2017. Effect of methane–sugar interaction on the solubility of methane in an aqueous solution. Journal of Colloid and Interface Science 500, pp. 113-118.
119. Copolovici, L., Niinemets, U., 2007. Salting-in and salting-out effects of ionic and neutral osmotica on limonene and linalool Henry's law constants and octanol/water partition coefficients. Chemosphere 69, pp. 621-629.
120. Rischbieter, E., Schumpe, A., Wunder, V., 1996. Gas solubilities in aqueous solutions of organic substances. Journal of Chemical and Engineering Data 41, pp. 809-812.
121. Held, C., Sadowski, G., Carneiro, A., Rodríguez, O., Macedo, E.A., 2013. Modeling thermodynamic properties of aqueous single-solute and multi-solute sugar solutions with PC-SAFT. AIChE Journal 59, pp. 4794-4805.
122. Strickley, R.G., 2004. Solubilizing Excipients in Oral and Injectable Formulations. Pharmaceutical Research 21, pp. 201-230.
123. Jambhekar, S.S., Breen, P., 2016. Cyclodextrins in pharmaceutical formulations II: Solubilization, binding constant, and complexation efficiency. Drug Discovery Today 21, pp. 363-368.
124. Davis, M.E., Brewster, M.E., 2004. Cyclodextrin-based pharmaceutics: Past, present and future. Nature Reviews Drug Discovery 3, pp. 1023-1035.
125. Harris, D.C., Lucy, C.A., 2015. Quantitative Chemical Analysis, 9th Edition. W. H. Freeman.
126. Sweetana, S., Akers, M.J., 1996. Solubility principles and practices for parenteral drug dosage form development. PDA Journal of Pharmaceutical Science and Technology 50, pp. 330-342.
127. Mao, X., Jiang, R., Xiao, W., Yu, J., 2015. Use of surfactants for the remediation of contaminated soils: A review. Journal of Hazardous Materials 285, pp. 419-435.
128. Palmer, M., Hatley, H., 2018. The role of surfactants in wastewater treatment: Impact, removal and future techniques: A critical review. Water Research 147, pp. 60-72.
129. Labows, J.N., 1992. Surfactant solubilization behavior via headspace analysis. Journal of the American Oil Chemists Society 69, pp. 34-38.
130. Lloyd, N.W., Kardaras, E., Ebeler, S.E., Dungan, S.R., 2011. Measuring local equilibrium flavor distributions in SDS solution using headspace solid-phase microextraction. Journal of Physical Chemistry B 115, pp. 14484-14492.
131. Malmsten, M., 2002. Surfactants and polymers in drug delivery. CRC Press.

132. Jones, M.T., Mahler, H.C., Yadav, S., Bindra, D., Corvari, V., Fesinmeyer, R.M., Gupta, K., Harmon, A.M., Hinds, K.D., Koulov, A., Liu, W., Maloney, K., Wang, J., Yeh, P.Y., Singh, S.K., 2018. Considerations for the Use of Polysorbates in Biopharmaceuticals. Pharmaceutical Research 35. doi:10.1007/s11095-018-2430-5.
133. Israelachvili, J.N., Mitchell, D.J., Ninham, B.W., 1976. Theory of self-assembly of hydrocarbon amphiphiles into micelles and bilayers. Journal of the Chemical Society, Faraday Transactions 2: Molecular and Chemical Physics 72, pp. 1525-1568.
134. Tanford, C., 1974. Theory of micelle formation in aqueous solutions. The Journal of Physical Chemistry 78, pp. 2469-2479.
135. Gouliarmou, V., Smith, K.E.C., De Jonge, L.W., Mayer, P., 2012. Measuring binding and speciation of hydrophobic organic chemicals at controlled freely dissolved concentrations and without phase separation. Analytical Chemistry 84, pp. 1601-1608.
136. Zhang, S.-X., Chai, X.-S., Barnes, D.G., 2017. Determination of Critical Micelle Concentration of Surfactants by Headspace Gas Chromatography. Journal of Surfactants and Detergents 20, pp. 1395-1400.
137. Zhong, H., Yang, L., Zeng, G., Brusseau, M.L., Wang, Y., Li, Y., Liu, Z., Yuan, X., Tan, F., 2015. Aggregate-based sub-CMC solubilization of hexadecane by surfactants. RSC Advances 5, pp. 78142-78149.
138. Hill, A.J., Ghoshal, S., 2002. Micellar Solubilization of Naphthalene and Phenanthrene from Nonaqueous-Phase Liquids. Environmental Science & Technology 36, pp. 3901-3907.
139. Mohamed, A., Mahfoodh, A.S.M., 2006. Solubilization of naphthalene and pyrene by sodium dodecyl sulfate (SDS) and polyoxyethylenesorbitan monooleate (Tween 80) mixed micelles. Colloids and Surfaces A: Physicochemical and Engineering Aspects 287, pp. 44-50.
140. Sepulveda, L., Lissi, E., Quina, F., 1986. Interactions of neutral molecules with ionic micelles. Advances in Colloid and Interface Science 25, pp. 1-57.
141. Falconer, R.J., 2019. Advances in liquid formulations of parenteral therapeutic proteins. Biotechnology Advances 37. doi:10.1016/j.biotechadv.2019.06.011.
142. Griffin, W.C., 1949. Classification of Surface-Active Agents by “HLB”. Journal of Cosmetic Science 1, pp. 311-326.
143. Bernardez, L.A., Ghoshal, S., 2004. Selective Solubilization of Polycyclic Aromatic Hydrocarbons from Multicomponent Nonaqueous-Phase Liquids into Nonionic Surfactant Micelles. Environmental Science & Technology 38, pp. 5878-5887.
144. Ilko, D., Braun, A., Germershaus, O., Meinel, L., Holzgrabe, U., 2015. Fatty acid composition analysis in polysorbate 80 with high performance liquid chromatography coupled to charged aerosol detection. European Journal of Pharmaceutics and Biopharmaceutics 94, pp. 569-574.
145. Tani, T.H., Moore, J.M., Patapoff, T.W., 1997. Single step method for the accurate concentration determination of polysorbate 80. Journal of Chromatography A 786, pp. 99-106.
146. Akers, M.J., 2002. Excipient-drug interactions in parenteral formulations. Journal of Pharmaceutical Sciences 91, pp. 2283-2300.
147. Christiansen, A., Backensfeld, T., Kühn, S., Weitschies, W., 2011. Stability of the non-ionic surfactant polysorbate 80 investigated by HPLC-MS and charged aerosol detector. Pharmazie 66, pp. 666-671.
148. Kerwin, B.A., 2008. Polysorbates 20 and 80 used in the formulation of protein biotherapeutics: Structure and degradation pathways. Journal of Pharmaceutical Sciences 97, pp. 2924-2935.
149. Braun, A.C., Ilko, D., Merget, B., Gieseler, H., Germershaus, O., Holzgrabe, U., Meinel, L., 2015. Predicting critical micelle concentration and micelle molecular weight of polysorbate 80 using compendial methods. European Journal of Pharmaceutics and Biopharmaceutics 94, pp. 559-568.
150. Zdravkovic, S.A., 2019. Comparison of the Extraction Properties of Binary Polysorbate 80/Water and Isopropanol/Water Solutions for Organic Substances Originating from a

Parenteral Infusion Pump. PDA Journal of Pharmaceutical Science and Technology. doi:10.5731/pdajpst.2018.009753.
151. Moulik, S.P., Gupta, S., Das, A.R., 1989. Hydration studies on some polyhydroxy non-electrolytes and non-ionic surfactants. Canadian Journal of Chemistry 67, pp. 356-364.
152. Wan, L.S.C., Lee, P.F.S., 1974. CMC of Polysorbates. Journal of Pharmaceutical Sciences 63, pp. 136-137.
153. Tiefenbach, K.J., Durchschlag, H., Jaenicke, R., 1999. Spectroscopic and hydrodynamic investigations of nonionic and zwitterionic detergents, Progress in Colloid and Polymer Science, pp. 135-141.
154. Farhadieh, B., 1973. Determination of cmc and partial specific volume of polysorbates 20, 60, and 80 from densities of their aqueous solutions. Journal of Pharmaceutical Sciences 62, pp. 1685-1688.
155. Mandal, A., Gupta, S., Moulik, S., 1985. Characterisation of Tween 20 & Tween 80 Micelles in Aqueous Medium from Transport Studies. Indian Journal of Chemistry - Section A Inorganic, Physical, Theoretical and Analytical Chemistry 24A, pp. 670-673.
156. Acharya, K.R., Bhattacharya, S.C., Moulik, S.P., 1997. Salt effects on surfactant aggregation and dye-micelle complexation. Indian Journal of Chemistry - Section A Inorganic, Physical, Theoretical and Analytical Chemistry 36, pp. 137-143.
157. Nayem, J., Zhang, Z., Tomlinson, A., Zarraga, I.E., Wagner, N.J., Liu, Y., 2020. Micellar Morphology of Polysorbate 20 and 80 and Their Ester Fractions in Solution via Small-Angle Neutron Scattering. Journal of Pharmaceutical Sciences 109, pp. 1498-1508.
158. Fredenslund, A., Jones, R.L., Prausnitz, J.M., 1975. Group-contribution estimation of activity coefficients in nonideal liquid mixtures. AIChE Journal 21, pp. 1086-1099.
159. Dearden, J.C., 1985. Partitioning and lipophilicity in quantitative structure-activity relationships. Environmental Health Perspectives VOL. 61, pp. 203-228.
160. Valsaraj, K.T., Thibodeaux, L.J., 1990. On the estimations of Micelle-Water partition constants for solutes from their Octanol-Water partition constants, normal boiling points, aqueous solubilities, and group and bond contribution schemes. Separation Science and Technology 25, pp. 369-395.
161. Goss, K.-U., Schwarzenbach, R.P., 2001. Linear Free Energy Relationships Used To Evaluate Equilibrium Partitioning of Organic Compounds. Environmental Science & Technology 35, pp. 1-9.
162. Klamt, A., 2011. The COSMO and COSMO-RS solvation models. Wiley Interdisciplinary Reviews: Computational Molecular Science 1, pp. 699-709.
163. Sangster, J.M., 1997. Octanol-water partition coefficients: fundamentals and physical chemistry. John Wiley & Sons.
164. Alvarez-Núñez, F.A., Yalkowsky, S.H., 2000. Relationship between Polysorbate 80 solubilization descriptors and octanol-water partition coefficients of drugs. International Journal of Pharmaceutics 200, pp. 217-222.
165. Mokrushina, L., Buggert, M., Smirnova, I., Arlt, W., Schomäcker, R., 2007. COSMO-RS and UNIFAC in Prediction of Micelle/Water Partition Coefficients. Industrial & Engineering Chemistry Research 46, pp. 6501-6509.
166. Ingram, T., Mehling, T., Smirnova, I., 2013. Partition coefficients of ionizable solutes in aqueous micellar two-phase systems. Chemical Engineering Journal 218, pp. 204-213.
167. Klamt, A., Huniar, U., Spycher, S., Keldenich, J., 2008. COSMOmic: A mechanistic approach to the calculation of membrane-water partition coefficients and internal distributions within membranes and micelles. Journal of Physical Chemistry B 112, pp. 12148-12157.
168. Ingram, T., Storm, S., Kloss, L., Mehling, T., Jakobtorweihen, S., Smirnova, I., 2013. Prediction of micelle/water and liposome/water partition coefficients based on molecular dynamics simulations, COSMO-RS, and COSMOmic. Langmuir 29, pp. 3527-3537.
169. Taft, R.W., Abboud, J.L.M., Kamlet, M.J., Abraham, M.H., 1985. Linear solvation energy relations. Journal of Solution Chemistry 14, pp. 153-186.

170. Vitha, M., Carr, P.W., 2006. The chemical interpretation and practice of linear solvation energy relationships in chromatography. Journal of Chromatography A 1126, pp. 143-194.
171. Abraham, M.H., 1993. Scales of solute hydrogen-bonding: Their construction and application to physicochemical and biochemical processes. Chemical Society Reviews 22, pp. 73-83.
172. Abraham, M.H., Ibrahim, A., Zissimos, A.M., 2004. Determination of sets of solute descriptors from chromatographic measurements. Journal of Chromatography A 1037, pp. 29-47.
173. Endo, S., Goss, K.U., 2014. Predicting partition coefficients of polyfluorinated and organosilicon compounds using polyparameter linear free energy relationships (PP-LFERs). Environmental Science and Technology 48, pp. 2776-2784.
174. Gruber, A.D., Widenhouse, C.W., Mathes, S., Gruber, R.P., 2000. Exhaustive Soxhlet extraction for the complete removal of residual compounds to provide a nonleaching silicone elastomer. Journal of Biomedical Materials Research 53, pp. 445-448.
175. Dearden, J.C., Bentley, D., 2002. The components of the "critical quartet" log Kow values assessed by four commercial software packages. SAR and QSAR in environmental research 13, pp. 185-197.
176. Endo, S., Goss, K.U., 2014. Applications of polyparameter linear free energy relationships in environmental chemistry. Environmental Science and Technology 48, pp. 12477-12491.
177. Hansen, C.M., 2004. 50 Years with solubility parameters - Past and future. Progress in Organic Coatings 51, pp. 77-84.
178. Panayiotou, C., 2012. Redefining solubility parameters: The partial solvation parameters. Physical Chemistry Chemical Physics 14, pp. 3882-3908.
179. Panayiotou, C., 2012. Partial solvation parameters and LSER molecular descriptors. The Journal of Chemical Thermodynamics 51, pp. 172-189.
180. Panayiotou, C., Mastrogeorgopoulos, S., Aslanidou, D., Avgidou, M., Hatzimanikatis, V., 2017. Redefining solubility parameters: Bulk and surface properties from unified molecular descriptors. Journal of Chemical Thermodynamics 111, pp. 207-220.
181. Niederquell, A., Wyttenbach, N., Kuentz, M., Panayiotou, C., 2019. Partial solvation parameters of drugs as a new thermodynamic tool for pharmaceutics. Pharmaceutics 11. doi:10.3390/pharmaceutics11010017.
182. Hsieh, M.-K., Fu, C.-T., Wu, S.-c., 2011. Simultaneous Estimation of Glass–Water Distribution and PDMS–Water Partition Coefficients of Hydrophobic Organic Compounds Using Simple Batch Method. Environmental Science & Technology 45, pp. 7785-7791.
183. Dearden, J.C., Bresnen, G.M., 1988. The Measurement of Partition Coefficients. Quantitative Structure-Activity Relationships 7, pp. 133-144.
184. Sallee, V.L., 1974. Apparent monomer activity of saturated fatty acids in micellar bile salt solutions measured by a polyethylene partitioning system. Journal of Lipid Research 15, pp. 56-64.
185. Hussam, A., Basu, S.C., Hixon, M., Olumee, Z., 1995. General Method for the Study of Solute-Surfactant Association Equilibria of Volatile Solutes by Head Space Gas Chromatography. Analytical Chemistry 67, pp. 1459-1464.
186. Berthod, A., Garcia-Alvarez-Coque, C., 2000. Micellar Liquid Chromatography. Taylor & Francis.
187. Sprunger, L.M., Gibbs, J., Acree Jr, W.E., Abraham, M.H., 2009. Linear Free Energy Relationship Correlation of The Distribution of Solutes Between Water And Cetytrimethylammonium Bromide (CTAB) Micelles. QSAR & Combinatorial Science 28, pp. 72-88.
188. Abraham, M.H., Chadha, H.S., Dixon, J.P., Rafols, C., Treiner, C., 1995. Hydrogen bonding. Part 40. Factors that influence the distribution of solutes between water and sodium dodecylsulfate micelles. Journal of the Chemical Society, Perkin Transactions 2. pp. 887-894.
189. Sprunger, L., Acree Jr, W.E., Abraham, M.H., 2007. Linear free energy relationship correlation of the distribution of solutes between water and Sodium Dodecyl Sulfate (SDS)

micelles and between gas and SDS micelles. Journal of Chemical Information and Modeling 47, pp. 1808-1817.
190. Niederquell, A., Kuentz, M., 2018. Biorelevant Drug Solubility Enhancement Modeled by a Linear Solvation Energy Relationship. Journal of Pharmaceutical Sciences 107, pp. 503-506.
191. Abraham, M.H., Andonian-Haftvan, J., Whiting, G.S., Leo, A., Taft, R.S., 1994. Hydrogen bonding. Part 34. The factors that influence the solubility of gases and vapours in water at 298 K, and a new method for its determination. Journal of the Chemical Society, Perkin Transactions 2. pp. 1777-1791.
192. Cohen–Adad, R., Cohen–Adad, M.T., 2003. Solubility of Solids in Liquids, in: Hefter, G.T., Tomkins, R.P.T. (Eds.), The Experimental Determination of Solubilities. John Wiley & Sons, Ltd, pp. 257-314.
193. Jenke, D., 2015. Safety risk categorization of organic extractables associated with polymers used in packaging, delivery and manufacturing systems for parenteral drug products. Pharmaceutical Research 32, pp. 1105-1127.
194. Poole, C.F., Atapattu, S.N., Poole, S.K., Bell, A.K., 2009. Determination of solute descriptors by chromatographic methods. Analytica Chimica Acta 652, pp. 32-53.
195. Ariyasena, T.C., Poole, C.F., 2014. Determination of descriptors for polycyclic aromatic hydrocarbons and related compounds by chromatographic methods and liquid–liquid partition in totally organic biphasic systems. Journal of Chromatography A 1361, pp. 240-254.
196. Sprunger, L.M., Achi, S.S., Acree Jr, W.E., Abraham, M.H., 2010. Development of correlations for describing solute transfer into acyclic alcohol solvents based on the Abraham model and fragment-specific equation coefficients. Fluid phase equilibria 288, pp. 139-144.
197. Ariyasena, T.C., Poole, C.F., 2013. Evaluation of triethylamine as a counter solvent in totally organic biphasic liquid–liquid partition systems. Chromatographia 76, pp. 1031-1039.
198. Sprunger, L., Proctor, A., Acree Jr, W.E., Abraham, M.H., 2007. Characterization of the sorption of gaseous and organic solutes onto polydimethyl siloxane solid-phase microextraction surfaces using the Abraham model. Journal of Chromatography A 1175, pp. 162-173.
199. Ahsan, S.S., Blaug, S.M., 1960. Interactions of tweens with some pharmaceuticals. Drug standards 28, pp. 95-100.
200. Vinarov, Z., Katev, V., Radeva, D., Tcholakova, S., Denkov, N.D., 2018. Micellar solubilization of poorly water-soluble drugs: effect of surfactant and solubilizate molecular structure. Drug Development and Industrial Pharmacy 44, pp. 677-686.
201. Long, J., Li, L., Jin, Y., Sun, H., Zheng, Y., Tian, S., 2016. Synergistic solubilization of polycyclic aromatic hydrocarbons by mixed micelles composed of a photoresponsive surfactant and a conventional non-ionic surfactant. Separation and Purification Technology 160, pp. 11-17.
202. Cheng, M., Zeng, G., Huang, D., Yang, C., Lai, C., Zhang, C., Liu, Y., 2018. Tween 80 surfactant-enhanced bioremediation: toward a solution to the soil contamination by hydrophobic organic compounds. Critical Reviews in Biotechnology 38, pp. 17-30.
203. Ulrich, N., Endo, S., Brown, T.N., Watanabe, N., Bronner, G., Abraham, M.H., Goss, K.U., 2017. UFZ-LSER database v 3.2 [Internet].
204. Luning Prak, D.J., 2007. Solubilization of nitrotoluenes in micellar nonionic surfactant solutions. Chemosphere 68, pp. 1961-1967.
205. Feng, S., Catron, N.D., Zhu, A.D., Lipari, J.M., Wu, J., Gao, Y., Zhang, G.G.Z., 2018. Predictive Modeling of Micellar Solubilization by Single and Mixed Nonionic Surfactants. Journal of Pharmaceutical Sciences 107, pp. 2079-2090.
206. Cheng, K.Y., Wong, J.W.C., 2006. Effect of synthetic surfactants on the solubilization and distribution of PAHS in water/soil-water systems. Environmental Technology 27, pp. 835-844.
207. Kawakami, K., Oda, N., Miyoshi, K., Funaki, T., Ida, Y., 2006. Solubilization behavior of a poorly soluble drug under combined use of surfactants and cosolvents. European Journal of Pharmaceutical Sciences 28, pp. 7-14.
208. Li, P., Zhao, L., 2002. Cosolubilization of non-polar drugs in polysorbate 80 solutions. International Journal of Pharmaceutics 249, pp. 211-217.

209. Li, P., Zhao, L., 2003. Solubilization of flurbiprofen in pH-surfactant solutions. Journal of Pharmaceutical Sciences 92, pp. 951-956.
210. Rodrigues, R., Betelu, S., Colombano, S., Masselot, G., Tzedakis, T., Ignatiadis, I., 2017. Influence of Temperature and Surfactants on the Solubilization of Hexachlorobutadiene and Hexachloroethane. Journal of Chemical and Engineering Data 62, pp. 3252-3260.
211. Liu, C., Desai, K.G.H., Tang, X., Chen, X., 2005. Solubility of rofecoxib in the presence of aqueous solutions of glycerol, propylene glycol, ethanol, Span 20, Tween 80, and sodium lauryl sulfate at (298.15, 303.15, and 308.15) K. Journal of Chemical and Engineering Data 50, pp. 2061-2064.
212. Hadžiabdić, J., Elezović, A., Imamović, B., Bečić, E., 2012. The improvement of lorazepam solubility by cosolvency, micellization and complexation. Jordan Journal of Pharmaceutical Sciences 5, pp. 141-154.
213. Ismail, A.A., Gouda, M.W., Motawi, M.M., 1970. Micellar solubilization of barbiturates I: Solubilities of certain barbiturates in polysorbates of varying hydrophobic chain length. Journal of Pharmaceutical Sciences 59, pp. 220-224.
214. Hamid, I.A., Parrott, E.L., 1971. Effect of temperature on solubilization and hydrolytic degradation of solubilized benzocaine and homatropine. Journal of Pharmaceutical Sciences 60, pp. 901-906.
215. Patel, N.K., Kostenbauder, H.B., 1958. Interaction of Preservatives with Macromolecules I.: Binding of Parahydroxybenzoic Acid Esters by Polyoxyethylene 20 Sorbitan Monooleate (Tween 80). Journal of the American Pharmaceutical Association 47, pp. 289-293.
216. Shihab, F.A., Ebian, A.R., Mustafa, R.M., 1979. Effect of polyethylene glycol, sodium lauryl sulfate and polysorbate-80 on the solubility of furosemide. International Journal of Pharmaceutics 4, pp. 13-20.
217. Sjökvist, E., Nyström, C., Aldén, M., Caram-Lelham, N., 1992. Physicochemical aspects of drug release. XIV. The effects of some ionic and non-ionic surfactants on properties of a sparingly soluble drug in solid dispersions. International Journal of Pharmaceutics 79, pp. 123-133.
218. Gerakis, A.M., Koupparis, M.A., Efstathiou, C.E., 1993. Micellar acid-base potentiometric titrations of weak acidic and/or insoluble drugs. Journal of Pharmaceutical and Biomedical Analysis 11, pp. 33-41.
219. Abraham, M.H., Acree, J.W.E., 2010. The transfer of neutral molecules, ions and ionic species from water to wet octanol. Physical Chemistry Chemical Physics 12, pp. 13182-13188.
220. Abraham, M.H., Chadha, H.S., Whiting, G.S., Mitchell, R.C., 1994. Hydrogen bonding. 32. An analysis of water-octanol and water-alkane partitioning and the Δlog P parameter of Seiler. Journal of pharmaceutical sciences 83, pp. 1085-1100.
221. Könczöl, Á., Dargó, G., 2018. Brief overview of solubility methods: Recent trends in equilibrium solubility measurement and predictive models. Drug discovery today. Technologies 27, pp. 3-10.
222. Sales, P.S., de Rossi, R.H., Fernández, M.A., 2011. Different behaviours in the solubilization of polycyclic aromatic hydrocarbons in water induced by mixed surfactant solutions. Chemosphere 84, pp. 1700-1707.
223. Poerschmann, J., Goärecki, T., Kopinke, F.D., 2000. Sorption of very hydrophobic organic compounds onto poly(dimethylsiloxane) and dissolved humic organic matter. 1. Adsorption or partitioning of VHOC on PDMS-coated solid-phase microextraction fibers - A never-ending story? Environmental Science and Technology 34, pp. 3824-3830.
224. Schacht, V., Grant, S., Escher, B., Hawker, D., Gaus, C., 2016. Solubility enhancement of dioxins and PCBs by surfactant monomers and micelles quantified with polymer depletion techniques. Chemosphere 152, pp. 99-106.
225. Treiner, C., Mannebach, M.H., 1987. Correlation analysis of solubilization data in aqueous cationic and anionic micellar solutions: Case of the halocarbons. Journal of Colloid And Interface Science 118, pp. 243-251.

226. Samaha, M.W., Gadalla, M.A.F., 1987. Solubilization of carbamazepin by different classes of nonionic surfactants and a bile salt. Drug Development and Industrial Pharmacy 13, pp. 93-112.
227. ter Mors, B.P., D.; Lehmann, L.; Lorson, T.; Meinel, L., 2020. Comparison of polysorbate 20 qualities. Pharm. Ind. 82, pp. 1064-1071.
228. U.S. EPA. 2012. Estimation Programs Interface Suite for Microsoft Windows, v4.11. United Sates Environmental Protection Agency, Washington, DC, USA.
229. OECD, 2021. eChemPortal, v3.4,. Organisation for Economic Co-operation and Development (OECD), Paris, France. https://www.echemportal.org/.
230. Gamsjäger, H., Lorimer, J.W., Salomon, M., Shaw, D.G., Tomkins, R.P.T., 2010. The IUPAC-NIST Solubility Data Series: A guide to preparation and use of compilations and evaluations (IUPAC Technical Report). Pure and Applied Chemistry 82, pp. 1137-1159.
231. Bergström, C.A.S., 2005. Computational models to predict aqueous drug solubility, permeability and intestinal absorption. Expert Opinion on Drug Metabolism & Toxicology 1, pp. 613-627.
232. Dearden, J.C., 2006. In silico prediction of aqueous solubility. Expert Opinion on Drug Discovery 1, pp. 31-52.
233. Bourget, P., Amin, A., Dupont, C., Abely, M., Desmazes-Dufeu, N., Dubus, J.C., Jouani, B.L., Merlette, C., Nové-Josserand, R., Pages, J., Panzo, R., Vidal, F., Voge, F., Hubert, D., 2014. How to minimize toxic exposure to pyridine during continuous infusion of ceftazidime in patients with cystic fibrosis. Antimicrobial Agents and Chemotherapy 58, pp. 2849-2855.
234. Millard, J.W., Alvarez-Núñez, F.A., Yalkowsky, S.H., 2002. Solubilization by cosolvents: Establishing useful constants for the log–linear model. International Journal of Pharmaceutics 245, pp. 153-166.
235. Huang, J.B., Mao, M., Zhu, B.Y., 1999. The surface physico-chemical properties of surfactants in ethanol-water mixtures. Colloids and Surfaces A: Physicochemical and Engineering Aspects 155, pp. 339-348.
236. Zhang, W.C., Li, G.Z., Shen, Q., Mu, J.H., 2000. Effect of benzyl alcohol on the rheological properties of CTAB/KBr micellar systems. Colloids and Surfaces A: Physicochemical and Engineering Aspects 170, pp. 59-64.
237. Meler, J., Pluta, J., 1999. Influence of auxiliary substances on the critical micellar concentration of Tweens®. Pharmazie 54, pp. 439-440.
238. Rhee, Y.S., Park, C.W., Kim, K.J., Chi, S.C., Park, E.S., 2007. Behavior of itraconazole and benzyl alcohol in aqueous solution containing nonionic surfactants. Archives of Pharmacal Research 30, pp. 240-248.
239. Emerson, M.F., Holtzer, A., 1967. On the ionic strength dependence of micelle number. II. The Journal of Physical Chemistry 71, pp. 1898-1907.
240. Hayashi, S., Ikeda, S., 1980. Micelle size and shape of sodium dodecyl sulfate in concentrated NaCl solutions. Journal of Physical Chemistry 84, pp. 744-751.
241. Bendedouch, D., Chen, S.H., 1984. Effect of an attractive potential on the interparticle structure of ionic micelles at high salt concentration. Journal of Physical Chemistry 88, pp. 648-652.
242. Berr, S.S., Jones, R.R.M., 1988. Effect of Added Sodium and Lithium Chlorides on Intermicellar Interactions and Micellar Size of Aqueous Dodecyl Sulfate Aggregates As Determined by Small-Angle Neutron Scattering. Langmuir 4, pp. 1247-1251.
243. Kumar, S., David, S.L., Aswal, V.K., Goyal, P.S., Kabir ud, D., 1997. Growth of sodium dodecyl sulfate micelles in aqueous ammonium salts. Langmuir 13, pp. 6461-6464.
244. Aswal, V.K., Goyal, P.S., 2000. Counterions in the growth of ionic micelles in aqueous electrolyte solutions: A small-angle neutron scattering study. Physical Review E - Statistical Physics, Plasmas, Fluids, and Related Interdisciplinary Topics 61, pp. 2947-2953.
245. Hansson, P., 2001. Self-assembly of ionic surfactants in polyelectrolyte solutions: A model for mixtures of opposite charge. Langmuir 17, pp. 4167-4180.

246. Sammalkorpi, M., Karttunen, M., Haataja, M., 2009. Ionic surfactant aggregates in saline solutions: Sodium dodecyl sulfate (SDS) in the presence of excess sodium chloride (NaCl) or calcium chloride (CaCl2). Journal of Physical Chemistry B 113, pp. 5863-5870.
247. Mukerjee, P., 1965. Salt effects on nonionic association colloids. Journal of Physical Chemistry 69, pp. 4038-4040.
248. Gordon, J.E., 1970. Salt effects on the critical micelle concentrations of nonionic amphiphiles. Journal of Physical Chemistry 74, pp. 3823-3824.
249. Carale, T.R., Pham, Q.T., Blankschtein, D., 1994. Salt Effects on Intramicellar Interactions and Micellization of Nonionic Surfactants in Aqueous Solutions. Langmuir 10, pp. 109-121.
250. Baner, A.L., 1992. Partition Coefficients of Aroma Compounds between Polyethylene and Aqueous Ethanol and Their Estimation Using UNIFAC and GCFEOS. Michigan State University, Department of Food Science and Human Nutrition.
251. Twist, J.N., Zatz, J.L., 1988. Membrane–solvent–solute interaction in a model permeation system. Journal of Pharmaceutical Sciences 77, pp. 536-540.
252. Fritz, L., Hofmann, D., 1998. Behaviour of water/ethanol mixtures in the interfacial region of different polysiloxane membranes - A molecular dynamics simulation study. Polymer 39, pp. 2531-2536.
253. Montemezzo, M., Ferrari, M.D., Kerstner, E., Santos, V.D., Victorazzi Lain, V., Wollheim, C., Frozza, C.O.D.S., Roesch-Ely, M., Baldo, G., Brandalise, R.N., 2021. PHMB-loaded PDMS and its antimicrobial properties for biomedical applications. Journal of Biomaterials Applications. doi:10.1177/08853282211011921.

10. Appendix

10.1 Experimental Test Solutes with Physicochemical Parameters and LSER Substance Descriptors

Table A1. Experimental test solutes with physicochemical parameters and LSER substance descriptors used in this work. Model leachables for migration case study (4.4) in bold text.

Solute	CAS-RN	M[a)]	LSER descriptors					$\log K_{i,O/W}$[b)]	Literature source[c)]
			E_i	S_i	A_i	B_i^0	V_i		
1,2,3-Trichloropropane	96-18-4	147.43	0.55	0.65	0.03	0.31	0.899	2.27	1
1,2-Benzanthraquinone	2498-66-0	258.27	2.5	2.06	0.00	0.64	1.898	3.76	Abraham Absolv[d)]
1-Bromo-2-chloroethane	107-04-0	143.41	0.57	0.70	0.10	0.09	0.688	1.86	1
1-Naphthol	90-15-3	144.17	1.43	1.16	0.74	0.32	1.144	2.85	2
2,2,4-Trimethylpentane	540-84-1	114.22	0.00	0.00	0.00	0.00	1.236	4.43	1
2,2-Dimethylbutane	75-83-2	86.18	0.00	0.00	0.00	0.00	0.954	3.67	1
2,2-Dimethylpentane	590-35-2	100.21	0.00	0.00	0.00	0.00	1.095	3.82	3
2,4,4-Trimethylpent-2-ene	107-40-4	112.21	0.14	0.08	0.00	0.07	1.193	4.14	Abraham Absolv
2,4-Dichlorophenol	120-83-2	163.00	0.96	0.82	0.54	0.17	1.020	3.06	4
2,4-Dinitrotoluene	121-14-2	182.13	1.15	1.60	0.00	0.47	1.206	1.98	5
3,5-Di-tert-butyl-4-hydroxybenzaldehyde	1620-98-0	234.33	1.05	1.17	0.48	0.77	2.060	4.15	ACD/Absolv[e)]
2-Bromophenol	95-56-7	173.01	1.04	0.90	0.35	0.31	0.950	2.35	4
2-Chloroaniline	95-51-2	127.57	1.03	0.99	0.25	0.38	0.939	1.88	2
2-Chlorotoluene	95-49-8	126.58	0.76	0.65	0.00	0.07	0.980	3.27	1
2-Ethyl-1-hexanol	104-76-7	130.23	0.21	0.39	0.37	0.48	1.290	2.72	6
2-Hexanone	591-78-6	100.16	0.14	0.68	0.00	0.51	0.970	1.69	2
2-Hydroxybiphenyl	90-43-7	170.21	1.55	1.40	0.56	0.49	1.383	3.09	6
2-Iodophenol	533-58-4	220.01	1.36	1.00	0.40	0.35	1.033	2.65	4
2-Methylaniline	95-53-4	107.15	0.96	1.04	0.18	0.53	0.957	1.32	2
3-Methylpentane	96-14-0	86.18	0.00	0.00	0.00	0.00	0.954	3.60	1
4-Aminobiphenyl	92-67-1	169.22	1.57	1.48	0.26	0.58	1.424	2.88	7
4-Iodoaniline	540-37-4	219.02	1.53	1.28	0.31	0.40	1.074	2.32	8
4-Nitroanisole	100-17-4	153.14	0.97	1.29	0.00	0.40	1.090	2.03	9
4-tert-Butylphenol	98-54-4	150.22	0.81	0.89	0.56	0.39	1.339	3.42	9
9-Phenylcarbazole	1150-62-5	243.30	2.40	1.74	0.00	0.31	1.923	5.06	Abraham Absolv
Acenaphthene	83-32-9	154.21	1.50	0.99	0.00	0.22	1.259	3.92	2
Acenaphthylene	208-96-8	152.19	1.56	1.17	0.00	0.20	1.216	3.85	2
Acetanisole	100-06-1	150.17	0.92	1.58	0.00	0.53	1.214	1.74	10
Aniline	62-53-3	93.13	0.96	0.10	0.25	0.51	0.816	0.90	2
Benzidine	92-87-5	184.24	1.88	1.57	0.23	0.80	1.524	1.34	11

Benzophenone	119-61-9	182.00	1.19	1.31	0.00	0.57	1.481	3.20	[2]
Benzothiazole	95-16-9	135.19	1.30	1.21	0.00	0.47	0.969	2.01	[11]
Butyraldehyde	123-72-8	72.11	0.17	0.64	0.00	0.43	0.688	0.88	[2]
Butyronitrile	109-74-0	69.11	0.19	0.90	0.00	0.36	0.686	0.53	[1]
Carbazole	86-74-8	167.21	2.22	1.61	0.40	0.25	1.315	3.72	[2]
Chlorobenzene	108-90-7	112.56	0.72	0.65	0.00	0.06	0.839	2.84	[2]
Cyclohexane	110-82-7	84.16	0.31	0.10	0.00	0.00	0.845	3.44	[10]
Decane	124-18-5	142.29	0.00	0.00	0.00	0.00	1.518	5.01	[1]
Di(2-ethylhexyl) phthalate	117-81-7	390.56	0.69	1.16	0.00	1.19	3.401	7.60	[12]
Dibutyl phthalate	84-74-2	278.34	0.69	1.32	0.00	0.93	2.274	4.45	[2]
Diethyl disulfide	110-81-6	122.25	0.67	0.54	0.00	0.27	0.999	2.91	[1]
Diethyl ether	60-29-7	74.12	0.04	0.26	0.00	0.50	0.731	0.89	[13]
Diphenylamine	122-39-4	169.23	1.70	1.28	0.15	0.53	1.424	3.50	[12]
Dodecane	112-40-3	170.34	0.00	0.00	0.00	0.00	1.799	6.10	[10]
Ethyl acrylate	140-88-5	100.12	0.21	0.64	0.00	0.42	0.845	1.32	Abraham Absolv
Ethyl hexanoate	123-66-0	144.21	0.04	0.59	0.00	0.45	1.310	2.30	[2]
FTOH 4:2	2043-47-2	264.09	-0.51	-0.43	0.84	0.41	1.172	3.30	[14]
FTOH 6:2	647-42-7	364.1	-0.82	-0.89	0.79	0.54	1.525	4.54	[14]
Hept-1-yne	628-71-7	96.17	0.16	0.23	0.12	0.10	1.009	3.18	[15]
Heptane	142-82-5	100.21	0.00	0.00	0.00	0.00	1.095	4.66	[1]
Hexanal	66-25-1	100.16	0.16	0.64	0.00	0.43	0.970	1.78	[2]
Hexane	110-54-3	86.18	0.00	0.00	0.00	0.00	0.954	3.90	[1]
Iodobenzene	591-50-4	203.01	1.19	0.77	0.00	0.13	0.975	3.25	[2]
Isoamyl acetate	123-92-2	130.19	0.05	0.57	0.00	0.47	1.169	2.25	[1]
Methyl ethyl ketone	78-93-3	72.11	0.17	0.68	0.00	0.51	0.688	0.29	[2]
Methyl methacrylate	80-62-6	100.12	0.25	0.51	0.00	0.44	0.845	1.38	[1]
Methyl salicylate	119-36-8	152.14	0.85	0.82	0.01	0.48	1.131	2.55	[16]
Methyl-4-chlorobenzoate	1126-46-1	170.59	0.80	1.15	0.00	0.30	1.195	2.87	[6]
N,N-Diethylaniline	91-66-7	149.23	0.95	0.80	0.00	0.50	1.380	3.31	[6]
Naphthalene	91-20-3	128.17	1.22	0.92	0.00	0.19	1.085	3.30	[2]
n-Butyl methacrylate	97-88-1	142.2	0.17	0.49	0.00	0.45	1.267	2.75	Abraham Absolv
N-Methylaniline	100-61-8	107.15	0.95	0.90	0.17	0.48	0.957	1.66	[6]
Non-1-ene	124-11-8	126.24	0.09	0.08	0.00	0.07	1.334	4.89	[15]
Nonanal	124-19-6	142.24	0.14	0.64	0.00	0.43	1.392	3.56	[2]
n-Propylbenzene	103-65-1	120.2	0.60	0.48	0.00	0.14	1.139	3.69	[2]
Oct-1-ene	111-66-0	112.22	0.09	0.08	0.00	0.07	1.193	4.41	[15]
Octane	111-65-9	114.23	0.00	0.00	0.00	0.00	1.236	5.18	[1]
Oleamide	301-02-0	281.48	0.61	0.53	0.31	0.56	2.717	7.98	ACD/Absolv
Pentane	109-66-0	72.15	0.00	0.00	0.00	0.00	0.813	3.39	[1]

S-Limonene	5989-54-8	136.23	0.49	0.35	0.00	0.16	1.323	4.58	2
Tetrachloroethene	127-18-4	165.83	0.64	0.44	0.00	0.00	0.837	2.88	1
Tetrahydrofuran	109-99-9	72.11	0.30	0.53	0.00	0.46	0.622	0.46	2
Tetralin	119-64-2	132.2	0.89	0.65	0.00	0.17	1.170	3.96	2
Thiophene	110-02-1	84.14	0.69	0.57	0.00	0.15	0.641	1.81	1
Toluene	108-88-3	92.14	0.61	0.50	0.00	0.14	0.857	2.60	2
Trichloroethene	79-01-6	131.39	0.52	0.37	0.08	0.03	0.715	2.53	1
Trichloromethane	67-66-3	119.38	0.43	0.49	0.15	0.02	0.617	1.92	1
Triphenyl phosphate	115-86-6	326.28	1.83	1.66	0.00	1.10	2.371	4.60	17
Undecane	1120-21-4	156.31	0.00	0.00	0.00	0.00	1.659	5.74	15
Valerophenone	1009-14-9	162.23	0.78	1.00	0.00	0.50	1.437	3.20	2

a) Molar mass in g mol^{-1}.
b) Logarithmic octanol water partition coefficient retrieved from EPI Suite™ v4.11.
c) Chosen literature source from UFZ database (UFZ) or from Poole's database [2].
d) Personal database of M.H. Abraham included in UFZ tool.
e) Advanced Chemistry Development, Inc. (ACD/Labs), ACD/Absolv tool v5.0.0.184.

Table A2. Solutes used in the literature with physicochemical properties and LSER substance descriptors.

Solute	CAS-RN	M	LSER descriptors					log	Source
			E_i	S_i	A_i	B_i^0	V_i	$K_{i,O/W}$	
2,3-Dinitrotoluene	602-01-7	182.14	1.15	1.70	0.00	0.40	1.206	1.43	Abraham Absolv
2,4,6-Trinitrotoluene	118-96-7	227.13	1.39	2.03	0.06	0.69	1.380	1.60	Abraham Absolv
2,4-Dinitrophenol	51-28-5	184.11	1.20	1.49	0.09	0.56	1.124	1.67	4
2,6-Dinitrotoluene	606-20-2	182.14	1.15	1.55	0.00	0.45	1.206	2.10	Abraham Absolv
3-Methylbenzoic acid	99-04-7	136.15	0.73	0.89	0.60	0.40	1.073	2.37	Abraham Absolv
3-Nitrobenzoic acid	121-92-6	167.12	0.99	1.18	0.73	0.52	1.106	1.83	18
4-Hydroxybenzoic acid	99-96-7	138.12	0.93	0.90	0.81	0.56	0.990	1.58	16
4-Nitrotoluene	99-99-0	137.14	0.90	1.17	0.00	0.27	1.032	2.37	2
4-tert-Butylbenzoic acid	98-73-7	178.23	0.73	0.84	0.59	0.41	1.495	3.85	Abraham Absolv
Acetylsalicylic acid	50-78-2	180.16	0.78	1.69	0.71	0.67	1.290	1.19	16
Allobarbital	52-43-7	208.21	1.29	1.32	0.51	1.26	1.570	1.15	Abraham Absolv
Amobarbital	57-43-2	226.27	1.03	1.11	0.47	1.23	1.800	2.07	19
Barbital	57-44-3	184.19	1.03	1.14	0.47	1.18	1.370	0.65	19
Benzocaine	94-09-7	165.19	1.03	1.31	0.31	0.69	1.310	1.86	18
Benzoic acid	65-85-0	122.12	0.73	0.90	0.59	0.40	0.930	1.87	16
Butobarbital	77-28-1	212.25	1.03	1.14	0.47	1.18	1.660	1.73	19
Cyclobarbital	52-31-3	236.27	1.44	1.35	0.49	1.45	1.790	1.77	Abraham Absolv
Cyclosporin	59865-13-3	1202.6	4.23	10.6	1.20	7.60	10.02	2.80	Abraham Absolv
Ethinylestradiol	57-63-6	296.40	2.01	2.34	0.98	1.23	2.395	3.67	Abraham Absolv
Flurbiprofen	5104-49-4	244.26	1.44	1.45	0.62	0.76	1.839	4.16	16

Furosemide	54-31-9	330.74	2.31	2.19	1.03	1.50	2.100	2.03	Abraham Absolv
Griseofulvin	126-07-8	352.80	1.75	2.64	0.00	1.44	2.390	2.18	Abraham Absolv
Hexachlorobuta-1,3-diene	87-68-3	260.76	1.02	0.42	0.00	0.16	1.321	4.78	[20]
Hexachloroethane	67-72-1	236.74	0.68	0.68	0.00	0.00	1.125	4.03	[1]
Hydrocortison	50-23-7	362.46	2.03	3.49	0.71	1.90	2.798	1.61	[3]
Lorazepam	846-49-1	321.20	2.51	1.28	0.45	1.63	2.114	3.53	[19]
Methyl paraben	99-76-3	138.12	0.90	1.37	0.69	0.45	1.131	1.96	[16]
Naproxen	22204-53-1	230.26	1.51	2.02	0.60	0.67	1.782	3.18	[18]
Phenanthrene	85-01-8	178.23	1.92	1.28	0.00	0.29	1.454	4.46	[11]
Phenobarbital	50-06-6	232.23	1.63	1.80	0.73	1.15	1.700	1.47	[9]
Phenytoin	57-41-0	252.27	1.71	2.19	0.85	1.00	1.869	2.47	[19]
Pyrene	129-00-0	202.25	2.28	1.46	0.00	0.29	1.585	4.88	[2]
Rofecoxib	162011-90-7	314.36	1.66	3.10	0.00	1.30	2.232	1.58	Abraham Absolv
Salicylic acid	69-72-7	138.12	0.90	0.85	0.73	0.37	0.990	2.26	[16]
Secobarbital	76-73-3	238.28	1.16	1.20	0.49	1.31	1.890	1.97	Abraham Absolv
Simvastatin	79902-63-9	418.57	1.35	2.55	0.32	1.86	3.427	4.68	Abraham Absolv
β-Estradiol	50-28-2	272.38	1.80	1.77	0.86	1.10	2.199	4.01	Abraham Absolv

10.2 Instrumental Parameters

Table A3. HS-GC/MS instrumental conditions.

SYSTEM CONFIGURATION				
GC-System	**Agilent 7890**			
Sampler	**Perkin Elmer Turbomatrix 40 Headspace Sampler**			
	direct coupling to analytical column (bypassing SSI)			
	Perkin Elmer Turbomatrix 40 Headspace Sampler			
Sampling Unit				
Carrier gas	**Helium 5.0 60.0 kPa**			
Equilibration	25°C, 10 min			
Temperatures	Transfer line: 125°C		Needle: 125°C	
Injection	Pressurization time: 0 min		Dwell time: 0.2 min	
	Injection time: 0.04 min			
Separation				
Analytical column	**Restek Rxi 624 SilMS, 30 m, 0.32 mm ID, 1.8 µm df**			
Oven Program	**Hold time (min)**	**Temperature (°C)**	**Rate (°C/min)**	**Flow (mL/min)**
	2.0	40	10	0.8
	0.0	100	15	0.8
	0.0	160	20	0.8
	0.0	240	30	0.9
	1.0	270	-	1.2
Detection	**Agilent 5975 C Inert XL MSD**			
Mode	**EI 70.3 eV, Single Ion Monitoring (SIM)**			
SIM conditions	Ions per compound	2		
	Resolution	High		
	Dwell time	25-100 ms		
	EM offset	200 V		
Transfer line	280°C			
Ion source	230°C			
Quadrupol	150°C			
Data Acquisition	**Agilent Mass Hunter GC/MS B.07.03 (2129)**			

Table A4. LC/UV instrumental conditions.

SYSTEM CONFIGURATION				
LC/UV-System	**Agilent 1200 Series**			
Degasser	G1322 A			
Pump	Binary SL G1312 B			
Autosampler	1200 HiP SL G1367C			
Column Thermostat	TCC SL G 1316 P			
Detectors	DAD SL G1315C			
Injection				
Injection volume	8 µL			
Sampling unit	Ambient			
Separation				
Temperature	40°C			
Analytical column	**Phenomenex Synergi 2.5µ Hydro-RP 100 A 100x3.0mm 2.5 µm**			
Mobile Phase A	**10 mM KH_2PO_4 pH 2.5**			
Mobile Phase B	**Acetonitrile**			
Gradient	**Time (min)**	**%A**	**%B**	**Flow (mL/min)**
	0.0	94	6	0.8
	2.0	94	6	0.8
	6.0	58	42	0.8
	8.0	40	60	0.9
	18.0	20	80	1.2
	20.0	0	100	1.7
	24.0	0	100	1.9
	24.5	40	60	0.8
	25.5	94	6	0.8
	28.0	94	6	0.8
	0.0	94	6	0.8
Detection				
	Detection wavelength was individually chosen based on absorption maxima of target compounds, for up to eight wavelengths.			
	Bandwidth 10 nm			
	Reference wavelength 550 nm			
Data Acquisition	**Empower 3 Build 3471**			

Table A5. LC/MS instrumental conditions.

SYSTEM CONFIGURATION				
LC-System	**Thermo Fisher U3000**			
Degasser	SRD-3600			
Pump	HPG-3400SD			
Autosampler	WPS-3000			
Column Thermostat	TCC-3100			
Detector	Q Exactive™ Focus Orbitrap™			
Injection				
Injection volume	25 µL			
Sampling unit	Ambient			
Separation				
Temperature	60 °C			
Analytical column	**Phenomenex Kinetex F5 C18 100 A 100x4.6 mm 2.6 µm**			
Mobile Phase A	**80% 0.1% v/v formic acid, 20% methanol**			
Mobile Phase B	**0.1% v/v formic acid in methanol**			
Gradient	**Time (min)**	**%A**	**%B**	**Flow (mL/min)**
	0.0	90	0	1.0
	6.0	90	70	1.0
	13.0	45	85	1.0
	16.0	45	98	1.0
	23.0	10	99	1.0
	23.1	10	0	1.0
	27.0	90	0	1.0
Detection	**Thermo Q Exactive™ Focus Orbitrap™**			
Mode	**APCI, Single Ion Monitoring (SIM)**			
Capillary temperature	320°C			
S-lens RF level	50			
Resolution	17 500			
Data Acquisition	**TraceFinder™ 4.1 (2016)**			

10.3 LSER Validation Sets

Table A6. Calibration set for LSER accuracy. Predicted $\log K_{i,PS80/W}$ from eq. (31) – calibration set and eq (28) – complete data set.

Solute	CAS-RN	Exp. $\log K_{i,PS80/W}$	Eq. (31) $\log K_{i,PS80/W}$	|Delta| Exp./Eq. (31)	Eq. (28) $\log K_{i,PS80/W}$
Aniline	62-53-3	1.13	0.82	0.31	0.87
Acenaphthene	83-32-9	3.84	4.03	0.19	4.04
Phenytoin	57-41-0	2.61	2.43	0.18	2.46
Dodecane	112-40-3	6.64	6.37	0.27	6.33
Cyclohexane	110-82-7	3.21	3.02	0.19	3.05
2-Hexanone	591-78-6	0.98	1.04	0.06	1.03
Hept-1-yne	628-71-7	2.96	2.99	0.03	3.01
Thiophene	110-02-1	1.56	1.64	0.08	1.67
2,4-Dinitrophenol	51-28-5	1.72	1.58	0.14	1.58
Furosemide	54-31-9	2.42	2.10	0.32	2.15
4-Nitrotoluene	99-99-0	1.99	2.28	0.29	2.28
2,4,4-Trimethylpent-2-ene	107-40-4	3.66	3.93	0.27	3.94
Benzothiazole	95-16-9	1.77	1.70	0.07	1.71
Methyl-4-chlorobenzoate	1126-46-1	2.57	2.72	0.15	2.70
4-tert-Butylbenzoic acid	98-73-7	3.02	3.53	0.51	3.58
Tetrachloroethene	127-18-4	2.93	2.95	0.02	2.98
Nonanal	124-19-6	2.86	2.91	0.05	2.89
Amobarbital	57-43-2	1.83	1.94	0.11	1.95
Lorazepam	846-49-1	3.09	2.95	0.14	2.97
Heptane	142-82-5	3.84	3.75	0.09	3.77
4-Iodoaniline	540-37-4	2.68	2.39	0.29	2.43
Simvastatin	79902-63-9	4.87	4.76	0.11	4.60
Diethyl disulfide	110-81-6	2.53	2.57	0.04	2.59
Acetanisole	100-06-1	1.56	1.70	0.14	1.66
Hexanal	66-25-1	1.34	1.37	0.03	1.36
Benzidine	92-87-5	2.54	2.76	0.22	2.76
n-Butyl methacrylate	97-88-1	2.41	2.55	0.14	2.53
2,2,4-Trimethylpentane	540-84-1	4.36	4.28	0.08	4.28
2-Chlorotoluene	95-49-8	3.04	3.15	0.11	3.16
Diphenylamine	122-39-4	3.55	3.44	0.11	3.45
N,N-Diethylaniline	91-66-7	2.70	3.21	0.51	3.19
1-Bromo-2-chloroethane	107-04-0	1.54	1.75	0.21	1.79
Carbazole	86-74-8	4.10	4.09	0.01	4.14
3-Methylbenzoic acid	99-04-7	1.81	1.95	0.14	2.02

2,6-Dinitrotoluene	606-20-2	2.09	2.18	0.09	2.15
4-Aminobiphenyl	92-67-1	3.02	2.93	0.09	2.94
2,4-Dinitrotoluene	121-14-2	2.00	2.06	0.06	2.03
3-Methylpentane	96-14-0	3.51	3.23	0.28	3.25
Iodobenzene	591-50-4	2.93	3.20	0.27	3.22
Griseofulvin	126-07-8	2.7	2.70	0.00	2.58
FTOH 6:2	647-42-7	3.22	3.76	0.54	3.79
Undecane	1120-21-4	6.29	5.84	0.45	5.82
Benzocaine	94-09-7	1.89	1.79	0.10	1.81
Secobarbital	76-73-3	2.05	2.03	0.02	2.03
2,3-Dinitrotoluene	602-01-7	2.24	2.20	0.04	2.17
Butyronitrile	109-74-0	0.50	0.31	0.19	0.32
Pentane	109-66-0	3.16	2.71	0.45	2.74
Ethyl hexanoate	123-66-0	2.43	2.49	0.06	2.47
4-hydroxybenzoic acid	99-96-7	1.11	1.22	0.11	1.33
Butyraldehyde	123-72-8	0.45	0.33	0.12	0.35
Trichloroethene	79-01-6	2.30	2.34	0.04	2.38
Ethinylestradiol	57-63-6	3.85	3.69	0.16	3.71
N-Methylaniline	100-61-8	1.61	1.56	0.05	1.59
1-Naphthol	90-15-3	3.11	2.81	0.30	2.91
FTOH 4:2	2043-47-2	2.18	2.70	0.52	2.74
Flurbiprofen	5104-49-4	3.98	3.67	0.31	3.70
Rofecoxib	162011-90-7	2.28	2.02	0.26	1.92
Allobarbital	52-43-7	1.24	1.04	0.20	1.03
Non-1-ene	124-11-8	4.63	4.38	0.25	4.40
ß-Estradiol	50-28-2	3.41	3.79	0.38	3.84
Triphenyl phosphate	115-86-6	4.63	4.86	0.23	4.73
Naproxen	22204-53-1	2.79	3.22	0.43	3.28
Diethyl ether	60-29-7	0.30	0.51	0.21	0.52
Hexane	110-54-3	3.41	3.21	0.20	3.25
Dibutyl phthalate	84-74-2	4.13	4.29	0.16	4.22
2-Ethyl-1-hexanol	104-76-7	2.20	2.53	0.33	2.60
Acetylsalicylic acid	50-78-2	1.21	1.00	0.21	1.12
Toluene	108-88-3	2.03	2.47	0.44	2.48
Methyl ethyl ketone	78-93-3	0.14	0.02	0.12	0.03
Octane	111-65-9	4.38	4.25	0.13	4.28
1,2,3-Trichloropropane	96-18-4	2.06	1.84	0.22	1.86
Phenanthrene	85-01-8	4.59	4.65	0.06	4.60
2,2-Dimethylbutane	75-83-2	3.71	3.21	0.50	3.25

Isoamyl acetate	123-92-2	1.88	1.90	0.02	1.91
Valerophenone	1009-14-9	2.84	3.06	0.22	3.04

Table A7. Validation set for LSER accuracy. Predicted $\log K_{i,PS80/W}$ from eq. (31) – calibration set and eq. (28) – complete data set.

Solute	CAS-RN	Exp. $\log K_{i,PS80/W}$	Eq. (31) $\log K_{i,PS80/W}$	|Delta| Exp./Eq. (31)	Eq. (28) $\log K_{i,PS80/W}$
Tetrahydrofuran	109-99-9	0.16	0.20	0.04	0.23
Salicylic acid	69-72-7	1.86	1.90	0.04	2.00
Ethyl acrylate	140-88-5	0.93	0.97	0.04	0.98
2-Chloroaniline	95-51-2	2.04	1.80	0.24	1.84
Cyclobarbital	52-31-3	1.56	1.29	0.27	1.31
Hexachlorobuta-1,3-diene	87-68-3	4.65	4.57	0.08	4.58
2,4,6-Trinitrotoluene	118-96-7	1.74	1.74	0.00	1.70
Tetralin	119-64-2	3.45	3.64	0.19	3.64
Chlorobenzene	108-90-7	2.43	2.63	0.20	2.65
Trichloromethane	67-66-3	1.67	1.79	0.12	1.84
S-Limonene	5989-54-8	3.92	4.16	0.24	4.15
2-Methylaniline	95-53-4	1.21	1.28	0.07	1.31
Decane	124-18-5	5.69	5.32	0.37	5.31
Phenobarbital	50-06-6	1.77	1.64	0.13	1.68
Acenaphthylene	208-96-8	3.73	3.81	0.08	3.81
Cyclosporin	59865-13-3	3.46	4.31	0.85	3.62
Hydrocortison	50-23-7	1.99	1.89	0.10	1.80
Methyl salicylate	119-36-8	2.24	2.24	0.00	2.24
3-Nitrobenzoic acid	121-92-6	1.62	1.58	0.04	1.67
4-tert-Butylphenol	98-54-4	3.06	3.05	0.01	3.11
Benzoic acid	65-85-0	1.57	1.41	0.16	1.49
2,4-Dichlorophenol	120-83-2	3.25	2.83	0.42	2.91
Methyl paraben	99-76-3	1.86	1.66	0.20	1.72
Benzophenone	119-61-9	2.76	3.05	0.29	3.02
Naphthalene	91-20-3	3.15	3.29	0.14	3.30
Methyl methacrylate	80-62-6	1.04	1.07	0.03	1.08
Butethal	77-28-1	1.51	1.56	0.05	1.58
n-Propylbenzene	103-65-1	3.41	3.52	0.11	3.53
Pyrene	129-00-0	5.14	5.27	0.13	5.25
Barbital	57-44-3	0.77	0.48	0.29	0.52
2,2-Dimethylpentane	590-35-2	4.06	3.75	0.31	3.77
2-Bromophenol	95-56-7	2.50	2.14	0.36	2.20
2-Iodophenol	533-58-4	2.87	2.50	0.37	2.56

Hexachloroethane	67-72-1	3.42	3.82	0.40	3.82
4-Nitroanisole	100-17-4	2.08	2.01	0.07	2.00
Oct-1-ene	111-66-0	4.11	3.89	0.22	3.89
2-Hydroxybiphenyl	90-43-7	3.27	3.06	0.21	3.11

10.4 Migration Case Study

Table A8. Predicted and experimental logarithmic partition coefficients between PDMS and PS 80 solutions.

	$\log K_{i,P/f_{PS80=0.01\%}}$		$\log K_{i,P/f_{PS80=0.1\%}}$		$\log K_{i,P/f_{PS80=0.5\%}}$	
Compound	Predicted	Experimental	Predicted	Experimental	Predicted	Experimental
1,2-Benzanthraquinone	2.31	2.91	1.38	1.99	0.69	1.16
Di-(2-ethylhexyl) phthalate	2.95	n.d.[a)]	1.95	2.85	1.25	1.94
9-Phenylcarbazole	2.78	3.29	1.78	2.20	1.09	1.49
Oleamide	2.95	3.49	1.95	1.93	1.25	1.38
3,5-Di-tert-butyl-4-hydroxybenzaldehyde	3.15	3.21	2.47	2.51	1.82	1.74

a) Not determined in medium, therefore no calculation of $\log K_i$ possible.

Table A9. Predicted and experimental logarithmic partition coefficients between PDMS and placebo solutions.

	$\log K_{i,P/Placebo\ 1}$		$\log K_{i,P/Placebo\ 2}$		$\log K_{i,P/Placebo\ 3}$	
Compound	Predicted	Experimental	Predicted	Experimental	Predicted	Experimental
1,2-Benzanthraquinone	0.69	0.93	0.69	0.95	0.69	1.43
Di-(2-ethylhexyl) phthalate	1.25	1.82	1.25	1.87	1.25	2.29
9-Phenylcarbazole	1.09	1.42	1.09	1.41	1.09	1.88
Oleamide	1.25	0.86	1.25	0.97	1.25	0.95
3,5-Di-tert-butyl-4-hydroxybenzaldehyde	1.82	1.56	1.82	1.57	1.82	1.88

Table A10. Predicted and experimental logarithmic partition coefficients between PDMS and ethanol-water mixtures or water.

	$\log K_{i,P/f_{EtOH=20\%}}$		$\log K_{i,P/f_{EtOH=50\%}}$		$\log K_{i,P/W}$	
Compound	Predicted	Experimental	Predicted	Experimental	Predicted	Experimental
1,2-Benzanthraquinone	2.14	3.13	0.35	0.52	3.13	n.d.
Di-(2-ethylhexyl) phthalate	4.66	n.d.	1.36	2.00	6.52	n.d.
9-Phenylcarbazole	3.68	3.93	1.31	1.34	4.97	n.d.
Oleamide	4.87	n.d.	1.52	0.96	6.68	n.d.
3,5-Di-tert-butyl-4-hydroxybenzaldehyde	2.20	2.31	-0.05	0.02	3.38	n.d.

Table A11. Predicted and experimental logarithmic partition coefficients between LDPE and a 0.5% PS 80 solution.

	$\log K_{i,P/f_{PS80=0.5\%}}$	
Compound	Predicted	Experimental
1,2-Benzanthraquinone	0.99	2.49
Di-(2-ethylhexyl) phthalate	0.83	2.21
9-Phenylcarbazole	1.56	2.18
Oleamide	0.93	1.68
3,5-Di-tert-butyl-4-hydroxybenzaldehyde	1.41	2.13

10.5 Equations

PDMS/water

$$\log K_{i,PDMS/W} = 0.268 + 0.601\,E_i - 1.416\,S_i - 2.523\,A_i - 4.107\,B_i + 3.637\,V_i \quad (A1)$$

n = 170, R^2 = 0.993, SD = 0.171

LDPE/water

$$\log K_{i,LDPE/W} = -0.529 + 1.098\,E_i - 1.557\,S_i - 2.991\,A_i - 4.617\,B_i + 3.886\,V_i \quad (A2)$$

n = 156, R^2 = 0.991, SD = 0.264

NaCl Setschenow constant

$$k_{i,S} = 0.112 - 0.020\,E_i - 0.042\,S_i - 0.047\,A_i - 0.060\,B_i + 0.171\,V_i \quad (A3)$$

n = 43, R^2 = 0.83, SD = 0.031

10% ethanol/ water

$$\log K_{i,f_{EtOH=10\%}/W} = -0.173 - 0.023\,E_i - 0.001\,S_i + 0.065\,A_i - 0.372\,B_i + 0.454\,V_i \quad (A4)$$

n = 73, R^2 = 0.749, SD = 0.122

20% ethanol/ water

$$\log K_{i,f_{EtOH=20\%}/W} = -0.252 + 0.042\,E_i - 0.040\,S_i + 0.096\,A_i - 0.823\,B_i + 0.916\,V_i \quad (A5)$$

n = 73, R^2 = 0.739, SD = 0.263

30% ethanol/ water

$$\log K_{i,f_{EtOH=30\%}/W} = -0.269 + 0.107\,E_i - 0.098\,S_i + 0.133\,A_i - 1.316\,B_i + 1.414\,V_i \quad (A6)$$

n = 73, R^2 = 0.838, SD = 0.302

40% ethanol/ water

$$\log K_{i,f_{EtOH=40\%}/W} = -0.221 + 0.131\,E_i - 0.159\,S_i + 0.171\,A_i - 1.809\,B_i + 1.918\,V_i \quad (A7)$$

n = 73, R^2 = 0.892, SD = 0.317

50% ethanol/ water	$\log K_{i,f_{EtOH=50\%}/W} = -0.142 + 0.124\ E_i - 0.252\ S_i + 0.251\ A_i - 2.275\ B_i + 2.415\ V_i$ n = 73, R^2 = 0.93, SD = 0.313	(A8)
10% isopropanol/ water	$\log K_{i,f_{IPA=10\%}/W} = -0.030 - 0.117\ E_i + 0.098\ S_i - 0.044\ A_i - 0.457\ B_i + 0.400\ V_i$ n = 46, SD = 0.154	(A9)
20% isopropanol/ water	$\log K_{i,f_{IPA=20\%}/W} = -0.001 - 0.217\ E_i + 0.126\ S_i - 0.151\ A_i - 0.860\ B_i + 0.802\ V_i$ n = 46, SD = 0.287	(A10)
30% isopropanol/ water	$\log K_{i,f_{IPA=30\%}/W} = -0.028 - 0.189\ E_i + 0.098\ S_i - 0.068\ A_i - 1.433\ B_i + 1.252\ V_i$ n = 46, SD = 0.355	(A11)
40% isopropanol/ water	$\log K_{i,f_{IPA=40\%}/W} = 0.115 - 0.156\ E_i - 0.054\ S_i - 0.102\ A_i - 1.937\ B_i + 1.725\ V_i$ n = 46, SD = 0.441	(A12)
50% isopropanol/ water	$\log K_{i,f_{IPA=50\%}/W} = 0.167 - 0.091\ E_i - 0.169\ S_i - 0.080\ A_i - 2.382\ B_i + 2.132\ V_i$ n = 46, SD = 0.488	(A13)

10.6 Appendix References

1. Abraham, M.H., Ibrahim, A., Acree Jr, W.E., 2007. Partition of compounds from gas to water and from gas to physiological saline at 310 K: linear free energy relationships. Fluid phase equilibria 251, pp. 93-109.
2. Poole, C.F., 2020. Wayne State University experimental descriptor database for use with the solvation parameter model. Journal of Chromatography A 1617. doi:10.1016/j.chroma.2019.460841.
3. Abraham, M.H., Acree, W.E., 2012. Linear free-energy relationships for water/hexadec-1-ene and water/deca-1, 9-diene partitions, and for permeation through lipid bilayers; comparison of permeation systems. New Journal of Chemistry 36, pp. 1798-1806.
4. Abraham, M.H., Acree Jr, W.E., 2010. Solute descriptors for phenoxide anions and their use to establish correlations of rates of reaction of anions with iodomethane. The Journal of organic chemistry 75, pp. 3021-3026.
5. Houser, E.J., Mlsna, T.E., Nguyen, V.K., Chung, R., Mowery, R.L., McGill, R.A., 2001. Rational materials design of sorbent coatings for explosives: applications with chemical sensors. Talanta 54, pp. 469-485.
6. Hoover, K.R., Acree Jr, W.E., Abraham, M.H., 2005. Chemical toxicity correlations for several fish species based on the Abraham solvation parameter model. Chemical research in toxicology 18, pp. 1497-1505.
7. Abraham, M.H., 1993. Hydrogen bonding. 31. Construction of a scale of solute effective or summation hydrogen-bond basicity. Journal of physical organic chemistry 6, pp. 660-684.
8. Abraham, M.H., 1993. Hydrogen bonding: XXVII. Solvation parameters for functionally substituted aromatic compounds and heterocyclic compounds, from gas—liquid chromatographic data. Journal of Chromatography A 644, pp. 95-139.
9. Gunatilleka, A.D., Poole, C.F., 2000. Models for estimating the non-specific toxicity of organic compounds in short-term bioassays. Analyst 125, pp. 127-132.
10. Abraham, M.H., Acree Jr, W.E., 2004. Correlation and prediction of partition coefficients between the gas phase and water, and the solvents dodecane and undecane. New Journal of Chemistry 28, pp. 1538-1543.
11. Ariyasena, T.C., Poole, C.F., 2014. Determination of descriptors for polycyclic aromatic hydrocarbons and related compounds by chromatographic methods and liquid–liquid partition in totally organic biphasic systems. Journal of Chromatography A 1361, pp. 240-254.
12. Ariyasena, T.C., Poole, C.F., 2013. Evaluation of triethylamine as a counter solvent in totally organic biphasic liquid–liquid partition systems. Chromatographia 76, pp. 1031-1039.
13. Endo, S., Schmidt, T.C., 2006. Partitioning properties of linear and branched ethers: Determination of linear solvation energy relationship (LSER) descriptors. Fluid phase equilibria 246, pp. 143-152.
14. Abraham, M.H., Acree, W.E., 2021. Descriptors for fluorotelomere alcohols. Calculation of physicochemical properties. Physics and Chemistry of Liquids. pp. 1-6. doi:doi:10.1080/00319104.2021.1888094.
15. Abraham, M.H., Chadha, H.S., Whiting, G.S., Mitchell, R.C., 1994. Hydrogen bonding. 32. An analysis of water-octanol and water-alkane partitioning and the Δlog P parameter of Seiler. Journal of pharmaceutical sciences 83, pp. 1085-1100.
16. Abraham, M.H., Acree Jr, W.E., Leo, A.J., Hoekman, D., 2009. Partition of compounds from water and from air into the wet and dry monohalobenzenes. New Journal of Chemistry 33, pp. 1685-1692.
17. Abraham, M.H., Acree Jr, W.E., 2013. Descriptors for the prediction of partition coefficients and solubilities of organophosphorus compounds. Separation science and technology 48, pp. 884-897.
18. Sprunger, L.M., Achi, S.S., Acree Jr, W.E., Abraham, M.H., 2010. Development of correlations for describing solute transfer into acyclic alcohol solvents based on the Abraham model and fragment-specific equation coefficients. Fluid phase equilibria 288, pp. 139-144.

19. Abraham, M.H., Ibrahim, A., Zhao, Y., Acree Jr, W.E., 2006. A data base for partition of volatile organic compounds and drugs from blood/plasma/serum to brain, and an LFER analysis of the data. Journal of pharmaceutical sciences 95, pp. 2091-2100.
20. Abraham, M.H., Sánchez-Moreno, R., Gil-Lostes, J., Acree Jr, W.E., Cometto-Muñiz, J.E., Cain, W.S., 2010. The biological and toxicological activity of gases and vapors. Toxicology in Vitro 24, pp. 357-362.